5
Parametric Cycle Analysis of Ideal Engines

5.1 Introduction

Cycle analysis studies the thermodynamic changes of the working fluid (air and products of combustion in most cases) as it flows through the engine. It is divided into two types of analysis: *parametric cycle analysis* (also called *design-point* or *on-design)* and *engine performance analysis* (also called *off-design).* Parametric cycle analysis determines the performance of engines at different flight conditions and values of design choice (e.g., compressor pressure ratio) and design limit (e.g., combustor exit temperature) parameters. Engine performance analysis determines the performance of a specific engine at all flight conditions and throttle settings.

In both forms of analysis, the components of an engine are characterized by the change in properties they produce. For example, the compressor is described by a total pressure ratio and efficiency. A certain engine's behavior is determined by its geometry, and a compressor will develop a certain total pressure ratio for a given geometry, speed, and airflow. Because the geometry is not included in parametric cycle analysis, the plots of specific thrust $F/\dot{m}_0$, and thrust specific fuel consumption S vs, say, Mach number or compressor pressure ratio are not portraying the behavior of a specific engine. Each point on such plots represents a different engine. The geometry for each plotted engine will be different, and thus we say that parametric cycle analysis represents a "rubber engine." Parametric cycle analysis is also called *designpoint analysis* or *on-design analysis* because each plotted engine is operating at its so-called design point.[4,12,28,29]

The main objective of parametric cycle analysis is to relate the engine performance parameters (primarily thrust F and thrust specific fuel consumption S) to design choices (compressor pressure ratio, fan pressure ratio, bypass ratio, etc.), to design limitations (burner exit temperature, compressor exit pressure, etc.), and to flight environment (Mach number, ambient temperature, etc.). From parametric cycle analysis, we can easily determine which engine type (e.g., turbofan) and component design characteristics (range of design choices) best satisfy a particular need.

Supporting Material for this chapter is available electronically. See page 869 for instructions to download.

The value of parametric cycle analysis depends directly on the realism with which the engine components are characterized. For example, if a compressor is specified by the total pressure ratio and the isentropic efficiency, and if the analysis purports to select the best total pressure ratio for a particular mission, then the choice may depend on the variation of efficiency with pressure ratio. For the conclusions to be useful, a realistic variation of efficiency with total pressure ratio must be included in the analysis.

The parametric cycle analysis of engines will be developed in stages. First the general steps applicable to the parametric cycle analysis of engines will be introduced. Next these steps will be followed to analyze engines where all engine components are taken to be ideal. Trends of these ideal engines will be analyzed, given that only basic conclusions can be deduced. The parametric cycle analysis of ideal engines allows us to look at the characteristics of aircraft engines in the simplest possible ways so that they can be compared. Following this, realistic assumptions as to component losses will be introduced in Chapter 6 and the parametric cycle analysis repeated for the different aircraft engines in Chapter 7. Performance trends of these engines with losses (real engines) will also be analyzed in Chapter 8.

In the last chapter on engine cycle analysis, models will be developed for the performance characteristics of the engine components. The aerothermodynamic relationships between the engine components will be analyzed for several types of aircraft engines. Then the performance of specific engines at all flight conditions and throttle settings will be predicted.

5.2 Notation

The *total* or *stagnation temperature* is defined as that temperature reached when a steadily flowing fluid is brought to rest (stagnated) adiabatically. If T_t denotes the total temperature, T the static (thermodynamic) temperature, and V the flow velocity, then application of the first law of thermodynamics to a calorically perfect gas gives $T_t = T + V^2/(2g_c c_p)$. However, the Mach number $M = V/a = V/\sqrt{\gamma g_c RT}$ can be introduced into the preceding equation to give

$$T_t = T\left(1 + \frac{\gamma - 1}{2} M^2\right) \tag{5.1}$$

The *total or stagnation pressure* P_t is defined as the pressure reached when a steady flowing stream is brought to rest adiabatically and reversibly (i.e., isentropically). Since $P_t/P = (T_t/T)^{\gamma/(\gamma-1)}$ then

$$P_t = P\left(1 + \frac{\gamma - 1}{2} M^2\right)^{\gamma/(\gamma-1)} \tag{5.2}$$

Ratios of total temperatures and pressures will be used extensively in this text, and a special notation is adopted for them. We denote a *ratio of total pressures* across a component by π, with a subscript indicating the component: d for diffuser (inlet), c for compressor, b for burner, t for turbine, n for nozzle,

and f for fan:

$$\pi_a = \frac{\text{total pressure leaving component } a}{\text{total pressure entering component } a} \tag{5.3}$$

Similarly, the *ratio of total temperatures* is denoted by τ, and

$$\tau_a = \frac{\text{total temperature leaving component } a}{\text{total temperature entering component } a} \tag{5.4}$$

There are the following exceptions:

1) We define the total/static temperature and pressure ratios of the freestream (τ_r and π_r) by

$$\tau_r = \frac{T_{t0}}{T_0} = 1 + \frac{\gamma - 1}{2} M_0^2 \tag{5.5}$$

$$\pi_r = \frac{P_{t0}}{P_0} = \left(1 + \frac{\gamma - 1}{2} M_0^2\right)^{\gamma/(\gamma-1)} \tag{5.6}$$

Thus the total temperature and pressure of the freestream can be written as

$$T_{t0} = T_0 \tau_r \quad P_{t0} = P_0 \pi_r$$

2) Also, τ_λ is defined as the ratio of the burner exit enthalpy $c_p T_t$ to the ambient enthalpy $c_p T_0$:

$$\tau_\lambda = \frac{h_{t\ \text{burner exit}}}{h_0} = \frac{(c_p T_t)_{\text{burner exit}}}{(c_p T)_0} \tag{5.7}$$

Figure 5.1 shows the cross section and station numbering of a turbofan engine with both afterburning and duct burning. This station numbering is in accordance with Aerospace Recommended Practice (ARP) 755A (see Ref. 30). Note that

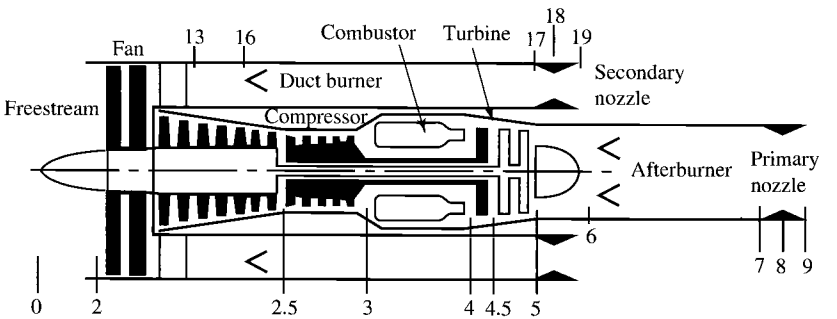

Fig. 5.1 Station numbering for gas turbine engines.

Table 5.1 Temperature and pressure relationships for all τ and π

Freestream			
$\tau_r = 1 + \frac{\gamma - 1}{2} M_0^2$		$\pi_r = \left(1 + \frac{\gamma-1}{2} M_0^2\right)^{\gamma/(\gamma-1)}$	
Core stream		Bypass stream	
$\tau_\lambda = \frac{c_{pt} T_{t4}}{c_{pc} T_0}$	$\tau_{\lambda AB} = \frac{c_{pAB} T_{t7}}{c_{pc} T_0}$	$\tau_{\lambda DB} = \frac{c_{pDB} T_{t17}}{c_{pc} T_0}$	
$\tau_d = \frac{T_{t2}}{T_{t0}}$	$\pi_d = \frac{P_{t2}}{P_{t0}}$	$\tau_f = \frac{T_{t13}}{T_{t2}}$	$\pi_f = \frac{P_{t13}}{P_{t2}}$
$\tau_c = \frac{T_{t3}}{T_{t2}}$	$\pi_c = \frac{P_{t3}}{P_{t2}}$	$\tau_{DB} = \frac{T_{t17}}{T_{t13}}$	$\pi_{DB} = \frac{P_{t17}}{P_{t13}}$
$\tau_b = \frac{T_{t4}}{T_{t3}}$	$\pi_b = \frac{P_{t4}}{P_{t3}}$	$\tau_{fn} = \frac{T_{t19}}{T_{t17}}$	$\pi_{fn} = \frac{P_{t19}}{P_{t17}}$
$\tau_t = \frac{T_{t5}}{T_{t4}}$	$\pi_t = \frac{P_{t5}}{P_{t4}}$		
$\tau_{AB} = \frac{T_{t7}}{T_{t5}}$	$\pi_{AB} = \frac{P_{t7}}{P_{t5}}$		
$\tau_n = \frac{T_{t9}}{T_{t7}}$	$\pi_n = \frac{P_{t9}}{P_{t7}}$		

the station numbers 13–19 are used for the bypass stream and decimal numbers such as station number 4.5 are used to indicate an intermediate station.

Table 5.1 contains most of the short-form notation temperature ratios τ and pressure ratios π that we will use in our analysis. (Note that the τ_λ are expressed for calorically perfect gases.) These ratios are shown in terms of the standard station numbering.[30]

5.3 Design Inputs

The total temperature ratios, total pressure ratios, etc., can be classified into one of four categories:

1) Flight conditions: P_0, T_0, M_0, c_p, τ_r, π_r
2) Design limits: $(c_p T_t)_{\text{burner exit}}$
3) Component performance: π_d, π_b, π_n, etc.
4) Design choices: π_c, π_f, etc.

5.4 Steps of Engine Parametric Cycle Analysis

The steps of engine parametric cycle analysis listed next are based on a jet engine with a single inlet and single exhaust. Thus these steps will use only the station numbers for the core engine flow (from 0 to 9) shown in Fig. 5.1. We will use these steps in this chapter and Chapter 7. When more than one

exhaust stream is present (e.g., high-bypass-ratio turbofan engine), the steps will be modified.

Parametric cycle analysis desires to determine how the engine performance (specific thrust and fuel consumption) varies with changes in the flight conditions (e.g., Mach number), design limits (e.g., main burner exit temperature), component performance (e.g., turbine efficiency), and design choices (e.g., compressor pressure ratio).

1) Starting with an equation for uninstalled engine thrust, we rewrite this equation in terms of the total pressure and total temperature ratios: the ambient pressure P_0, temperature T_0, and speed of sound a_0, and the flight Mach number M_0 as follows:

$$F = \frac{1}{g_c}(\dot{m}_9 V_e - \dot{m}_0 V_0) + A_9(P_9 - P_0)$$

$$\frac{F}{\dot{m}_0} = \frac{a_0}{g_c}\left(\frac{\dot{m}_9}{\dot{m}_0}\frac{V_9}{a_0} - M_0\right) + \frac{A_9 P_9}{\dot{m}_0}\left(1 - \frac{P_0}{P_9}\right)$$

2) Next express the velocity ratio(s) V_9/a_0 in terms of Mach numbers, temperatures, and gas properties of states 0 and 9:

$$\left(\frac{V_9}{a_0}\right)^2 = \frac{a_9^2 M_9^2}{a_0^2} = \frac{\gamma_9 R_9 g_c T_9}{\gamma_0 R_0 g_c T_0} M_9^2$$

3) Find the exit Mach number M_9. Since

$$P_{t9} = P_9\left(1 + \frac{\gamma - 1}{2} M_9^2\right)^{\gamma/(\gamma-1)}$$

then

$$M_9^2 = \frac{2}{\gamma - 1}\left[\left(\frac{P_{t9}}{P_9}\right)^{(\gamma-1)/\gamma} - 1\right]$$

where

$$\frac{P_{t9}}{P_9} = \frac{P_0}{P_9}\frac{P_{t0}}{P_0}\frac{P_{t2}}{P_{t0}}\frac{P_{t3}}{P_{t2}}\frac{P_{t4}}{P_{t3}}\frac{P_{t5}}{P_{t4}}\frac{P_{t7}}{P_{t5}}\frac{P_{t9}}{P_{t7}}$$

$$= \frac{P_0}{P_9}\pi_r \pi_d \pi_c \pi_b \pi_t \pi_{AB} \pi_n$$

4) Find the temperature ratio T_9/T_0:

$$\frac{T_9}{T_0} = \frac{T_{t9}/T_0}{T_{t9}/T_9} = \frac{T_{t9}/T_0}{(P_{t9}/P_9)^{(\gamma-1)/\gamma}}$$

where

$$\frac{T_{t9}}{T_0} = \frac{T_{t0}}{T_0}\frac{T_{t2}}{T_{t0}}\frac{T_{t3}}{T_{t2}}\frac{T_{t4}}{T_{t3}}\frac{T_{t5}}{T_{t4}}\frac{T_{t7}}{T_{t5}}\frac{T_{t9}}{T_{t7}} = \tau_r\tau_d\tau_c\tau_b\tau_t\tau_{AB}\tau_n$$

5) Apply the first law of thermodynamics to the burner (combustor), and find an expression for the fuel/air ratio f in terms of τ's, etc.:

$$\dot{m}_0 c_p T_{t3} + \dot{m}_f h_{PR} = \dot{m}_0 c_p T_{t4}$$

6) When applicable, find an expression for the total temperature ratio across the turbine τ_t by relating the turbine power output to the compressor, fan, and/or propeller power requirements. This allows us to find τ_t in terms of other variables.

7) Evaluate the specific thrust, using the preceding results.

8) Evaluate the thrust specific fuel consumption S, using the results for specific thrust and fuel/air ratio:

$$S = \frac{f}{F/\dot{m}_0} \tag{5.8}$$

9) Develop expressions for the thermal and propulsive efficiencies.

5.5 Assumptions of Ideal Cycle Analysis

For analysis of ideal cycles, we assume the following:

1) There are isentropic (reversible and adiabatic) compression and expansion processes in the inlet (diffuser), compressor, fan, turbine, and nozzle. Thus we have the following relationships:

$$\tau_d = \tau_n = 1 \qquad \pi_d = \pi_n = 1 \qquad \tau_c = \pi_c^{(\gamma-1)/\gamma} \qquad \tau_t = \pi_t^{(\gamma-1)/\gamma}$$

2) Constant-pressure combustion ($\pi_b = 1$) is idealized as a heat interaction into the combustor. The fuel flow rate is much less than the airflow rate through the combustor such that

$$\frac{\dot{m}_f}{\dot{m}_c} \ll 1 \qquad \text{and} \qquad \dot{m}_c + \dot{m}_f \cong \dot{m}_c$$

3) The working fluid is air that behaves as a perfect gas with constant specific heats.

4) The engine exhaust nozzles expand the gas to the ambient pressure ($P_9 = P_0$).

5.6 Ideal Ramjet

A schematic diagram of a ramjet engine is shown in Fig. 5.2, and the ideal cycle is plotted on a temperature-entropy (T-s) diagram and H-K diagram in

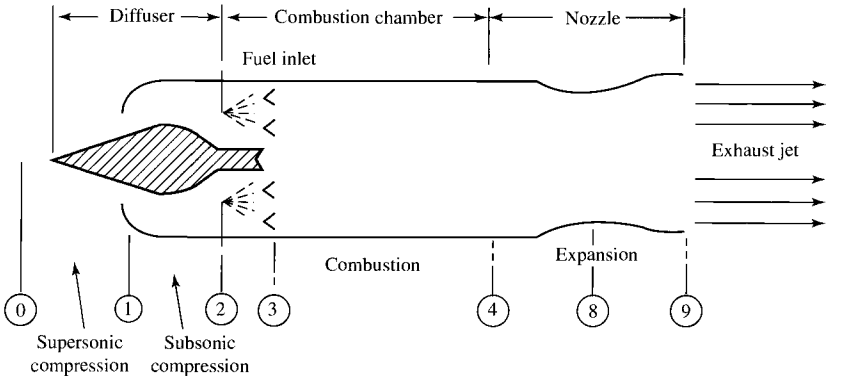

Fig. 5.2 Typical ramjet engine.

Fig. 5.3. A ramjet engine is conceptually the simplest aircraft engine and consists of an inlet or diffuser, a combustor or burner, and a nozzle. The inlet or diffuser slows the air velocity relative to the engine from the flight velocity V_0 to a smaller value V_2. This decrease in velocity increases both the static pressure P_2 and static temperature T_2. In the combustor or burner, fuel is added and its chemical energy is converted to thermal energy in the combustion process. This addition of thermal energy increases the static temperature T_4, and the combustion process occurs at a nearly constant pressure for $M_4 \ll 1$. The nozzle expands the gas to or near the ambient pressure, and

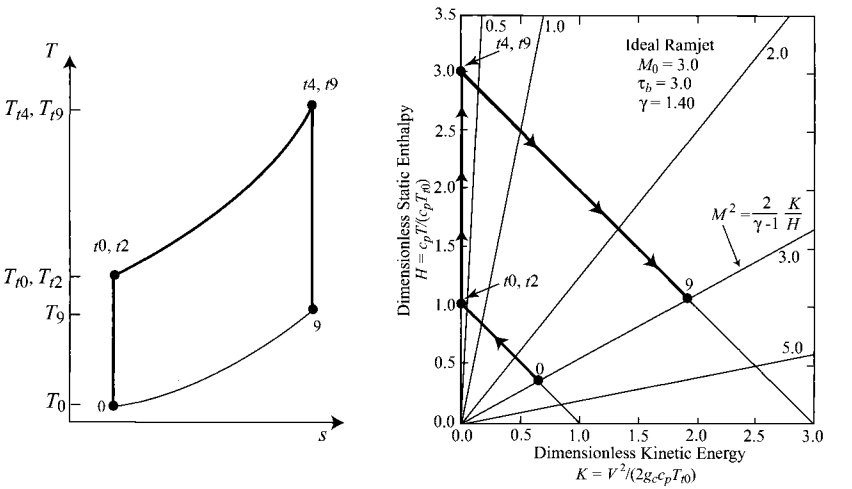

Fig. 5.3 The *T-s* diagram and *H-K* diagram of an ideal ramjet engine.

the temperature decreases from T_4 to T_9 with a corresponding increase in the kinetic energy per unit mass $(V_9^2 - V_4^2)/(2g_c)$.

5.6.1 Cycle Analysis

Application of the steps of cycle analysis to the ideal ramjet of Fig. 5.2 is presented next in the order listed in Section 5.4.

Step 1:

$$F = \frac{1}{g_c}(\dot{m}_9 V_9 - \dot{m}_0 V_0) + A_9(P_9 - P_0)$$

However, $P_9 = P_0$ and $\dot{m}_9 \cong \dot{m}_0$ for the ideal engine. Thus

$$F = \frac{\dot{m}_0}{g_c}(V_9 - V_0) = \frac{\dot{m}_0 a_0}{g_c}\left(\frac{V_9}{a_0} - M_0\right) \tag{5.9}$$

Step 2:

$$\left(\frac{V_9}{a_0}\right)^2 = \frac{a_9^2 M_9^2}{a_0^2} = \frac{\gamma_9 R_9 g_c T_9 M_9^2}{\gamma_0 R_0 g_c T_0}$$

However, $\gamma_9 = \gamma_0 = \gamma$ and $R_9 = R_0 = R$ for an ideal engine. Thus

$$\left(\frac{V_9}{a_0}\right)^2 = \frac{T_9}{T_0} M_9^2 \tag{5.10}$$

Step 3:

$$P_{t9} = P_0 \frac{P_{t0}}{P_0}\frac{P_{t2}}{P_{t0}}\frac{P_{t4}}{P_{t2}}\frac{P_{t9}}{P_{t4}} = P_0 \pi_r \pi_d \pi_b \pi_n$$

However, $\pi_d = \pi_b = \pi_n = 1$ for an ideal engine. Thus $P_{t9} = P_0 \pi_r$ and

$$\frac{P_{t9}}{P_9} = \frac{P_{t9}}{P_0}\frac{P_0}{P_9} = \pi_r \frac{P_0}{P_9} = \pi_r$$

$$M_9^2 = \frac{2}{\gamma - 1}\left[\left(\frac{P_{t9}}{P_9}\right)^{(\gamma-1)/\gamma} - 1\right] = \frac{2}{\gamma - 1}(\pi_r^{(\gamma-1)/\gamma} - 1)$$

However,

$$\pi_r^{(\gamma-1)/\gamma} = \tau_r$$

Thus

$$M_9^2 = \frac{2}{\gamma - 1}(\tau_r - 1) = M_0^2 \qquad \text{or} \qquad M_9 = M_0 \tag{5.11}$$

Step 4:

$$T_{t9} = T_0 \frac{T_{t0}}{T_0}\frac{T_{t2}}{T_{t0}}\frac{T_{t4}}{T_{t2}}\frac{T_{t9}}{T_{t4}} = T_0 \tau_r \tau_d \tau_b \tau_n = T_0 \tau_r \tau_b$$

$$\frac{T_{t9}}{T_0} = \left(\frac{P_{t9}}{P_9}\right)^{(\gamma-1)/\gamma}$$

$$\frac{T_9}{T_0} = \frac{T_{t9}/T_o}{T_{t9}/T_9} = \frac{\tau_r \tau_b}{(P_{t9}/P_9)^{(\gamma-1)/\gamma}} = \frac{\tau_r \tau_b}{\tau_r}$$

$$\frac{T_9}{T_0} = \tau_b \tag{5.12}$$

Step 5: Application of the steady flow energy equation (first law of thermodynamics) to the control volume about the burner or combustor shown in Fig. 5.4 gives

$$\dot{m}_0 h_{t2} + \dot{m}_f h_{PR} = (\dot{m}_0 + \dot{m}_f) h_{t4}$$

where h_{pR} is the thermal energy released by the fuel during combustion. For an ideal engine,

$$\dot{m}_0 + \dot{m}_f \cong \dot{m}_0 \qquad \text{and} \qquad c_{p2} = c_{p4} = c_p$$

Thus the preceding equation becomes

$$\dot{m}_0 c_p T_{t2} + \dot{m}_f h_{PR} = \dot{m}_0 c_p T_{t4}$$

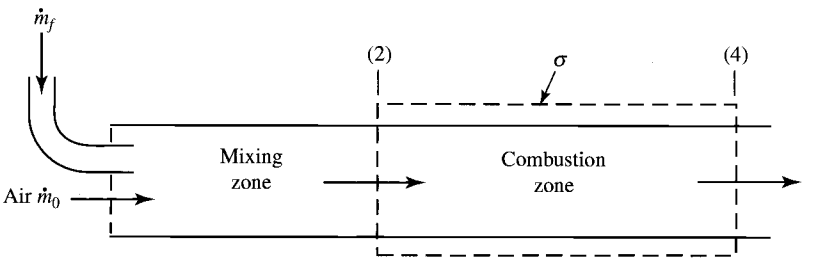

Fig. 5.4 Combustor model.

or

$$\dot{m}_f h_{PR} = \dot{m}_0 c_p (T_{t4} - T_{t2}) = \dot{m}_0 c_p T_{t2} \left(\frac{T_{t4}}{T_{t2}} - 1 \right)$$

The fuel/air ratio f is defined as

$$f \equiv \frac{\dot{m}_f}{\dot{m}_0} = \frac{c_p T_{t2}}{h_{PR}} \left(\frac{T_{t4}}{T_{t2}} - 1 \right) \tag{5.13a}$$

For the ideal ramjet, $T_{t0} = T_{t2} = T_0 \tau_r$ and $T_{t4}/T_{t2} = \tau_b$. Thus Eq. (5.13a) becomes

$$f = \frac{c_p T_0 \tau_r}{h_{PR}} (\tau_b - 1) \tag{5.13b}$$

However,

$$\tau_\lambda = \frac{c_{p4} T_{t4}}{c_{p0} T_0} = \frac{T_{t4}}{T_0} = \frac{T_{t2}}{T_0} \frac{T_{t4}}{T_{t2}} = \tau_r \tau_b$$

for the ramjet, and Eq. (5.13b) can be written as

$$f = \frac{c_p T_0}{h_{PR}} (\tau_\lambda - \tau_r) \tag{5.13c}$$

Step 6: This is not applicable for the ramjet engine.

Step 7: Since $M_9 = M_0$ and $T_9/T_0 = \tau_b$, then

$$\left(\frac{V_9}{a_0} \right)^2 = \frac{T_9}{T_0} M_9^2 = \tau_b M_0^2 \tag{5.14}$$

and the expression for thrust can be rewritten as

$$F = \frac{\dot{m}_0 a_0 M_0}{g_c} (\sqrt{\tau_b} - 1) = \frac{\dot{m}_0 a_0 M_0}{g_c} \left(\sqrt{\frac{\tau_\lambda}{\tau_r}} - 1 \right) \tag{5.15a}$$

or

$$\frac{F}{\dot{m}_0} = \frac{a_0 M_0}{g_c} (\sqrt{\tau_b} - 1) = \frac{a_0 M_0}{g_c} \left(\sqrt{\frac{\tau_\lambda}{\tau_r}} - 1 \right) \tag{5.15b}$$

Step 8:

$$S = \frac{f}{F/\dot{m}_0}$$

$$S = \frac{c_p T_0 g_c (\tau_\lambda - \tau_r)}{a_0 M_0 h_{PR} (\sqrt{\tau_\lambda/\tau_r} - 1)} \tag{5.16a}$$

or

$$S = \frac{c_p T_0 g_c \tau_r (\tau_b - 1)}{a_0 M_0 h_{PR} (\sqrt{\tau_b} - 1)} \tag{5.16b}$$

Step 9: Development of the following efficiency expressions is left to the reader.

Thermal efficiency:

$$\eta_T = 1 - \frac{1}{\tau_r} \tag{5.17a}$$

Propulsive efficiency:

$$\eta_P = \frac{2}{\sqrt{\tau_\lambda/\tau_r} + 1} \tag{5.17b}$$

Overall efficiency:

$$\eta_O = \eta_T \eta_P = \frac{2(\tau_r - 1)}{\sqrt{\tau_\lambda \tau_r} + \tau_r} \tag{5.17c}$$

5.6.2 Summary of Equations—Ideal Ramjet

INPUTS:

$$M_0,\ T_0(\mathrm{K},\ ^\circ\mathrm{R}),\ \gamma,\ c_p\left(\frac{\mathrm{kJ}}{\mathrm{kg}\cdot\mathrm{K}},\ \frac{\mathrm{Btu}}{\mathrm{lbm}\cdot{}^\circ\mathrm{R}}\right),\ h_{PR}\left(\frac{\mathrm{kJ}}{\mathrm{kg}},\ \frac{\mathrm{Btu}}{\mathrm{lbm}}\right),\ T_{t4}(\mathrm{K},\ ^\circ\mathrm{R})$$

OUTPUTS:

$$\frac{F}{\dot{m}_0}\left(\frac{\mathrm{N}}{\mathrm{kg/s}},\ \frac{\mathrm{lbf}}{\mathrm{lbm/s}}\right),\ f,\ S\left(\frac{\mathrm{mg/s}}{\mathrm{N}},\ \frac{\mathrm{lbm/h}}{\mathrm{lbf}}\right),\ \eta_T,\ \eta_P,\ \eta_O$$

EQUATIONS:

$$R = \frac{\gamma - 1}{\gamma} c_p \tag{5.18a}$$

$$a_0 = \sqrt{\gamma R g_c T_0} \tag{5.18b}$$

$$\tau_r = 1 + \frac{\gamma - 1}{2} M_0^2 \tag{5.18c}$$

$$\tau_\lambda = \frac{T_{t4}}{T_0} \tag{5.18d}$$

$$\frac{V_9}{a_0} = M_0 \sqrt{\frac{\tau_\lambda}{\tau_r}} \tag{5.18e}$$

$$\frac{F}{\dot{m}_0} = \frac{a_0}{g_c}\left(\frac{V_9}{a_0} - M_0\right) \tag{5.18f}$$

$$f = \frac{c_p T_0}{h_{PR}}(\tau_\lambda - \tau_r) \tag{5.18g}$$

$$S = \frac{f}{F/\dot{m}_0} \tag{5.18h}$$

$$\eta_T = 1 - \frac{1}{\tau_r} \tag{5.18i}$$

$$\eta_P = \frac{2}{\sqrt{\tau_\lambda/\tau_r} + 1} \tag{5.18j}$$

$$\eta_O = \eta_T \eta_P = \frac{2(\tau_r - 1)}{\sqrt{\tau_\lambda \tau_r} + \tau_r} \tag{5.18k}$$

Example 5.1

The performance of ideal ramjets is plotted in Figs. 5.5a–5.5d vs flight Mach number M_0 for different values of the total temperature leaving the combustor. Calculations were performed for the following input data:

$T_0 = 216.7\,\text{K}$, $\gamma = 1.4$, $c_p = 1.004\,\text{kJ/(kg} \cdot \text{K)}$, $h_{PR} = 42{,}800\,\text{kJ/kg}$

$T_{t4} = 1600$, 1900, and 2200 K

5.6.3 Optimum Mach Number

The plot of specific thrust vs Mach number (see Fig. 5.5a) shows that the maximum value of specific thrust is exhibited at a certain Mach number for each value of T_{t4}. An analytical expression for this optimum Mach number can be found by taking the partial derivative of the equation for specific thrust with respect to flight Mach number, setting this equal to zero, and solving as follows.

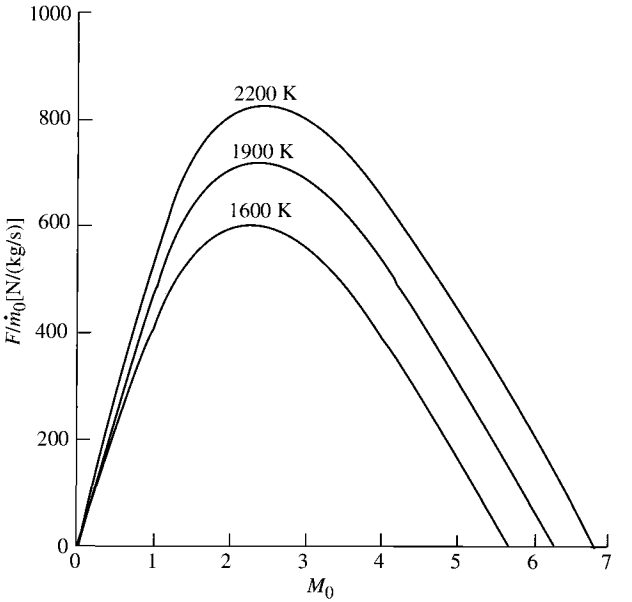

Fig. 5.5a Ideal ramjet performance vs Mach number: specific thrust.

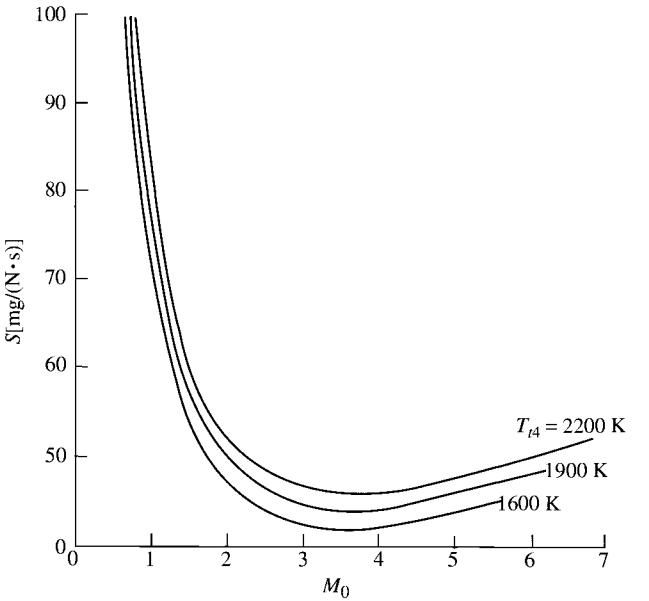

Fig. 5.5b Ideal ramjet performance vs Mach number: thrust-specific fuel consumption.

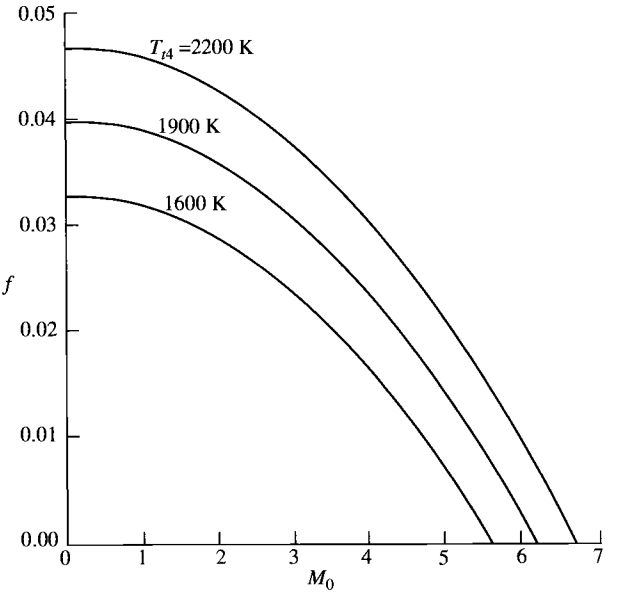

Fig. 5.5c Ideal ramjet performance vs Mach number: fuel/air ratio.

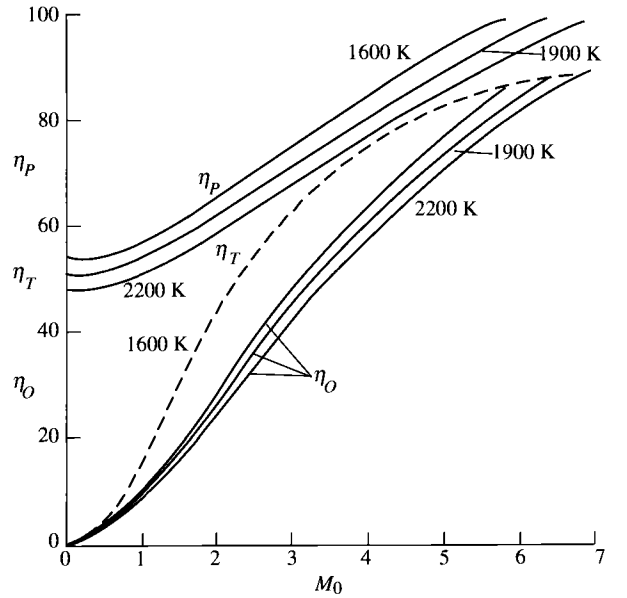

Fig. 5.5d Ideal ramjet performance vs Mach number: efficiencies.

Combining Eqs. (5.18e) and (5.18f) and differentiating gives

$$\frac{\partial}{\partial M_0}\left(\frac{F}{\dot{m}_0}\right) = \frac{a_0}{g_c}\frac{\partial}{\partial M_0}\left[M_0\left(\sqrt{\frac{\tau_\lambda}{\tau_r}} - 1\right)\right] = 0$$

$$\sqrt{\frac{\tau_\lambda}{\tau_r}} - 1 + M_0\sqrt{\tau_\lambda}\frac{\partial}{\partial M_0}\left(\frac{1}{\sqrt{\tau_r}}\right) = 0$$

Now

$$\frac{\partial}{\partial M_0}\left(\frac{1}{\sqrt{\tau_r}}\right) = -\frac{1}{2}\frac{1}{\tau_r^{3/2}}\frac{\partial \tau_r}{\partial M_0} = -\frac{1}{2\tau_r^{3/2}}\frac{\partial}{\partial M_0}\left(1 + \frac{\gamma - 1}{2}M_0^2\right)$$

$$= -\frac{(\gamma - 1)M_0}{2\tau_r^{3/2}}$$

Thus

$$\sqrt{\frac{\tau_\lambda}{\tau_r}} - 1 = M_0\sqrt{\tau_\lambda}\frac{(\gamma - 1)M_0}{2\tau_r^{3/2}}$$

or

$$\sqrt{\frac{\tau_\lambda}{\tau_r}} - 1 = \sqrt{\frac{\tau_\lambda}{\tau_r}}\frac{(\gamma - 1)M_0^2}{2\tau_r}$$

However,

$$\frac{\gamma - 1}{2}M_0^2 = \tau_r - 1$$

Then

$$\sqrt{\frac{\tau_\lambda}{\tau_r}} - 1 = \sqrt{\frac{\tau_\lambda}{\tau_r}}\frac{\tau_r - 1}{\tau_r} = \sqrt{\frac{\tau_\lambda}{\tau_r}} - \frac{\sqrt{\tau_\lambda}}{\tau_r^{3/2}} \quad \text{or} \quad \tau_r^3 = \tau_\lambda$$

Thus $F/\dot{m}_0$ is maximum when

$$\tau_{r\ \max\ F/\dot{m}_0} = \sqrt[3]{\tau_\lambda} \tag{5.19}$$

or

$$M_{0\ \max\ F/\dot{m}_0} = \sqrt{\frac{2}{\gamma - 1}(\sqrt[3]{\tau_\lambda} - 1)} \tag{5.20}$$

5.6.4 Mass Ingested by an Ideal Ramjet

Because the specific thrust of a ramjet has a maximum at the flight Mach number given by Eq. (5.20) and decreases at higher Mach numbers, one might question how the thrust of a given ramjet will vary with the Mach number. Does the thrust of a ramjet vary as its specific thrust? Because the thrust of a given ramjet will depend on its physical size (flow areas), the variation in thrust per unit area with Mach number will give the trend we seek. For a ramjet, the diffuser exit Mach number (station 2) is essentially constant over the flight Mach number operating range ($M_2 = 0.5$). Using this fact, we can find the engine mass flow rate in terms of A_2, M_0, M_2, and the ambient pressure and temperature. With this flow rate, we can then find the thrust per unit area at station 2 from

$$\frac{F}{A_2} = \frac{F}{\dot{m}_0}\frac{\dot{m}_0}{A_2}$$

As we shall see, the mass flow rate is a strong function of flight Mach number and altitude. For our case,

$$\frac{\dot{m}_0}{A_2} = \frac{\dot{m}_2}{A_2} = \frac{\dot{m}_2}{A_2^*}\frac{A_2^*}{A_2} = \frac{\dot{m}_2}{A_2^*}\left(\frac{A^*}{A}\right)_{M_2} \tag{i}$$

However, mass flow parameter (MFP),

$$\text{MFP}(M_i) = \frac{\dot{m}_i\sqrt{T_{ti}}}{A_i P_{ti}}$$

and

$$\text{MFP}^* = \text{MFF}(@M = 1) = \frac{\dot{m}\sqrt{T_t}}{A^* P_t}$$

Then

$$\frac{\dot{m}_2}{A_2^*} = \text{MFP}^*\frac{P_{t2}}{\sqrt{T_{t2}}}, \qquad T_{t2} = T_{t0}, \qquad \text{and} \qquad P_{t2} = \pi_d P_{t0} \tag{ii}$$

where

$$\frac{P_{t2}}{\sqrt{T_{t2}}} = \frac{\pi_d P_{t0}}{\sqrt{T_{t0}}} = \frac{\pi_d P_0}{\sqrt{T_0}}\frac{P_{t0}/P_0}{\sqrt{T_{t0}/T_0}} = \frac{\pi_d P_0}{\sqrt{T_0}}\frac{(T_{t0}/T_0)^{\gamma/(\gamma-1)}}{\sqrt{T_{t0}/T_0}}$$

or

$$\frac{P_{t2}}{\sqrt{T_{t2}}} = \frac{\pi_d P_0}{\sqrt{T_0}} \left(\frac{T_{t0}}{T_0}\right)^{\gamma/(\gamma-1)-1/2} = \frac{\pi_d P_0}{\sqrt{T_0}} (\tau_r)^{(\gamma+1)/[2(\gamma-1)]} \tag{iii}$$

For air, $\gamma = 1.4$ and $(\gamma + 1)/[2(\gamma - 1)] = 3$. Thus, combining Eqs. (i), (ii), and (iii), we get

$$\frac{\dot{m}_0}{A_2} = \text{MFP}^* \left(\frac{A^*}{A}\right)_{M_2} \frac{\pi_d P_0 \tau_r^3}{\sqrt{T_0}} \tag{5.21}$$

The variations of mass flow per unit area [Eq. (5.21)], specific thrust, and thrust per unit area at station 2 with flight Mach number are plotted in Fig. 5.6 for M_2 of 0.5, altitude of 12 km, T_{t4}, of 1900 K, and π_d of 1.0. Although the specific thrust variation with Mach number reaches a maximum at Mach 2.30 and then falls off, the thrust of an ideal ramjet continues to increase with flight Mach number until about Mach 5.25 due to the very rapid increase in mass flow per unit area.

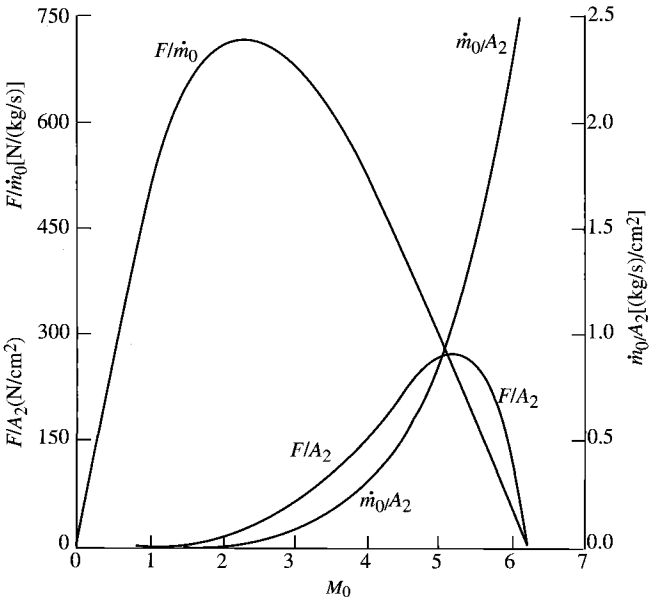

Fig. 5.6 Ideal ramjet thrust per unit area vs Mach number.

5.7 Ideal Turbojet

The thrust of a ramjet tends to zero as the Mach number goes to zero. This poor performance can be overcome by the addition of a compressor-turbine unit to the basic Brayton cycle, as shown in Fig. 5.7a. The thermal efficiency of this ideal cycle is now

$$\eta_T = 1 - \frac{T_0}{T_{t3}} = 1 - \frac{1}{\tau_r \tau_c} \tag{5.22}$$

Whereas an ideal ramjet's thermal efficiency is zero at Mach 0, a compressor having a pressure ratio of 10 will give a thermal efficiency of about 50% for the ideal turbojet at Mach 0.

For the ideal turbojet

$$\dot{W}_t = \dot{W}_c, \qquad T_{t4} > T_{t3}, \qquad \text{and} \qquad P_{t4} = P_{t3}$$

Thus the compressor-burner-turbine combination generates a higher pressure and temperature at its exit and is called, therefore, a *gas generator.* The gas leaving the gas generator may be expanded through a nozzle to form a turbojet, as depicted in Figs. 5.7a and 5.7b, or the gases may be expanded through a turbine to drive a fan (turbofan), a propeller (turboprop), a generator (gas turbine), an automobile (gas turbine), or a helicopter rotor (gas turbine).

We will analyze the ideal turbojet cycle as we did the ideal ramjet cycle and will determine the trends in the variation of thrust, thrust specific fuel consumption, and fuel/air ratio with compressor pressure ratio and flight Mach number.

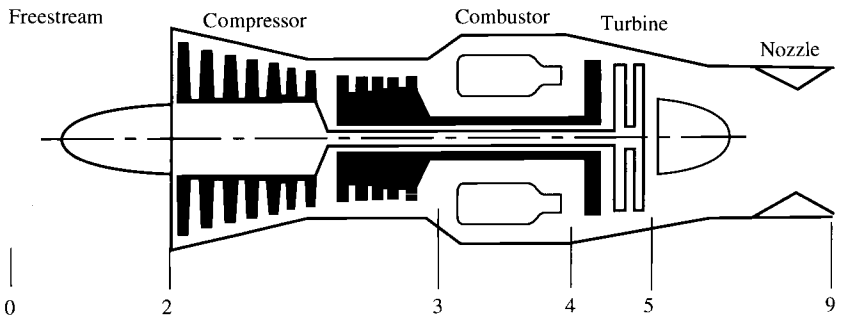

Fig. 5.7a Station numbering of ideal turbojet engine.

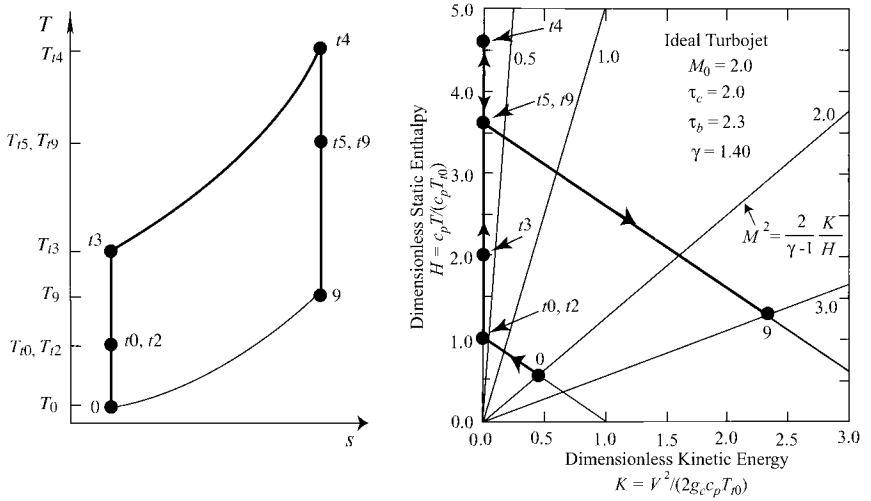

Fig. 5.7b The *T-s* diagram and *H-K* diagram of an ideal turbojet engine.

5.7.1 Cycle Analysis

Application of these steps of cycle analysis to the ideal turbojet engine is presented next in the order listed in Section 5.4.

Step 1:

$$\frac{F}{\dot{m}_0} = \frac{1}{g_c}(V_9 - V_0) = \frac{a_0}{g_c}\left(\frac{V_9}{a_0} - M_0\right)$$

Step 2:

$$\left(\frac{V_9}{a_0}\right)^2 = \frac{a_9^2 M_9^2}{a_0^2} = \frac{\gamma_9 R_9 g_c T_9 M_9^2}{\gamma_0 R_0 g_c T_0} = \frac{T_9}{T_0} M_9^2$$

Step 3:

$$P_{t9} = P_9\left(1 + \frac{\gamma - 1}{2} M_9^2\right)^{\gamma/(\gamma-1)}$$

and

$$P_{t9} = P_0 \frac{P_{t0}}{P_0}\frac{P_{t2}}{P_{t0}}\frac{P_{t3}}{P_{t2}}\frac{P_{t4}}{P_{t3}}\frac{P_{t5}}{P_{t4}}\frac{P_{t9}}{P_{t5}} = P_0 \pi_r \pi_d \pi_c \pi_b \pi_t \pi_n$$

However, $\pi_d = \pi_b = \pi_n = 1$; thus $P_{t9} = P_0 \pi_r \pi_c \pi_t$, and so

$$M_9^2 = \frac{2}{\gamma - 1}\left[\left(\frac{P_{t9}}{P_9}\right)^{(\gamma-1)/\gamma} - 1\right]$$

where

$$\frac{P_{t9}}{P_9} = \frac{P_{t9}}{P_0}\frac{P_0}{P_9} = \pi_r \pi_c \pi_t \frac{P_0}{P_9} = \pi_r \pi_c \pi_t$$

Then

$$M_9^2 = \frac{2}{\gamma - 1}[(\pi_r \pi_c \pi_t)^{(\gamma-1)/\gamma} - 1]$$

However, $\pi_r^{(\gamma-1)/\gamma} = \tau_r$ and for an ideal turbojet $\pi_c^{(\gamma-1)/\gamma} = \tau_c$ and $\pi_t^{(\gamma-1)/\gamma} = \tau_t$. Thus

$$M_9^2 = \frac{2}{\gamma - 1}(\tau_r \tau_c \tau_t - 1) \tag{5.23}$$

Step 4:

$$T_{t9} = T_0 \frac{T_{t0}}{T_0}\frac{T_{t2}}{T_{t0}}\frac{T_{t3}}{T_{t2}}\frac{T_{t4}}{T_{t3}}\frac{T_{t5}}{T_{t4}}\frac{T_{t9}}{T_{t5}} = T_0 \tau_r \tau_d \tau_c \tau_b \tau_t \tau_n = T_0 \tau_r \tau_c \tau_b \tau_t$$

Then

$$\frac{T_9}{T_0} = \frac{T_{t9}/T_0}{T_{t9}/T_9} = \frac{\tau_r \tau_c \tau_b \tau_t}{(P_{t9}/P_9)^{(\gamma-1)/\gamma}} = \frac{\tau_r \tau_c \tau_b \tau_t}{(\pi_r \pi_c \pi_t)^{(\gamma-1)/\gamma}} = \frac{\tau_r \tau_c \tau_b \tau_t}{\tau_r \tau_c \tau_t}$$

Thus

$$\frac{T_9}{T_0} = \tau_b \tag{5.24}$$

Step 5: Application of the steady flow energy equation to the burner gives

$$\dot{m}_0 h_{t3} + \dot{m}_f h_{PR} = (\dot{m}_0 + \dot{m}_f) h_{t4}$$

For an ideal cycle, $\dot{m}_0 + \dot{m}_f \cong \dot{m}_0$ and $c_{p3} = c_{p4} = c_p$. Thus

$$\dot{m}_0 c_p T_{t3} + \dot{m}_f h_{PR} = \dot{m}_0 c_p T_{t4}$$

$$\dot{m}_f h_{PR} = \dot{m}_0 c_p (T_{t4} - T_{t3}) = \dot{m}_0 c_p T_0 \left(\frac{T_{t4}}{T_0} - \frac{T_{t3}}{T_0}\right)$$

or

$$f = \frac{\dot{m}_f}{\dot{m}_0} = \frac{c_p T_0}{h_{PR}} \left(\frac{T_{t4}}{T_0} - \frac{T_{t3}}{T_0} \right)$$

However,

$$\tau_\lambda = \frac{T_{t4}}{T_0} \qquad \text{and} \qquad \tau_r \tau_c = \frac{T_{t3}}{T_0}$$

Then

$$f = \frac{\dot{m}_f}{\dot{m}_0} = \frac{c_p T_0}{h_{PR}} (\tau_\lambda - \tau_r \tau_c) \tag{5.25}$$

or

$$f = \frac{\dot{m}_f}{\dot{m}_0} = \frac{c_p T_0 \tau_r \tau_c}{h_{PR}} (\tau_b - 1) \tag{5.26}$$

Step 6: The power out of the turbine is

$$\dot{W}_t = (\dot{m}_0 + \dot{m}_f)(h_{t4} - h_{t5}) \cong \dot{m}_0 c_p (T_{t4} - T_{t5})$$
$$= \dot{m}_0 c_p T_{t4} \left(1 - \frac{T_{t5}}{T_{t4}} \right) = \dot{m}_0 c_p T_{t4} (1 - \tau_t)$$

The power required to drive the compressor is

$$\dot{W}_c = \dot{m}_0 (h_{t3} - h_{t2}) = \dot{m}_0 c_p (T_{t3} - T_{t2})$$
$$= \dot{m}_0 c_p T_{t2} \left(\frac{T_{t3}}{T_{t2}} - 1 \right) = \dot{m}_0 c_p T_{t2} (\tau_c - 1)$$

Since $\dot{W}_c = \dot{W}_t$ for the ideal turbojet, then

$$\dot{m}_0 c_p T_{t2} (\tau_c - 1) = \dot{m}_0 c_p T_{t4} (1 - \tau_t)$$

or

$$\tau_t = 1 - \frac{T_{t2}}{T_{t4}} (\tau_c - 1)$$

Thus

$$\tau_t = 1 - \frac{\tau_r}{\tau_\lambda} (\tau_c - 1) \tag{5.27}$$

Step 7:

$$\left(\frac{V_9}{a_0}\right)^2 = \frac{T_9}{T_0} M_9^2 = \frac{2}{\gamma - 1} \frac{\tau_\lambda}{\tau_r \tau_c} (\tau_r \tau_c \tau_t - 1) \tag{5.28}$$

However,

$$\frac{F}{\dot{m}_0} = \frac{a_0}{g_c} \left(\frac{V_9}{a_0} - M_0\right)$$

Thus

$$\frac{F}{\dot{m}_0} = \frac{a_0}{g_c} \left[\sqrt{\frac{2}{\gamma - 1} \frac{\tau_\lambda}{\tau_r \tau_c} (\tau_r \tau_c \tau_t - 1)} - M_0\right] \tag{5.29}$$

Step 8: According to Eq. (5.8),

$$S = \frac{f}{F/\dot{m}_0}$$

The thrust specific fuel consumption S can be calculated by first calculating the fuel/air ratio f and the thrust per unit of airflow $F/\dot{m}_0$, using Eqs. (5.25) and (5.29), respectively, and then substituting these values into the preceding equation. An analytical expression for S can be obtained by substituting Eqs. (5.25) and (5.29) into Eq. (5.8) to get the following:

$$S = \frac{c_p T_0 g_c (\tau_\lambda - \tau_r \tau_c)}{a_0 h_{PR} \left[\sqrt{\frac{2}{\gamma - 1} \frac{\tau_\lambda}{\tau_r \tau_c} (\tau_r \tau_c \tau_t - 1)} - M_0\right]} \tag{5.30}$$

Step 9: Again the development of these expressions is left to the reader.

Thermal efficiency:

$$\eta_T = 1 - \frac{1}{\tau_r \tau_c} \tag{5.31a}$$

Propulsive efficiency:

$$\eta_P = \frac{2M_0}{V_9/a_0 + M_0} \tag{5.31b}$$

Overall efficiency:

$$\eta_O = \eta_P \eta_T \tag{5.31c}$$

5.7.2 Summary of Equations—Ideal Turbojet

INPUTS:

$$M_0,\ T_0(\mathrm{K},\ ^\circ\mathrm{R}),\ \gamma,\ c_p\left(\frac{\mathrm{kJ}}{\mathrm{kg}\cdot\mathrm{K}},\ \frac{\mathrm{Btu}}{\mathrm{lbm}\cdot{}^\circ\mathrm{R}}\right),\ h_{PR}\left(\frac{\mathrm{kJ}}{\mathrm{kg}},\ \frac{\mathrm{Btu}}{\mathrm{lbm}}\right),\ T_{t4}(\mathrm{K},\ ^\circ\mathrm{R}),\ \pi_c$$

OUTPUTS:

$$\frac{F}{\dot{m}_0}\left(\frac{N}{\mathrm{kg/s}},\ \frac{\mathrm{lbf}}{\mathrm{lbm/s}}\right),\ f,\ S\left(\frac{\mathrm{mg/s}}{\mathrm{N}},\ \frac{\mathrm{lbm/h}}{\mathrm{lbf}}\right)\ \eta_T,\ \eta_P,\ \eta_O$$

EQUATIONS:

$$R = \frac{\gamma - 1}{\gamma} c_p \tag{5.32a}$$

$$a_0 = \sqrt{\gamma R g_c T_0} \tag{5.32b}$$

$$\tau_r = 1 + \frac{\gamma - 1}{2} M_0^2 \tag{5.32c}$$

$$\tau_\lambda = \frac{T_{t4}}{T_0} \tag{5.32d}$$

$$\tau_c = (\pi_c)^{(\gamma-1)/\gamma} \tag{5.32e}$$

$$\tau_t = 1 - \frac{\tau_r}{\tau_\lambda}(\tau_c - 1) \tag{5.32f}$$

$$\frac{V_9}{a_0} = \sqrt{\frac{2}{\gamma - 1}\frac{\tau_\lambda}{\tau_r \tau_c}(\tau_r \tau_c \tau_t - 1)} \tag{5.32g}$$

$$\frac{F}{\dot{m}_0} = \frac{a_0}{g_c}\left(\frac{V_9}{a_0} - M_0\right) \tag{5.32h}$$

$$f = \frac{c_p T_0}{h_{PR}}(\tau_\lambda - \tau_r \tau_c) \tag{5.32i}$$

$$S = \frac{f}{F/\dot{m}_0} \tag{5.32j}$$

$$\eta_T = 1 - \frac{1}{\tau_r \tau_c} \tag{5.32k}$$

$$\eta_P = \frac{2M_0}{V_9/a_0 + M_0} \tag{5.32l}$$

$$\eta_O = \eta_P \eta_T \tag{5.32m}$$

Example 5.2

In Figs. 5.8a–5.8d, the performance of ideal turbojets is plotted vs compressor pressure ratio π_c for different values of flight Mach number M_0. Figures 5.9a–5.9d plot the performance vs flight Mach number M_0 for different values of the compressor pressure ratio π_c. Calculations were performed for the following input data:

$$T_0 = 390°\text{R}, \qquad \gamma = 1.4, \qquad c_p = 0.24\,\text{Btu/(lbm} \cdot °\text{R)}$$
$$h_{PR} = 18{,}400\,\text{Btu/lbm}, \qquad T_{t4} = 3000°\text{R}$$

a) Figures 5.8a–5.8d. Figure 5.8a shows that for a fixed Mach number, there is a compressor pressure ratio that gives maximum specific thrust. The loci of the compressor pressure ratios that give maximum specific thrust are indicated by the dashed line in Fig. 5.8a. One can also see from Fig. 5.8a that a lower compressor pressure ratio is desired at high Mach numbers to obtain reasonable specific thrust. This helps explain why the compressor pressure ratio of a turbojet for a subsonic flight may be 24 and that for supersonic flight may be 10. Figure 5.8b shows the general trend that increasing the compressor pressure ratio will decrease the thrust specific fuel consumption. The decrease in fuel/air ratio with increasing compressor pressure ratio and Mach number is shown

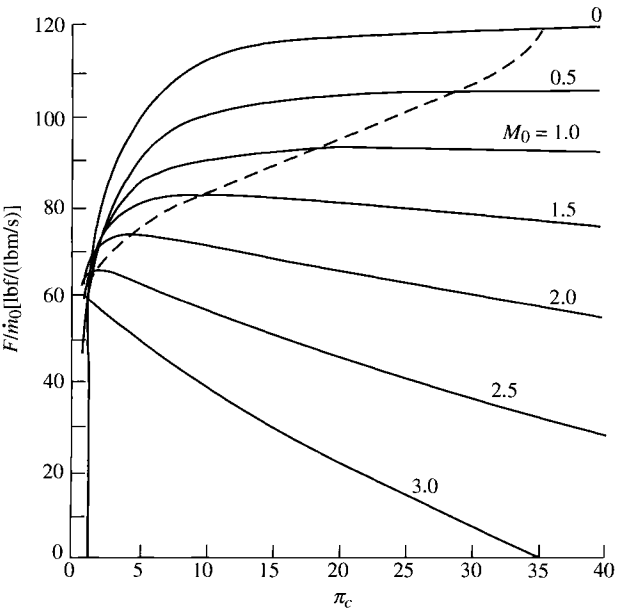

Fig. 5.8a Ideal turbojet performance vs compressor pressure ratio: specific thrust.

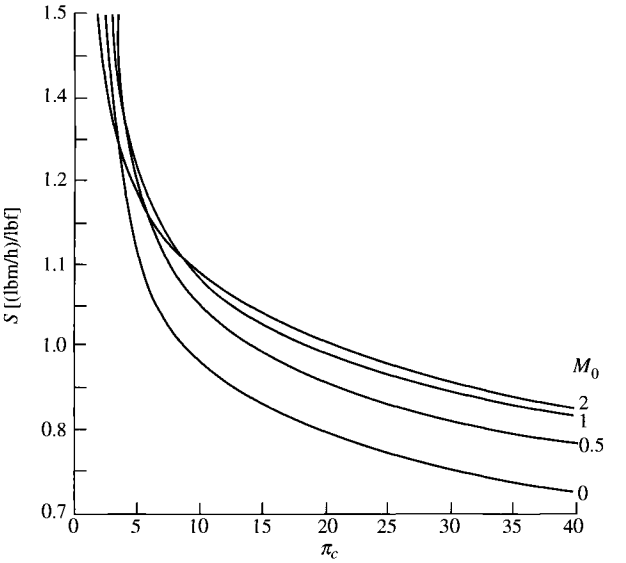

Fig. 5.8b Ideal turbojet performance vs compressor pressure ratio: thrust-specific fuel consumption.

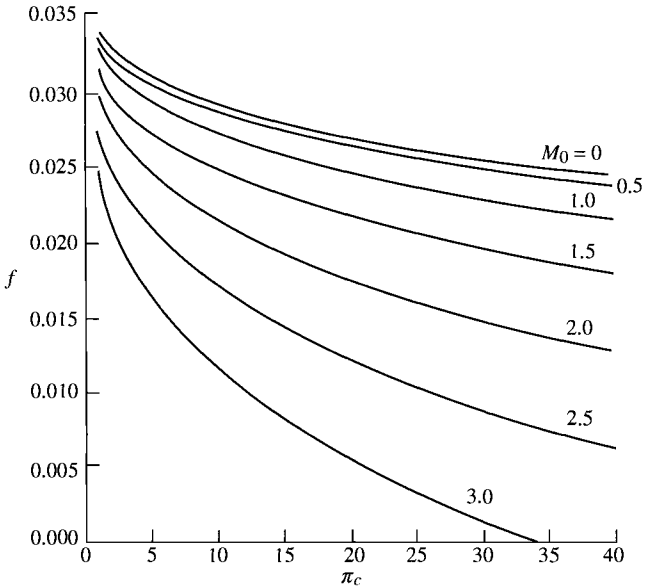

Fig. 5.8c Ideal turbojet performance vs compressor pressure ratio: fuel/air ratio.

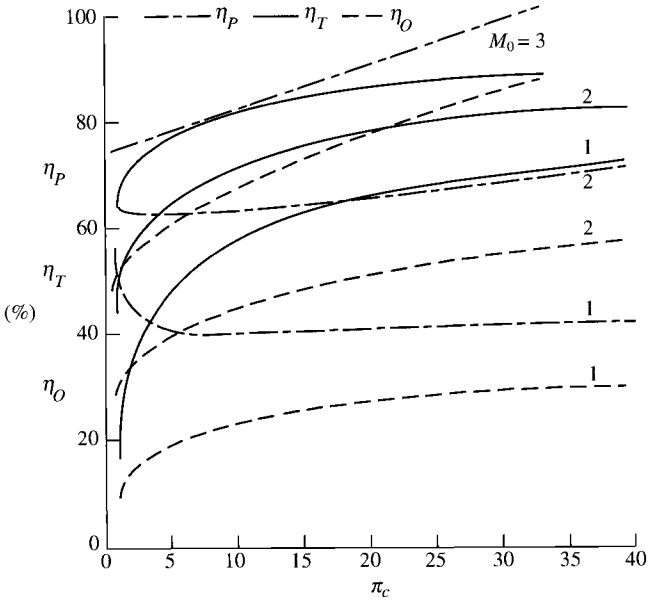

Fig. 5.8d Ideal turbojet performance vs compressor pressure ratio: efficiencies.

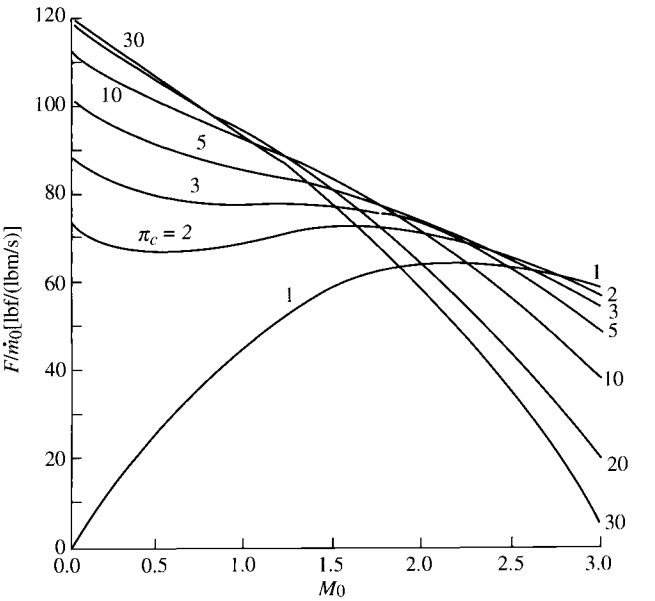

Fig. 5.9a Ideal turbojet performance vs flight Mach number: specific thrust.

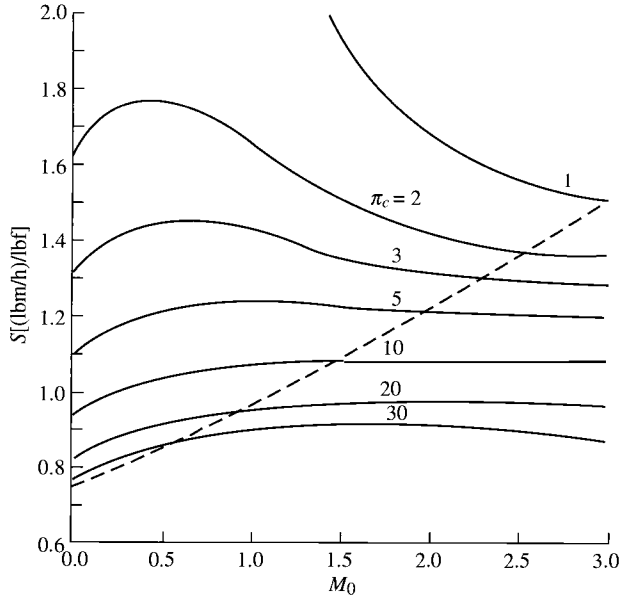

Fig. 5.9b Ideal turbojet performance vs flight Mach number: thrust-specific fuel consumption.

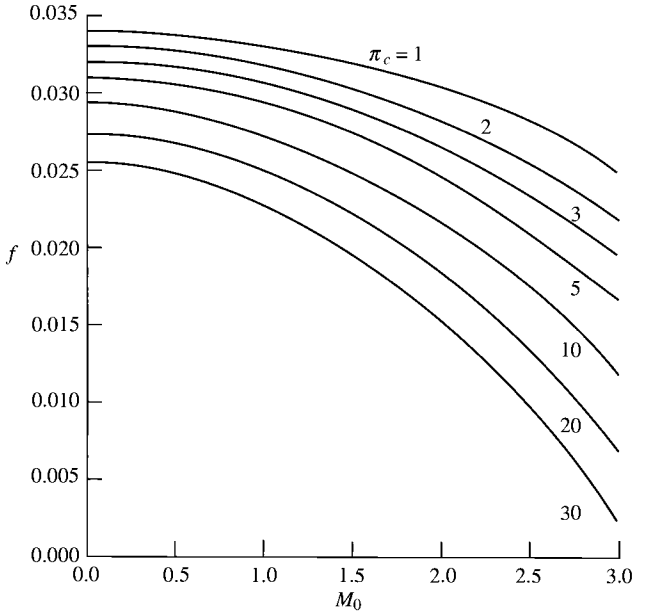

Fig. 5.9c Ideal turbojet performance vs flight Mach number: fuel/air ratio.

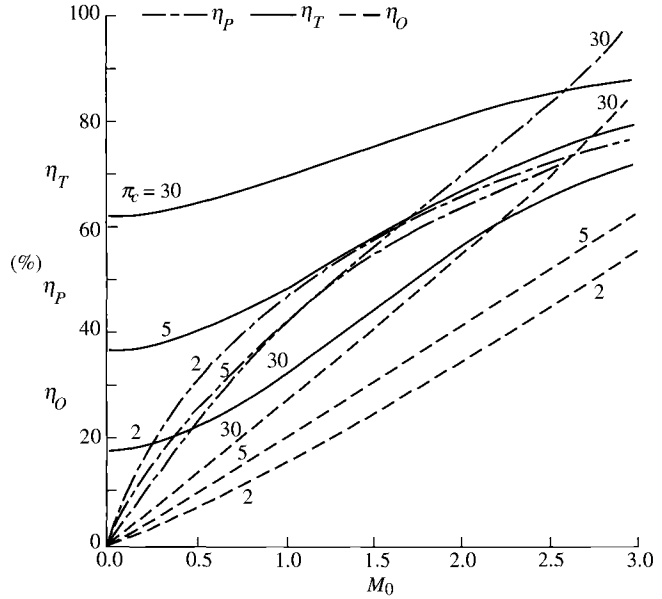

Fig. 5.9d Ideal turbojet performance vs flight Mach number: efficiencies.

in Fig. 5.8c. This is due to the increase in the total temperature entering the burner with increasing compressor pressure ratio and Mach number. Figure 5.8d shows the general increase in propulsive, thermal, and overall efficiencies with increasing compressor pressure ratio and flight Mach number.

b) Figures 5.9a–5.9d. These figures are another representation of the data of Figs. 5.8a–5.8d. Figures 5.9a and 5.9b show that a high compressor pressure ratio is desirable for subsonic flight for good specific thrust and low fuel consumption. However, some care must be used in selecting the compressor pressure ratio for the supersonic flight Mach number because of the rapid falloff in specific thrust with the compressor pressure ratio. The loci of the compressor pressure ratios that give maximum specific thrust are indicated by the dashed line in Fig. 5.9b. The decrease in fuel/air ratio with increasing Mach number and compressor pressure ratio is shown in Fig. 5.9c. Figure 5.9d shows the dominant influence of flight Mach number on propulsive efficiency. The performance of the ideal ramjet is shown in Figs. 5.9a–5.9c by curves for the compressor pressure ratio equal to 1.

5.7.3 Optimum Compressor Pressure Ratio

The plot of specific thrust vs the compressor pressure ratio (see Fig. 5.8a) shows that a maximum value is exhibited at a certain compressor pressure ratio at a given M_0, a_0, and τ_λ. The value of τ_c and hence of π_c to maximize

the specific thrust at a given M_0, a_0 and τ_λ can be found by differentiation. Because specific thrust will be maximum when V_9/a_0 is maximum, it is convenient to differentiate the expression for $(V_9/a_0)^2$ to find τ_c optimum. From Eq. (5.28), we have

$$\frac{\partial}{\partial \tau_c}\left[\left(\frac{V_9}{a_0}\right)^2\right] = \frac{2}{\gamma - 1}\frac{\partial}{\partial \tau_c}\left[\frac{\tau_\lambda}{\tau_r \tau_c}(\tau_r \tau_c \tau_t - 1)\right] = 0$$

Differentiating with respect to τ_c at constant M_0 (thus τ_r is constant) and constant τ_λ, we obtain

$$-\frac{\tau_\lambda}{\tau_r \tau_c^2}(\tau_r \tau_c \tau_t - 1) + \frac{\tau_\lambda}{\tau_r \tau_c}\left(\tau_r \tau_t + \tau_r \tau_c \frac{\partial \tau_t}{\partial \tau_c}\right) = 0$$

or

$$-\frac{\tau_\lambda \tau_t}{\tau_c} + \frac{\tau_\lambda}{\tau_r \tau_c^2} + \frac{\tau_\lambda \tau_t}{\tau_c} + \tau_\lambda \frac{\partial \tau_t}{\partial \tau_c} = 0$$

Then

$$\frac{1}{\tau_r \tau_c^2} + \frac{\partial \tau_t}{\partial \tau_c} = 0$$

where, using Eq. (5.27)

$$\frac{\partial \tau_t}{\partial \tau_c} = -\frac{\tau_t}{\tau_\lambda}$$

Thus

$$\frac{1}{\tau_r \tau_c^2} = \frac{\tau_t}{\tau_\lambda}$$

which results in

$$(\tau_c)_{\max F/\dot{m}_0} = \frac{\sqrt{\tau_\lambda}}{\tau_r} \tag{5.33a}$$

or

$$(\pi_c)_{\max F/\dot{m}_0} = (\tau_c)^{\gamma/(\gamma-1)}_{\max F/\dot{m}_0} \tag{5.33b}$$

An expression for the maximum V_9/a_0 can be found by substituting Eq. (5.33a) into Eqs. (5.28) and (5.27) to obtain

$$\frac{V_9}{a_0} = \sqrt{\frac{2}{\gamma - 1}\sqrt{\tau_\lambda}(\sqrt{\tau_\lambda}\tau_t - 1)}$$

and

$$\tau_t = 1 - \left(\frac{1}{\sqrt{\tau_\lambda}} - \frac{\tau_r}{\tau_\lambda}\right)$$

Thus

$$\frac{V_9}{a_0} = \sqrt{\frac{2}{\gamma - 1}[(\sqrt{\tau_\lambda} - 1)^2 + \tau_r - 1]} \tag{5.33c}$$

The specific thrust can then be written as

$$\frac{F}{\dot{m}_0} = \frac{a_0}{g_c}\left\{\sqrt{\frac{2}{\gamma - 1}[(\sqrt{\tau_\lambda} - 1)^2 + \tau_r - 1]} - M_0\right\} \tag{5.33d}$$

The fuel/air ratio f for the optimum turbojet can be written as

$$f = \frac{c_p T_0}{h_{PR}}(\tau_\lambda - \sqrt{\tau_\lambda}) \tag{5.33e}$$

and the thrust specific fuel consumption S as

$$S = \frac{c_p T_0 g_c(\tau_\lambda - \sqrt{\tau_\lambda})}{a_0 h_{PR}\{\sqrt{[2/(\gamma - 1)][(\sqrt{\tau_\lambda} - 1)^2 + \tau_r - 1]} - M_0\}} \tag{5.33f}$$

For the optimum ideal turbojet, it can be easily shown that $T_{t3} = T_9$. As the Mach number is changed in the optimum ideal turbojet at a fixed τ_λ and fixed altitude, the cycle and its enclosed area remain the same in the T-s diagram. The area enclosed by the cycle in the T-s diagram equals the net work output (kinetic energy change, for our case) of the cycle per unit mass flow. Even though this output is constant as M_0 increases, the thrust per unit mass flow decreases as M_0 increases. This can be shown as follows.

The kinetic energy change per unit mass is constant, and we can write

$$V_9^2 - V_0^2 = C$$

and therefore,

$$(V_9 - V_0)(V_9 + V_0) = C$$

or

$$\frac{F}{\dot{m}_0} = \frac{V_9 - V_0}{g_c} = \frac{C/g_c}{V_9 + V_0} \tag{5.34}$$

Referring to the T-s diagram of Fig. 5.7b, we see that as V_0 increases, T_{t2} increases and thus so does T_{t5}. However, if T_{t5} increases, V_9 increases also. Consequently $V_9 + V_0$ becomes larger as M_0 increases. Therefore, from Eq. (5.34), $V_9 - V_0$ must decrease as M_0 increases. It follows that the thrust per unit mass flow decreases with increasing M_0 even though the cycle work output per unit mass flow remains constant.

5.8 Ideal Turbojet with Afterburner

The thrust of a turbojet can be increased by the addition of a second combustion chamber, called an *afterburner*, aft of the turbine, as shown in Fig. 5.10. The total temperature leaving the afterburner has a higher limiting value than the total temperature leaving the main combustor because the gases leaving the afterburner do not have a turbine to pass through. The station numbering is indicated in Figs. 5.10, 5.11a, and 5.11b with 9′ representing the nozzle exit for the case of no afterburning.

5.8.1 Cycle Analysis

Rather than go through the complete steps of cycle analysis, we will use the results of the ideal turbojet and modify the equations to include afterburning. The gas velocity at the nozzle exit is given by

$$\frac{V_9^2}{2g_c c_p} = T_{t9} - T_9 = T_{t9}\left[1 - \left(\frac{P_9}{P_{t9}}\right)^{(\gamma-1)/\gamma}\right] \tag{5.35}$$

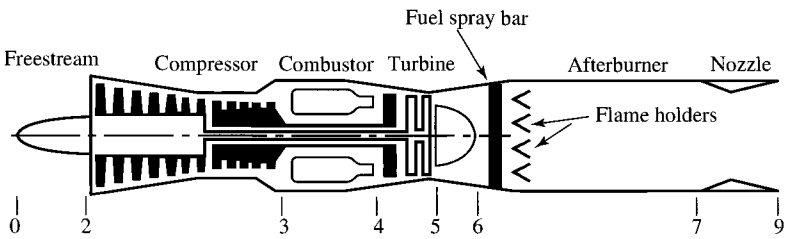

Fig. 5.10 Station numbering of an ideal afterburning turbojet engine.

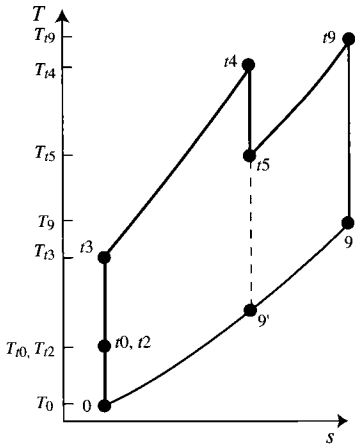

Fig. 5.11a The *T-s* diagram for an ideal afterburning turbojet engine.

and for the nonafterburning (subscript dry) and afterburning (subscript AB for afterburning) cases, we have

$$\frac{P_9}{P_{t9}} = \left(\frac{P_{9'}}{P_{t5}}\right)_{\text{dry}} = \left(\frac{P_9}{P_{t9}}\right)_{\text{AB}}$$

Thus we have

$$\left(\frac{V_9}{V_{9'}}\right)^2 = \frac{T_{t9}}{T_{t5}} \tag{5.36}$$

Equation (5.36) can be obtained directly from the *H-K* diagram in Fig. 5.11b. Since $(P_{9'}/P_{t5})_{\text{dry}} = (P_9/P_{t9})_{\text{AB}}$, $M_{9'} = M_9$. The triangle for the exit state of the turbojet with afterburner between points *t*9-9-origin is similar to that for the dry turbojet between points *t*5-9′-origin. Thus

$$\frac{K_9}{K_{9'}} = \frac{H_{t9}}{H_{t5}}$$

which can be rewritten as Eq. (5.36).

Consequently, we can find the velocity ratio $(V_9/a_0)^2$ for the afterburning turbojet by multiplying $(V_{9'}/a_0)^2$ from our nonafterburning turbojet analysis [Eq. (5.28)] by the total temperature ratio of the afterburner. That is,

$$\left(\frac{V_9}{a_0}\right)^2 = \frac{T_{t9}}{T_{t5}}\left(\frac{V_{9'}}{a_0}\right)^2 \tag{5.37}$$

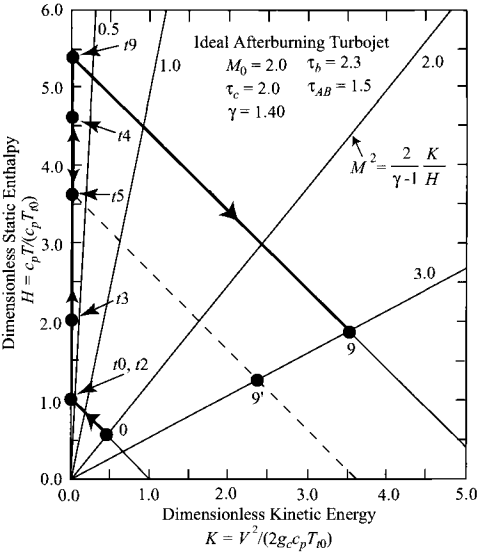

Fig. 5.11b *H-K* diagram for an ideal afterburning turbojet engine.

We define the temperature ratio $\tau_{\lambda AB}$ as

$$\tau_{\lambda AB} = \frac{T_{t7}}{T_0} \tag{5.38}$$

Thus we can write the total temperature ratio of the afterburner as

$$\frac{T_{t9}}{T_{t5}} = \frac{(T_{t9}/T_{t7})(T_{t7}/T_0)}{(T_{t5}/T_{t4})(T_{t4}/T_0)} = \frac{\tau_{\lambda AB}}{\tau_\lambda \tau_t} \tag{5.39}$$

Using Eqs. (5.27), (5.28), (5.37), and (5.39), we get the following expressions for V_9/a_0:

$$\left(\frac{V_9}{a_0}\right)^2 = \frac{2}{\gamma - 1}\frac{\tau_{\lambda AB}}{\tau_\lambda \tau_t}\frac{\tau_\lambda}{\tau_r \tau_c}(\tau_r \tau_c \tau_t - 1) = \frac{2}{\gamma - 1}\tau_{\lambda AB}\left(1 - \frac{1}{\tau_r \tau_c \tau_t}\right)$$

$$\left(\frac{V_9}{a_0}\right)^2 = \frac{2}{\gamma - 1}\tau_{\lambda AB}\left[1 - \frac{\tau_\lambda/(\tau_r \tau_c)}{\tau_\lambda - \tau_r(\tau_c - 1)}\right] \tag{5.40}$$

We find the total fuel flow rate to the burner and afterburner by an energy balance across the engine from station 0 to station 9, as sketched in Fig. 5.12.

The chemical energy of the fuel introduced between stations 0 and 9 is converted to thermal and kinetic energy of the gases, as measured by the total

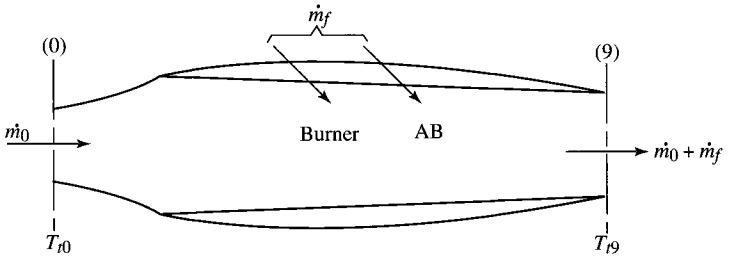

Fig. 5.12 Total fuel flow rate control volume.

temperature rise $T_{t9} - T_{t0}$. Thus we can write for this ideal engine

$$\dot{m}_{f\,\text{tot}} h_{PR} = \dot{m}_0 c_p (T_{t9} - T_{t0}) = \dot{m}_0 c_p T_0 \left(\frac{T_{t9}}{T_0} - \frac{T_{t0}}{T_0} \right)$$

Thus

$$f_{\text{tot}} = \frac{\dot{m}_f}{\dot{m}_0} = \frac{c_p T_0}{h_{PR}} (\tau_{\lambda \text{AB}} - \tau_r) \tag{5.41}$$

The thermal efficiency is given by

$$\eta_T = \frac{(\gamma - 1) c_p T_0 [(V_9/a_0)^2 - M_0^2]}{2 f_{\text{tot}} h_{PR}} \tag{5.42}$$

5.8.2 Summary of Equations—Ideal Turbojet with Afterburner

INPUTS:

$$M_0,\ T_0(\text{K, °R}),\ \gamma,\ c_p\left(\frac{\text{kJ}}{\text{kg} \cdot \text{K}}, \frac{\text{Btu}}{\text{lbm} \cdot \text{°R}}\right),\ h_{PR}\left(\frac{\text{kJ}}{\text{kg}}, \frac{\text{Btu}}{\text{lbm}}\right),$$

$$T_{t4}(\text{K, °R}),\ T_{t7}(\text{K, °R}),\ \pi_c$$

OUTPUTS:

$$\frac{F}{\dot{m}_0}\left(\frac{\text{N}}{\text{kg/s}}, \frac{\text{lbf}}{\text{lbm/s}}\right),\ f_{\text{tot}},\ S\left(\frac{\text{mg/s}}{\text{N}}, \frac{\text{lbm/h}}{\text{lbf}}\right),\ \eta_T,\ \eta_P,\ \eta_O$$

EQUATIONS:

Equations (5.32a–5.32f), (5.40), (5.32h), (5.41), (5.32j) with f replaced by f_{tot}, (5.42), (5.32l), and (5.32m).

Example 5.3

We consider the performance of an ideal turbojet engine with afterburner. For comparison with the nonafterburning (simple) turbojet of Example 5.2, we select the following input data:

$$T_0 = 390°\text{R}, \quad \gamma = 1.4, \quad c_p = 0.24\,\text{Btu/(lbm}\cdot°\text{R)}, \quad h_{PR} = 18{,}400\,\text{Btu/lbm}$$
$$T_{t4} = 3000°\text{R}, \quad T_{t7} = 4000°\text{R}$$

Figure 5.13 compares the performance of two turbojet engines with a compressor pressure ratio of 10, an afterburning turbojet and a simple turbojet. The graph of specific thrust vs M_0 indicates the thrust increase available by adding an afterburner to a simple turbojet. The afterburner increases the static thrust about 22% for the conditions shown and continues to provide significant thrust as the thrust of the simple turbojet goes to zero at about Mach 3.8. The graph of Fig. 5.13 also shows the cost in fuel consumption of the increased thrust provided by the afterburner. The cost is about a 20–30% increase in the fuel flow rate per unit thrust up to about $M_0 = 2.0$. In a nonideal turbojet, the same increase in S occurs up to about $M_0 = 2.0$. However, as the thrust of the simple turbojet approaches zero in the real case, its S rises above the afterburning engine's S so that the afterburning engine at the higher M_0 has a lower S and higher specific thrust than the simple turbojet.

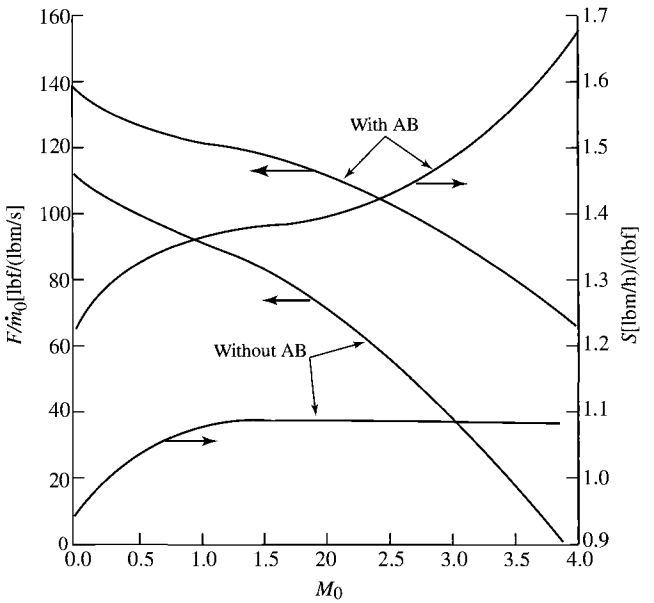

Fig. 5.13 Engine performance vs M_0 for an ideal afterburning turbojet.

Figures 5.14a–5.14d show the variation of engine performance with both Mach number and compressor pressure ratio for the afterburning turbojet. These should be compared to their counterparts in Figs. 5.8a–5.8d. For a fixed flight Mach number, the ideal afterburning turbojet has a compressor pressure ratio giving maximum specific thrust. The locus of these compressor pressure ratios is shown by a dashed line in Fig. 5.14a. Comparison of Figs. 5.14a–5.14d to Figs. 5.8a–5.8d yields the following general trends:

1) Afterburning increases both the specific thrust and the thrust specific fuel consumption.

2) Afterburning turbojets with moderate to high compressor pressure ratios give very good specific thrust at high flight Mach numbers.

3) The fuel/air ratio of the main burner f is unchanged. The afterburner fuel/air ratio f_{AB} increases with Mach number and compressor pressure ratio. The total fuel/air ratio decreases with Mach number and is not a function of π_c; see Eq. (5.41).

4) Thermal, propulsive, and overall efficiencies are reduced by afterburning.

5.8.3 Optimum Compressor Pressure Ratio with Afterburner

The value of the compressor pressure ratio to maximize the specific thrust at a given M_0, τ_r, τ_λ, and altitude can be found by differentiating V_9/a_0 with respect to

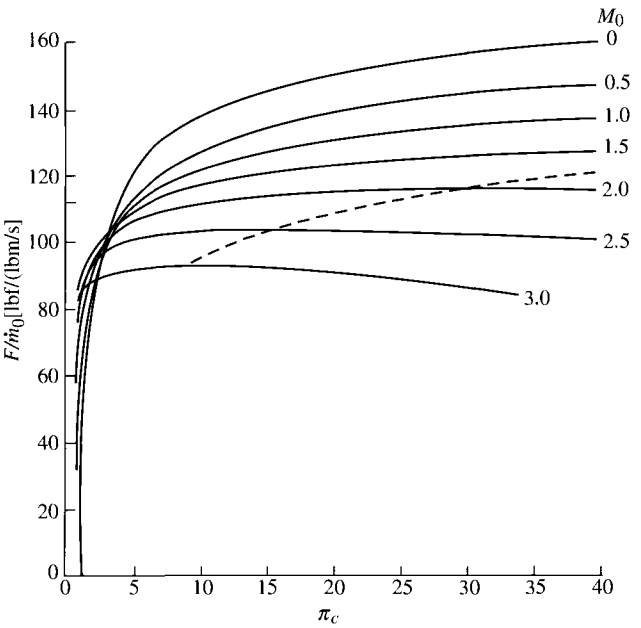

Fig. 5.14a Ideal afterburning turbojet engine performance vs compressor pressure ratio: specific thrust.

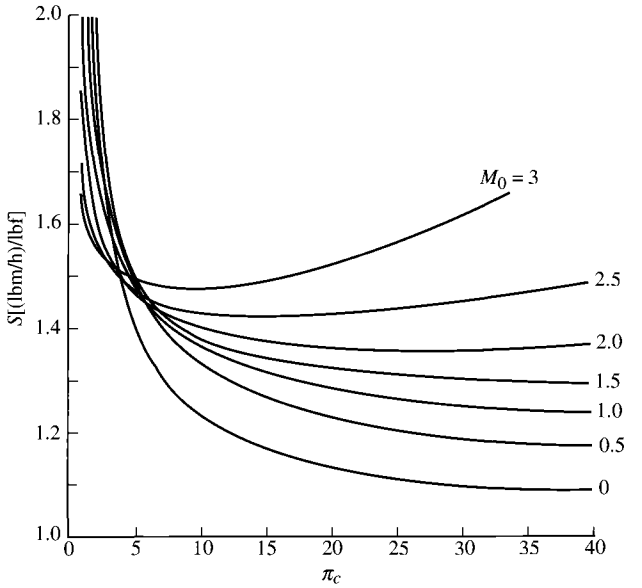

Fig. 5.14b Ideal afterburning turbojet engine performance vs compressor pressure ratio: thrust specific fuel consumption.

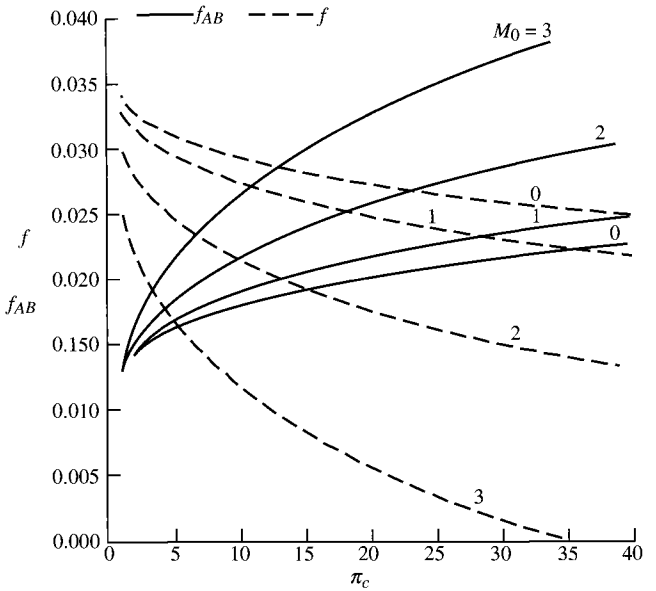

Fig. 5.14c Ideal afterburning turbojet engine performance vs compressor pressure ratio: fuel/air ratios.

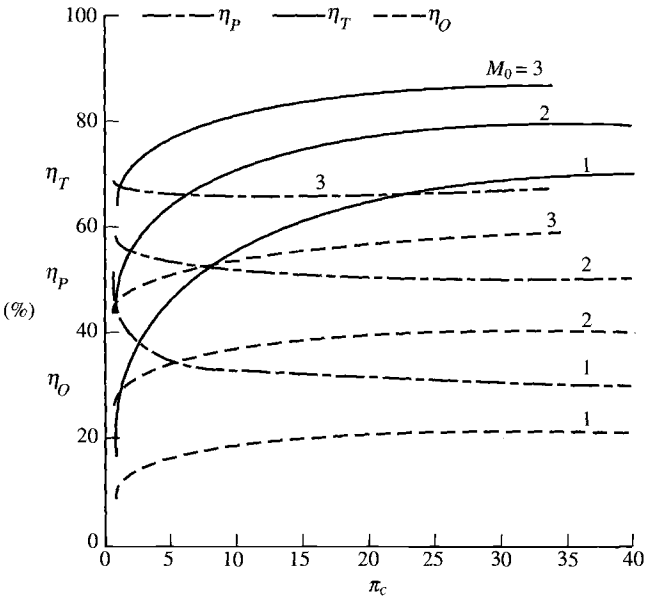

Fig. 5.14d Ideal afterburning turbojet engine performance vs compressor pressure ratio: efficiencies.

τ_c since the specific thrust depends on τ_c only through the ratio V_9/a_0 in the equation

$$\frac{F}{\dot{m}_0} = \frac{a_0}{g_c}\left(\frac{V_9}{a_0} - M_0\right)$$

We have for $(V_9/a_0)^2$, from Eq. (5.40),

$$\left(\frac{V_9}{a_0}\right)^2 = \frac{2}{\gamma - 1}\tau_{\lambda AB}\left[1 - \frac{\tau_\lambda/(\tau_r\tau_c)}{\tau_\lambda - \tau_r(\tau_c - 1)}\right]$$

Differentiating with respect to τ_c at constant M_0, τ_r, and τ_λ and setting it equal to zero, we get

$$\frac{\partial}{\partial\tau_c}\left[\left(\frac{V_9}{a_0}\right)^2\right] = \frac{2}{\gamma - 1}\tau_{\lambda AB}\frac{\partial}{\partial\tau_c}\left[1 - \frac{\tau_\lambda/(\tau_r\tau_c)}{\tau_\lambda - \tau_r(\tau_c - 1)}\right] = 0$$

Thus

$$\frac{\tau_\lambda}{\tau_r\tau_c^2}\frac{1}{\tau_\lambda - \tau_r(\tau_c - 1)} + \frac{\tau_\lambda/(\tau_r\tau_c)}{[\tau_\lambda - \tau_r(\tau_c - 1)]^2}(-\tau_r) = 0$$

or

$$\frac{1}{\tau_c} - \frac{\tau_r}{\tau_\lambda - \tau_r(\tau_c - 1)} = 0$$

which becomes

$$\tau_r\tau_c = \tau_\lambda - \tau_r(\tau_c - 1)$$

resulting in

$$\tau_{c\,\max F/\dot{m}\mathrm{AB}} = \frac{1}{2}\left(\frac{\tau_\lambda}{\tau_r} + 1\right) \tag{5.43}$$

Placing Eq. (5.43) into Eq. (5.40), we get

$$\left(\frac{V_9}{a_0}\right)^2 = \frac{2}{\gamma - 1}\tau_{\lambda\,\mathrm{AB}}\left[1 - \frac{4\tau_\lambda}{(\tau_\lambda + \tau_r)^2}\right] \tag{5.44}$$

so that

$$\frac{F}{\dot{m}_0} = \frac{a_0}{g_c}\left\{\sqrt{\frac{2}{\gamma - 1}\tau_{\lambda\,\mathrm{AB}}\left[1 - \frac{4\tau_\lambda}{(\tau_\lambda + \tau_r)^2}\right]} - M_0\right\} \tag{5.45}$$

The locus of specific thrust vs π_c and M_0 for optimum afterburning turbojets is plotted as a dashed line in Fig. 5.14a. Note that the pressure ratio giving the maximum specific thrust decreases with the flight Mach number.

5.8.4 Optimum Simple Turbojet and Optimum Afterburning Turbojet—Comparison

Figures 5.8a and 5.14a plot the thrust per unit mass flow vs the compressor pressure ratio for different values of the flight Mach number for the ideal turbojet without afterburner and the ideal turbojet with afterburner, respectively. These figures show that the thrust per unit mass flow is higher for the engine with afterburner and that the optimum compressor pressure ratio is also higher for the engine with afterburner. The thrust per unit mass flow, thrust specific fuel consumption, and compressor pressure ratio for an optimum simple and an optimum afterburning turbojet are shown vs the Mach number for representative conditions in Figs. 5.15 and 5.16. The optimum afterburning π_c and specific

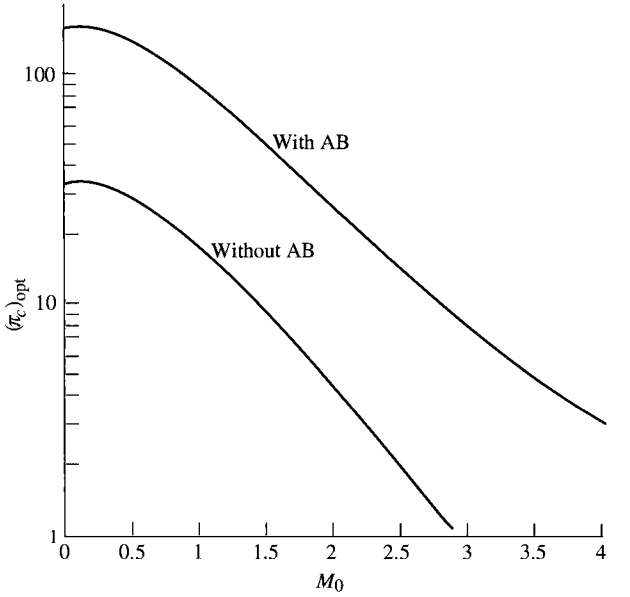

Fig. 5.15 Optimum ideal turbojet compressor pressure ratio ($\tau_\lambda = 7.5$).

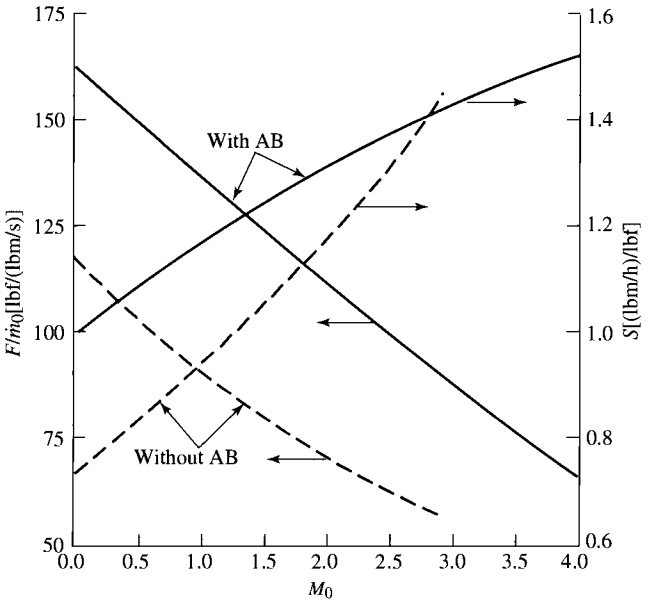

Fig. 5.16 Optimum ideal turbojet performance ($T_0 = 390°R$, $\tau_\lambda = 7.5$, $\tau_{\lambda AB} = 10$).

thrust are higher at all Mach numbers. Considering a given engine with, say, a compressor pressure ratio of 30, we see from Fig. 5.15 that it can operate optimally at Mach 2 with afterburning and near-optimum conditions subsonically without afterburning where less thrust is required and available and where the fuel consumption is much lower. Figure 5.16 shows that at $M_0 = 2.7$, the specific fuel consumption of an afterburning engine with $\pi_c = 12$ is the same as that of a simple turbojet with $\pi_c = 1.5$. From Fig. 5.16, we see that at $M_0 = 2.7$, the thrust per unit mass flow of the afterburning engine is 50% higher. Based on these data, which engine would you select for a supersonic transport (SST) to cruise at $M_0 = 2.7$?

The higher-pressure-ratio afterburning engine is the logical choice for cruise at $M_0 = 2.7$ because it provides a smaller engine with the same fuel consumption as the nonafterburning, low-pressure-ratio engine. The final choice of an engine depends on the engine's subsonic performance also.

The plots of Fig. 5.17 provide a comparison of the nonafterburning $\pi_c = 12$ and $\pi_c = 1.5$ engines at subsonic flight speeds. It is evident that the higher-pressure-ratio engine operating in the nonafterburning mode has the better subsonic performance. The higher-pressure-ratio engine is, therefore, the best choice overall.

Although our conclusions that an afterburning high-pressure-ratio ($\pi_c = 12$) turbojet engine is a proper engine for an SST are based on a simple ideal cycle analysis, they agree with practice. The Concorde uses four Olympus 593 afterburning turbojet engines (see Figs. 5.18a–5.18c) for supersonic cruise. In

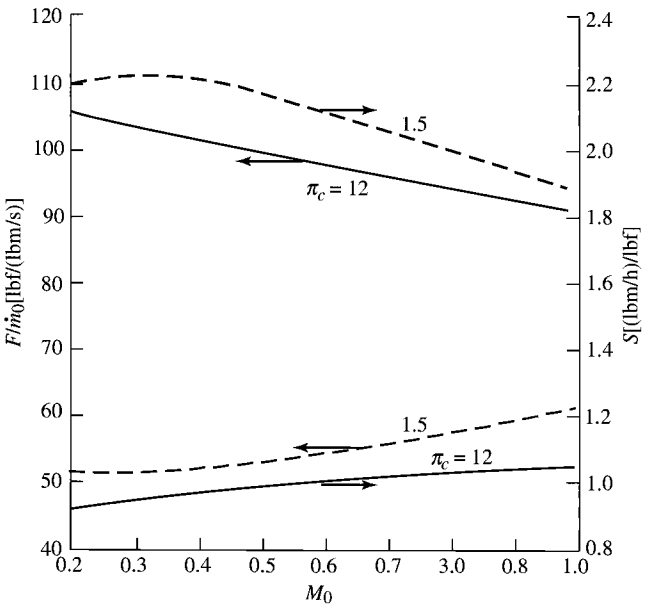

Fig. 5.17 Ideal turbojet without afterburning ($T_0 = 390°R$, $\tau_\lambda = 7.5$).

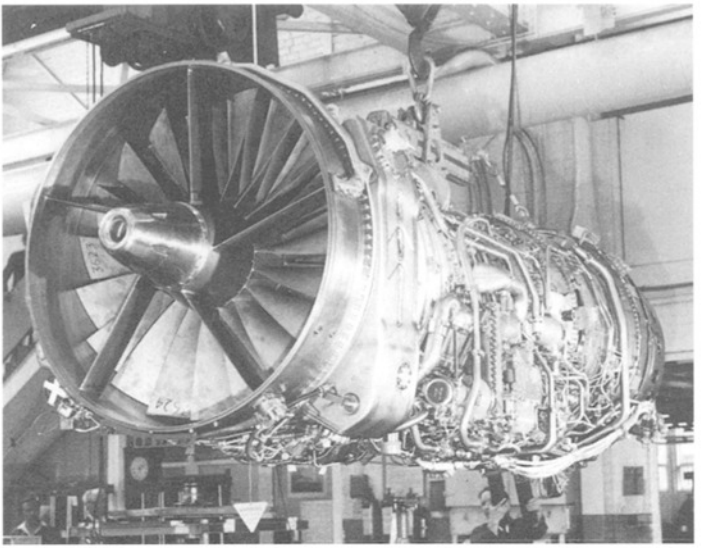

Fig. 5.18a Olympus 593 turbojet engine used in the Concorde. (Courtesy of Rolls-Royce.)

addition, the GE4 that was being developed by General Electric for the Boeing SST was an afterburning turbojet engine with a pressure ratio of about 12! This SST engine is shown in Fig. 5.19.

5.9 Ideal Turbofan

The propulsive efficiency of a simple turbojet engine can be improved by extracting a portion of the energy from the engine's gas generator to drive a ducted propeller, called a *fan*. The fan increases the propellant mass flow rate with an accompanying decrease in the required propellant exit velocity for a given thrust. Because the rate of production of "wasted" kinetic energy in the

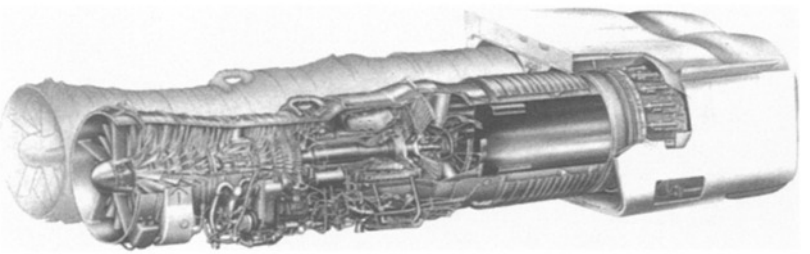

Fig. 5.18b Two Olympus engines, with thrust-reversing nozzles. (Courtesy of Rolls-Royce.)

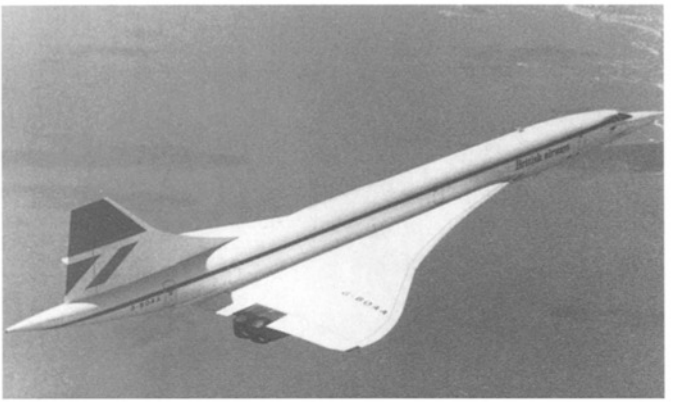

Fig. 5.18c Concorde supersonic transport. (Courtesy of Rolls-Royce.)

exit propellant gases varies as the first power with mass flow rate and as the square of the exit velocity, the net effect of increasing the mass flow rate and decreasing the exit velocity is to reduce the wasted kinetic energy production and to improve the propulsive efficiency.

Our station numbering for the turbofan cycle analysis is given in Fig. 5.20, and the *T-s* diagrams for ideal flow through the core engine and the fan are given in Figs. 5.21 and 5.22, respectively. The temperature drop through the turbine $(T_{t4} - T_{t5})$ is now greater than the temperature rise through the compressor $(T_{t3} - T_{t2})$ since the turbine drives the fan in addition to the compressor.

The fan exit is station 13, and the fan total pressure ratio and the fan total temperature ratio are π_f and τ_f, respectively. The fan flow nozzle exit is station

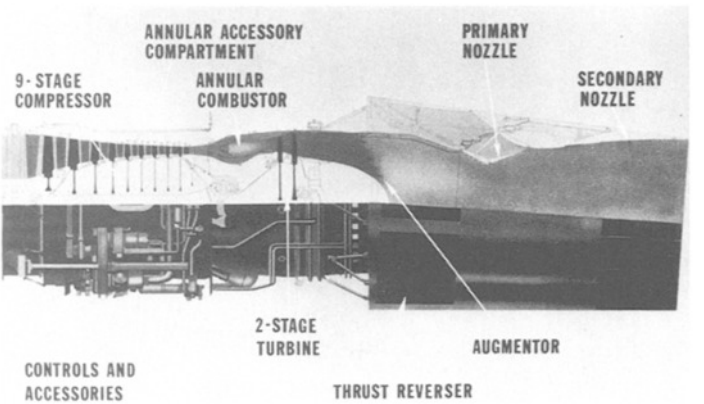

Fig. 5.19 General Electric GE4 turbojet engine (developed for Boeing SST). (Courtesy of General Electric.)

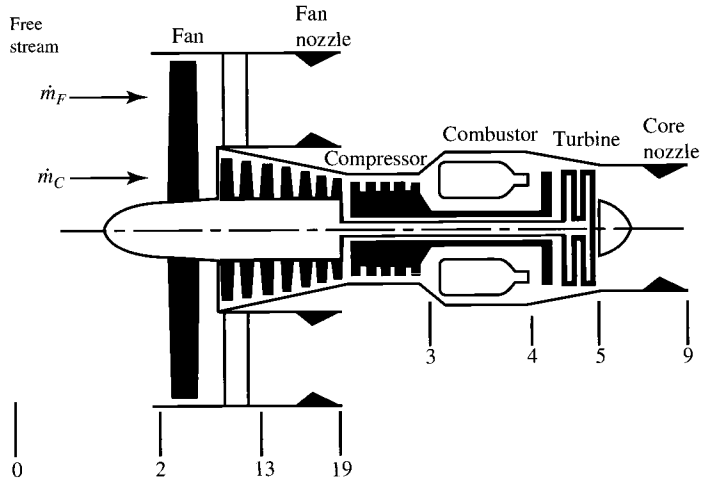

Fig. 5.20 Station numbering of a turbofan engine.

19, and the fan nozzle total pressure ratio and the fan nozzle total temperature ratio are π_{fn} and τ_{fn}, respectively. These four ratios are listed in the following:

$$\pi_f = \frac{P_{t13}}{P_{t2}} \qquad \tau_f = \frac{T_{t13}}{T_{t2}} \qquad \pi_{fn} = \frac{P_{t19}}{P_{t13}} \qquad \text{and} \qquad \tau_{fn} = \frac{T_{t19}}{T_{t13}}$$

The gas flow through the core engine is $\dot{m}_C$, and the gas flow through the fan is $\dot{m}_F$. The ratio of the fan flow to the core flow is defined as the *bypass ratio* and given the symbol alpha α. Thus

$$\text{Bypass ratio } \alpha = \frac{\dot{m}_F}{\dot{m}_C} \tag{5.46}$$

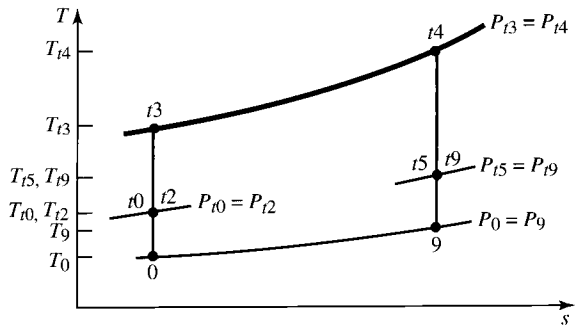

Fig. 5.21 The *T-s* diagram for core stream of ideal turbofan engine.

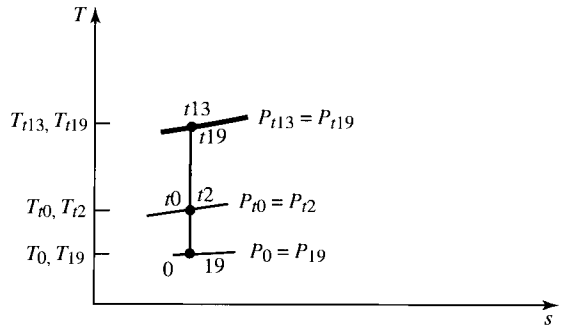

Fig. 5.22 The *T-s* diagram for fan stream of ideal turbofan engine.

The total gas flow is $\dot{m}_C + \dot{m}_F$, or $(1 + \alpha)\dot{m}_C$. We will also use $\dot{m}_0$ for the total gas flow. Thus

$$\dot{m}_0 = \dot{m}_C + \dot{m}_F = (1 + \alpha)\dot{m}_C \tag{5.47}$$

In the analysis of the ideal turbofan engine, we will assume that the mass flow rate of fuel is much less than the mass flow rate of gas through the engine core. We will also assume that both the engine core nozzle and the fan nozzle are designed so that $P_0 = P_9 = P_{19}$.

5.9.1 Cycle Analysis

Application of the steps of cycle analysis to the ideal turbofan engine of Figs. 5.20–5.22 is presented next in the order listed in Section 5.4.

Step 1: The thrust of the ideal turbofan engine is

$$F = \frac{\dot{m}_C}{g_c}(V_9 - V_0) + \frac{\dot{m}_F}{g_c}(V_{19} - V_0)$$

Thus

$$\frac{F}{\dot{m}_0} = \frac{a_0}{g_c}\frac{1}{1+\alpha}\left[\frac{V_9}{a_0} - M_0 + \alpha\left(\frac{V_{19}}{a_0} - M_0\right)\right] \tag{5.48}$$

Steps 2–4: First, the core stream of the turbofan encounters the same engine components as the ideal turbojet, and we can use its results. We have, from the analysis of the ideal turbojet,

$$\left(\frac{V_9}{a_0}\right)^2 = \frac{T_9}{T_0}M_9^2, \qquad \frac{T_9}{T_0} = \tau_b = \frac{\tau_\lambda}{\tau_r\tau_c}, \qquad \text{and} \qquad M_9^2 = \frac{2}{\gamma - 1}(\tau_r\tau_c\tau_t - 1)$$

Thus

$$\left(\frac{V_9}{a_0}\right)^2 = \frac{T_9}{T_0}M_9^2 = \frac{2}{\gamma - 1}\frac{\tau_\lambda}{\tau_r\tau_c}(\tau_r\tau_c\tau_t - 1) \tag{5.49}$$

Second, compared to the core stream, the fan stream of the turbofan contains a fan rather than a compressor and does not have either a combustor or a turbine. Thus the preceding equations for the core stream of the ideal turbofan can be adapted for the fan stream as follows:

$$\left(\frac{V_{19}}{a_0}\right)^2 = \frac{T_{19}}{T_0}M_{19}^2, \qquad T_{19} = T_0, \qquad \text{and} \qquad M_{19}^2 = \frac{2}{\gamma - 1}(\tau_r\tau_f - 1)$$

$$\left(\frac{V_{19}}{a_0}\right)^2 = M_{19}^2 = \frac{2}{\gamma - 1}(\tau_r\tau_f - 1) \tag{5.50}$$

Step 5: Application of the steady flow energy equation to the burner gives

$$\dot{m}_C c_p T_{t3} + \dot{m}_f h_{PR} = (\dot{m}_C + \dot{m}_f)c_p T_{t4}$$

We define the fuel/air ratio f in terms of the mass flow rate of air through the burner $\dot{m}_C$, and we obtain

$$f = \frac{\dot{m}_f}{\dot{m}_C} = \frac{c_p T_0}{h_{PR}}(\tau_\lambda - \tau_r\tau_c) \tag{5.51}$$

Step 6: The power out of the turbine is

$$\dot{W}_t = (\dot{m}_C + \dot{m}_f)c_p(T_{t4} - T_{t5}) \cong \dot{m}_C c_p T_{t4}(1 - \tau_t)$$

The power required to drive the compressor is

$$\dot{W}_c = \dot{m}_C c_p(T_{t3} - T_{t2}) = \dot{m}_C c_p T_{t2}(\tau_c - 1)$$

The power required to drive the fan is

$$\dot{W}_f = \dot{m}_F c_p(T_{t13} - T_{t2}) = \dot{m}_F c_p T_{t2}(\tau_f - 1)$$

Since $\dot{W}_t = \dot{W}_c + \dot{W}_f$ for the ideal turbofan, then

$$T_{t4}(1 - \tau_t) = T_{t2}(\tau_c - 1) + \alpha T_{t2}(\tau_f - 1)$$

$$\tau_t = 1 - \frac{T_{t2}}{T_{t4}}[\tau_c - 1 + \alpha(\tau_f - 1)]$$

$$\tau_t = 1 - \frac{\tau_r}{\tau_\lambda}[\tau_c - 1 + \alpha(\tau_f - 1)] \tag{5.52}$$

Step 7: Combining Eqs. (5.49) and (5.52), we get

$$\left(\frac{V_9}{a_0}\right)^2 = \frac{2}{\gamma - 1}\frac{\tau_\lambda}{\tau_r \tau_c}\left(\tau_r \tau_c \left\{1 - \frac{\tau_r}{\tau_\lambda}[\tau_c - 1 + \alpha(\tau_f - 1)]\right\} - 1\right)$$

which can be simplified to

$$\left(\frac{V_9}{a_0}\right)^2 = \frac{2}{\gamma - 1}\left\{\tau_\lambda - \tau_r[\tau_c - 1 + \alpha(\tau_f - 1)] - \frac{\tau_\lambda}{\tau_r \tau_c}\right\} \tag{5.53}$$

Thus the specific thrust of the ideal turbojet is given by Eqs. (5.48), (5.50), and (5.53).

Step 8:

$$S = \frac{\dot{m}_f}{F} = \frac{f}{F/\dot{m}_C} = \frac{f}{(\dot{m}_0/\dot{m}_C)(F/\dot{m}_0)}$$

$$S = \frac{f}{(1 + \alpha)(F/\dot{m}_0)} \tag{5.54}$$

Step 9: The thermal efficiency of an ideal turbofan engine is the same as that of an ideal turbojet engine. That is [Eq. (5.22)],

$$\eta_T = 1 - \frac{1}{\tau_r \tau_c}$$

This may seem surprising since the net power out of a turbojet is $\dot{m}_0(V_9^2 - V_0^2)/(2g_c)$, while for a turbofan it is $\dot{m}_C(V_9^2 - V_0^2)/(2g_c) + \dot{m}_F(V_{19}^2 - V_0^2)/(2g_c)$. The reason that the thermal efficiency is the same is that power extracted from the core stream of the turbofan engine is added to the bypass stream without loss in the ideal case. Thus the net power out remains the same.

One can easily show that the propulsive efficiency of the ideal turbofan engine is given by

$$\eta_P = 2\frac{V_9/V_0 - 1 + \alpha(V_{19}/V_0 - 1)}{V_9^2/V_0^2 - 1 + \alpha(V_{19}^2/V_0^2 - 1)} \tag{5.55}$$

A useful performance parameter for the turbofan engine is the ratio of the specific thrust per unit mass flow of the core stream to that of the fan stream. We give this *thrust ratio* the symbol FR and define

$$\text{FR} \equiv \frac{F_C/\dot{m}_C}{F_F/\dot{m}_F} \tag{5.56}$$

For the ideal turbofan engine, the thrust ratio FR can be expressed as

$$\text{FR} = \frac{V_9/a_0 - M_0}{V_{19}/a_0 - M_0} \tag{5.57}$$

We will discover in the analysis of optimum turbofan engines that we will want a certain thrust ratio for minimum thrust specific fuel consumption.

5.9.2 Summary of Equations—Ideal Turbofan

INPUTS:

$$M_0,\ T_0(\text{K},\ ^\circ\text{R}),\ \gamma,\ c_p\left(\frac{\text{kJ}}{\text{kg}\cdot\text{K}},\ \frac{\text{Btu}}{\text{lbm}\cdot{}^\circ\text{R}}\right),\quad h_{PR}\left(\frac{\text{kJ}}{\text{kg}},\ \frac{\text{Btu}}{\text{lbm}}\right)$$

$$T_{t4}(\text{K},\ ^\circ\text{R}),\ \pi_c,\ \pi_f,\ \alpha$$

OUTPUTS:

$$\frac{F}{\dot{m}_0}\left(\frac{\text{N}}{\text{kg/s}},\ \frac{\text{lbf}}{\text{lbm/s}}\right), f, S\left(\frac{\text{mg/s}}{\text{N}},\ \frac{\text{lbm/h}}{\text{lbf}}\right),\ \eta_T,\ \eta_P,\ \eta_O,\ \text{FR}$$

EQUATIONS:

$$R = \frac{\gamma - 1}{\gamma} c_p \tag{5.58a}$$

$$a_0 = \sqrt{\gamma R g_c T_0} \tag{5.58b}$$

$$\tau_r = 1 + \frac{\gamma - 1}{2} M_0^2 \tag{5.58c}$$

$$\tau_\lambda = \frac{T_{t4}}{T_0} \tag{5.58d}$$

$$\tau_c = (\pi_c)^{(\gamma-1)/\gamma} \tag{5.58e}$$

$$\tau_f = (\pi_f)^{(\gamma-1)/\gamma} \tag{5.58f}$$

$$\frac{V_9}{a_0} = \sqrt{\frac{2}{\gamma - 1}\left\{\tau_\lambda - \tau_r[\tau_c - 1 + \alpha(\tau_f - 1)] - \frac{\tau_\lambda}{\tau_r \tau_c}\right\}} \tag{5.58g}$$

$$\frac{V_{19}}{a_0} = \sqrt{\frac{2}{\gamma - 1}(\tau_r \tau_f - 1)} \tag{5.58h}$$

$$\frac{F}{\dot{m}_0} = \frac{a_0}{g_c}\frac{1}{1+\alpha}\left[\frac{V_9}{a_0} - M_0 + \alpha\left(\frac{V_{19}}{a_0} - M_0\right)\right] \tag{5.58i}$$

$$f = \frac{c_p T_0}{h_{PR}}(\tau_\lambda - \tau_r\tau_c) \tag{5.58j}$$

$$S = \frac{f}{(1+\alpha)(F/\dot{m}_0)} \tag{5.58k}$$

$$\eta_T = 1 - \frac{1}{\tau_r\tau_c} \tag{5.58l}$$

$$\eta_P = 2M_0\frac{V_9/a_0 - M_0 + \alpha(V_{19}/a_0 - M_0)}{V_9^2/a_0^2 - M_0^2 + \alpha(V_{19}^2/a_0^2 - M_0^2)} \tag{5.58m}$$

$$\eta_O = \eta_T\eta_P \tag{5.58n}$$

$$\text{FR} = \frac{V_9/a_0 - M_0}{V_{19}/a_0 - M_0} \tag{5.58o}$$

Example 5.4

The turbofan engine has three design variables: 1) compressor pressure ratio π_c, 2) fan pressure ratio π_f, and 3) bypass ratio α. Because this engine has two more design variables than the turbojet, this section contains many more plots of engine performance than were required for the turbojet. First, we will look at the variation of each of the three design variables for an engine that will operate at a flight Mach number of 0.9. Then we will look at the variation of design performance with flight Mach number. In all of the calculations for this section, the following values are held constant:

$$T_0 = 216.7\,\text{K}, \qquad \gamma = 1.4, \qquad c_p = 1.004\,\text{kJ/(kg}\cdot\text{K)}$$
$$h_{PR} = 42{,}800\,\text{kJ/kg}, \qquad T_{t4} = 1670\,\text{K}$$

a) Figures 5.23a–5.23e. Specific thrust and thrust specific fuel consumption are plotted vs the compressor pressure ratio for different values of the bypass ratio in Figs. 5.23a and 5.23b. The fan pressure ratio is held constant in these plots. Figure 5.23a shows that specific thrust remains essentially constant with respect to the compressor pressure ratio for values of π_c from 15 to 25, and that specific thrust decreases with increasing bypass ratio. Figure 5.23b shows that thrust-specific fuel consumption decreases with increasing compressor pressure ratio π_c and increasing bypass ratio α.

Figure 5.23c shows that the fuel/air ratio decreases with compressor pressure ratio, the thermal efficiency increases with compressor pressure ratio, and both are independent of the engine bypass ratio. From Fig. 5.23d, we can see that the propulsive efficiency increases with engine bypass ratio and varies very little with compressor pressure ratio. The overall efficiency, shown also in Fig. 5.23d, increases with both compressor pressure ratio and bypass ratio.

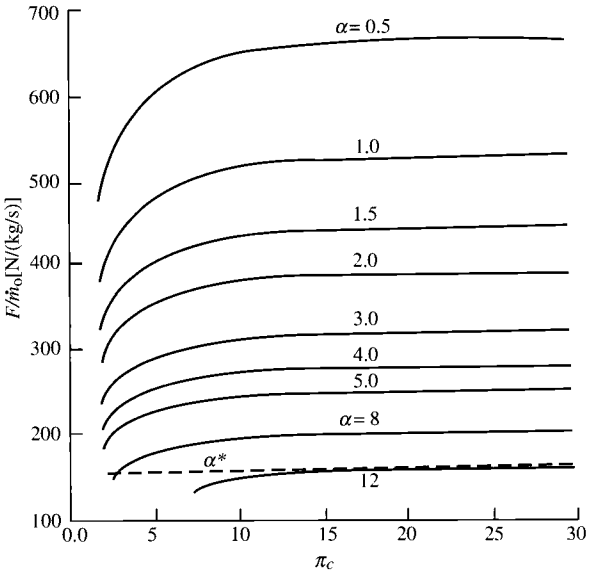

Fig. 5.23a Ideal turbofan performance vs π_c, for $\pi_f = 2$ and $M_0 = 0.9$: specific thrust.

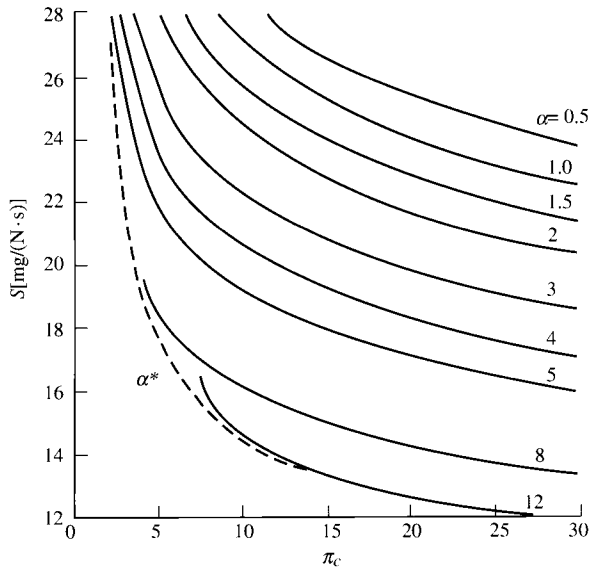

Fig. 5.23b Ideal turbofan performance vs π_c, for $\pi_f = 2$ and $M_0 = 0.9$: thrust-specific fuel consumption.

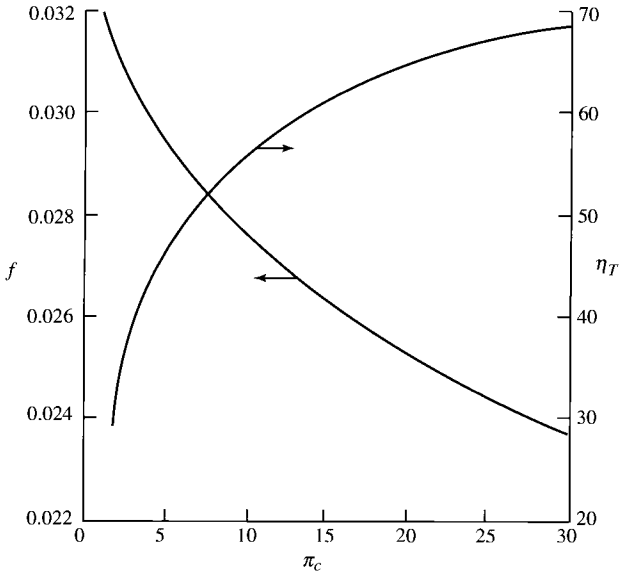

Fig. 5.23c Ideal turbofan performance vs π_c, for $\pi_f = 2$ and $M_0 = 0.9$: fuel/air ratio and thermal efficiency.

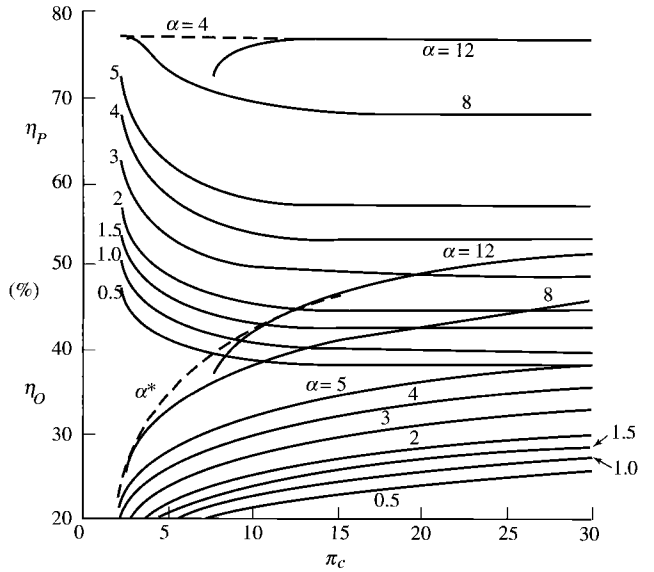

Fig. 5.23d Ideal turbofan performance vs π_c, for $\pi_f = 2$ and $M_0 = 0.9$: propulsive and overall efficiencies.

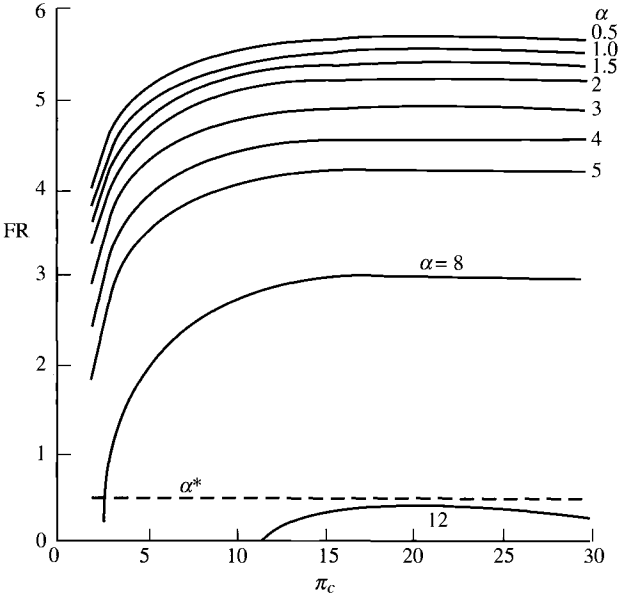

Fig. 5.23e Ideal turbofan performance vs π_c, for $\pi_f = 2$ and $M_0 = 0.9$: thrust ratio.

The thrust ratio is plotted vs compressor pressure ratio and bypass ratio in Fig. 5.23e. As can be seen, the thrust ratio decreases with increasing bypass ratio and varies very little with compressor pressure ratio.

b) Figures 5.24a–5.24e. Specific thrust and thrust-specific fuel consumption are plotted vs the compressor pressure ratio π_c for different values of the fan pressure ratio π_f. The bypass ratio α is held constant in these plots. Figure 5.24a shows that the specific thrust remains essentially constant with respect to the compressor pressure ratio for values of π_c from 15 to 25, and that the specific thrust has a maximum with respect to the fan pressure ratio π_f Figure 5.24b shows that thrust-specific fuel consumption decreases with increasing compressor pressure ratio π_c and that S has a minimum with respect to fan pressure ratio π_f. We will look at this optimum fan pressure ratio in more detail in another section of this chapter.

Propulsive and overall efficiencies are plotted vs compressor pressure ratio and fan pressure ratio in Figs. 5.24c and 5.24d. Figure 5.24c shows that propulsive efficiency increases with fan pressure ratio until a value of $\pi_f = 3.5$ and then decreases. There is a fan pressure ratio giving maximum propulsive efficiency. Propulsive efficiency is essentially constant for values of the compressor pressure ratio above 15. Also from Fig. 5.24d, we can see that overall efficiency increases with compressor pressure ratio and increases with fan pressure ratio until a value of $\pi_f = 3.5$ and then decreases. There is a fan pressure ratio giving maximum overall efficiency.

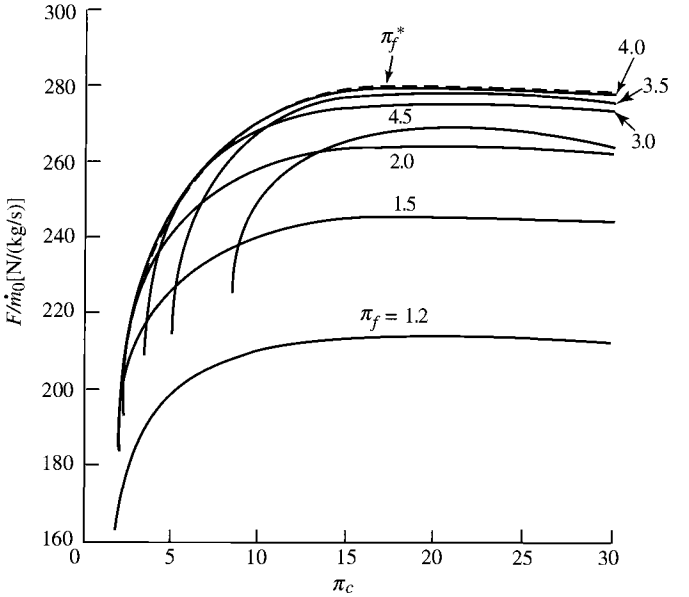

Fig. 5.24a Ideal turbofan performance vs π_c, for $\alpha = 5$ for $M_0 = 0.9$: specific thrust.

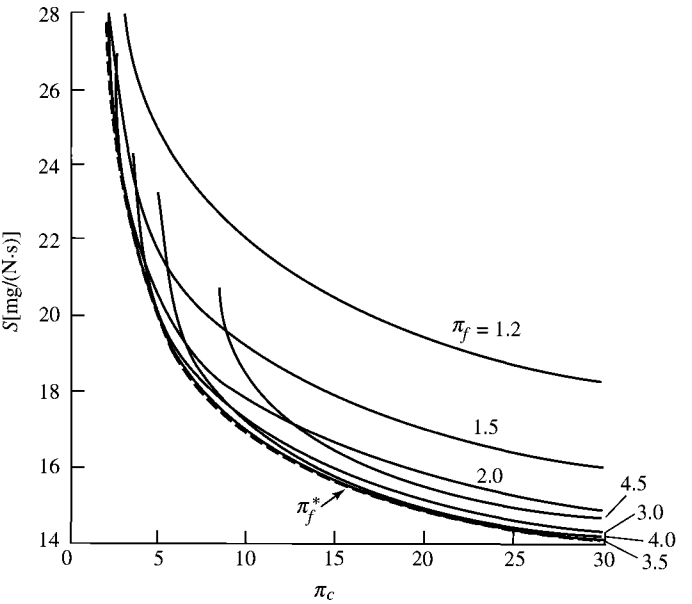

Fig. 5.24b Ideal turbofan performance vs π_c, for $\alpha = 5$ and $M_0 = 0.9$: thrust-specific fuel consumption.

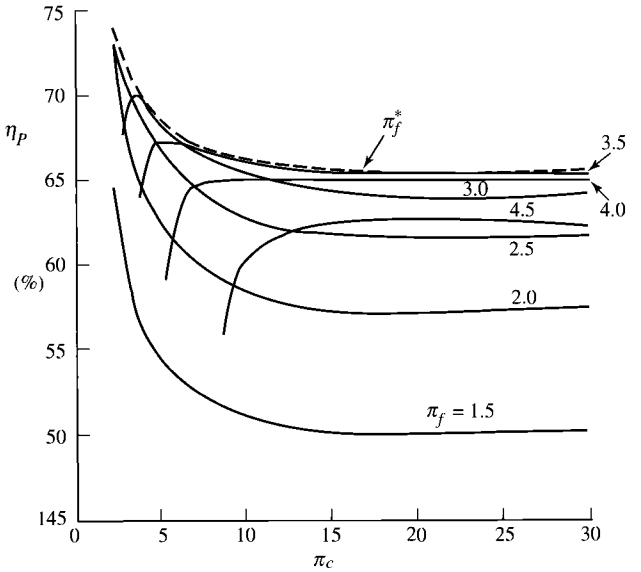

Fig. 5.24c Ideal turbofan performance vs π_c, for $\alpha = 5$ and $M_0 = 0.9$: propulsive efficiency.

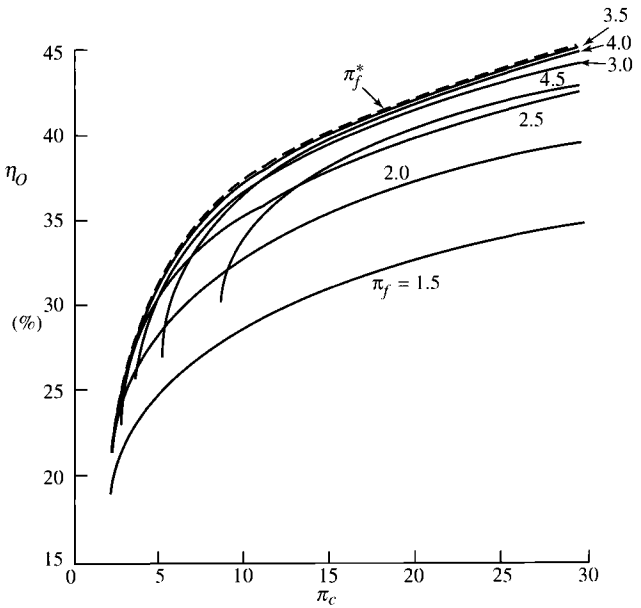

Fig. 5.24d Ideal turbofan performance vs π_c, for $\alpha = 5$ and $M_0 = 0.9$: overall efficiency.

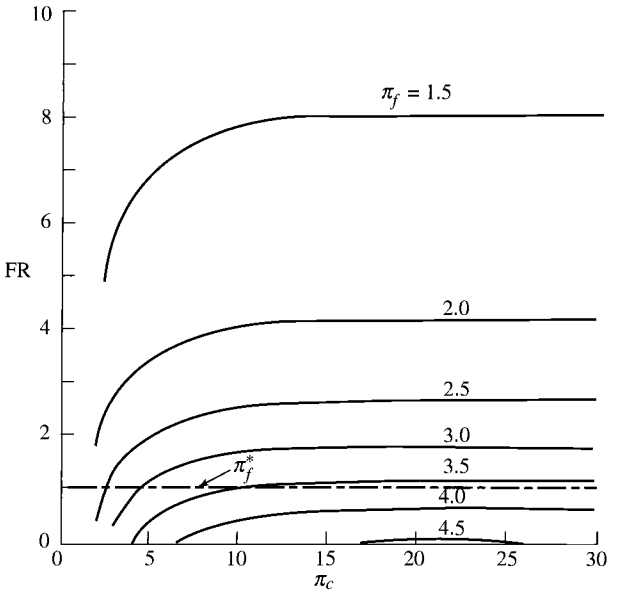

Fig. 5.24e Ideal turbofan performance vs π_c, for $\alpha = 5$ and $M_0 = 0.9$: thrust ratio.

The thrust ratio FR is plotted vs compressor pressure ratio and fan pressure ratio in Fig. 5.24e. As can be seen, the thrust ratio decreases with increasing fan pressure ratio and varies very little with compressor pressure ratio.

c) Figures 5.25a–5.25d. Specific thrust, thrust-specific fuel consumption, propulsive efficiency, and thrust ratio are plotted vs fan pressure ratio for different values of the bypass ratio in Figs. 5.25a, 5.25b, 5.25c, and 5.25d, respectively. The compressor pressure ratio is held constant in these plots. Figures 5.25a and 5.25b show there is an optimum fan pressure ratio for each bypass ratio that will maximize specific thrust while minimizing fuel consumption. Also Fig. 5.25c shows the optimum fan pressure ratio corresponds to maximum propulsive efficiency. We will look at this optimum fan pressure ratio in more detail in another section of this chapter. Figure 5.25d shows that thrust ratio decreases with increasing fan pressure ratio.

d) Figures 5.26a–5.26d. Specific thrust and thrust-specific fuel consumption are plotted vs the bypass ratio for different values of the fan pressure ratio in Figs. 5.26a and 5.26b. The compressor pressure ratio is held constant in these plots. Figure 5.26a shows the decreasing trend in specific thrust with increasing bypass ratio that is characteristic of turbofan engines. Figure 5.26b shows that there is an optimum bypass ratio for each fan pressure ratio that will minimize

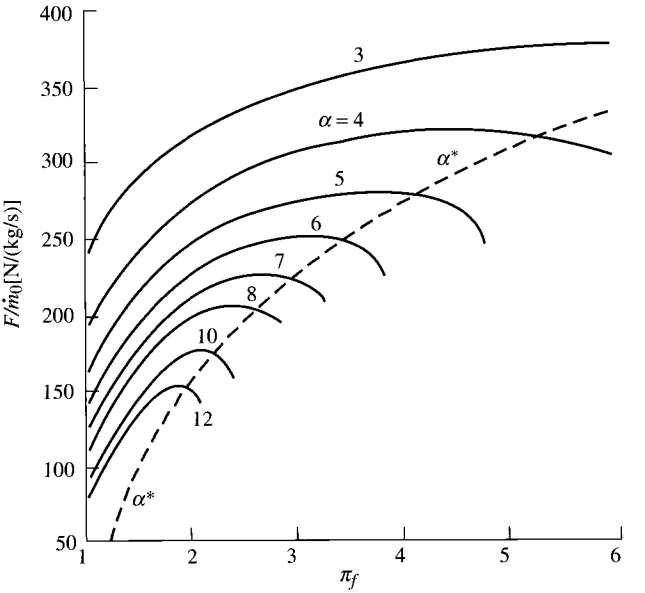

Fig. 5.25a Ideal turbofan performance vs π_f, for $\pi_c = 24$ and $M_0 = 0.9$: specific thrust.

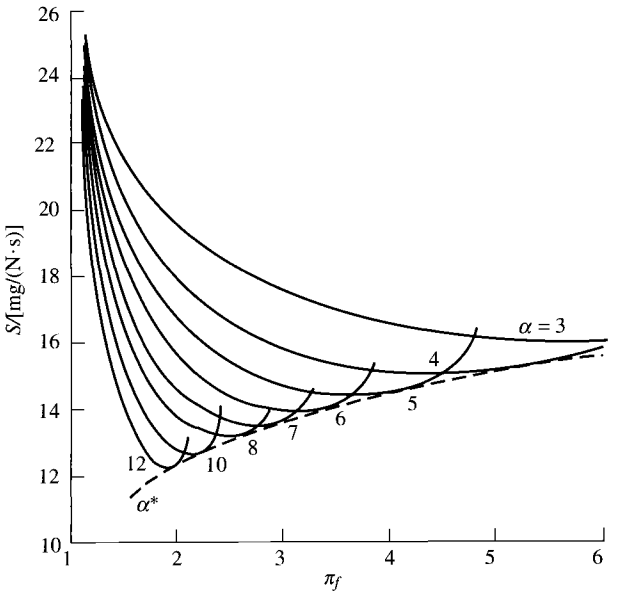

Fig. 5.25b Ideal turbofan performance vs π_f, for $\pi_c = 24$ and $M_0 = 0.9$: thrust-specific fuel consumption.

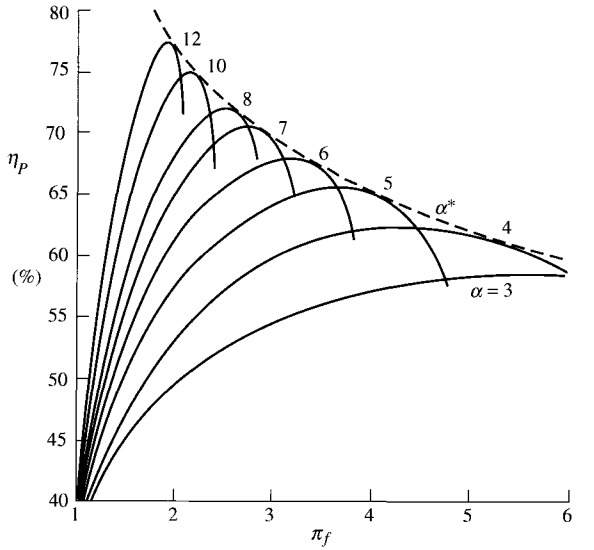

Fig. 5.25c Ideal turbofan performance vs π_f, for $\pi_c = 24$ and $M_0 = 0.9$: propulsive efficiency.

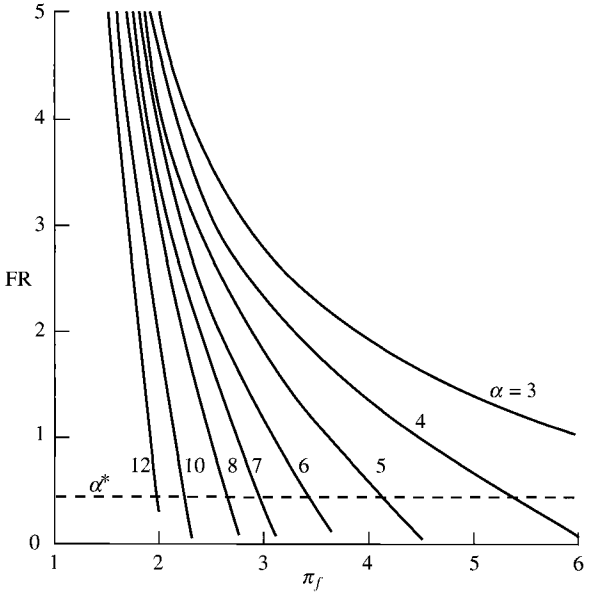

Fig. 5.25d Ideal turbofan performance vs π_f, for $\pi_c = 24$ and $M_0 = 0.9$: thrust ratio.

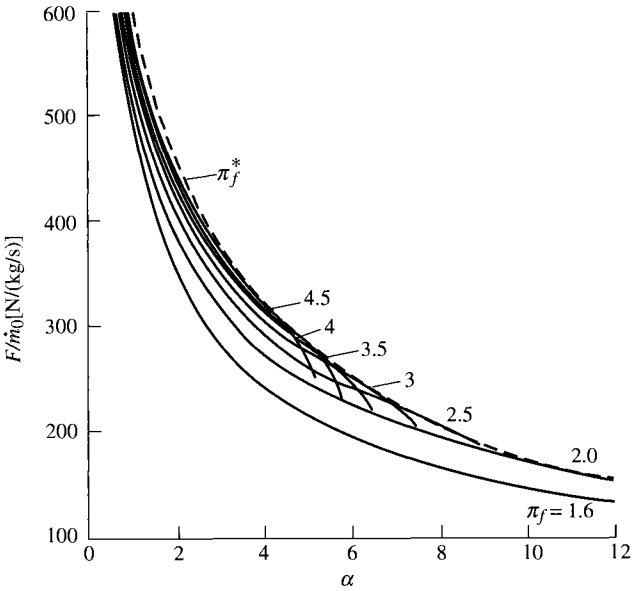

Fig. 5.26a Ideal turbofan performance vs α, for $\pi_c = 24$ and $M_0 = 0.9$: specific thrust.

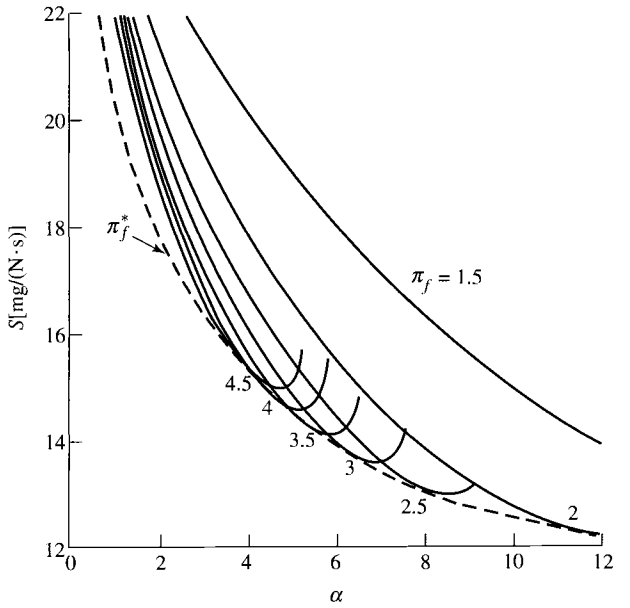

Fig. 5.26b Ideal turbofan performance vs α, for $\pi_c = 24$ and $M_0 = 0.9$: thrust-specific fuel consumption.

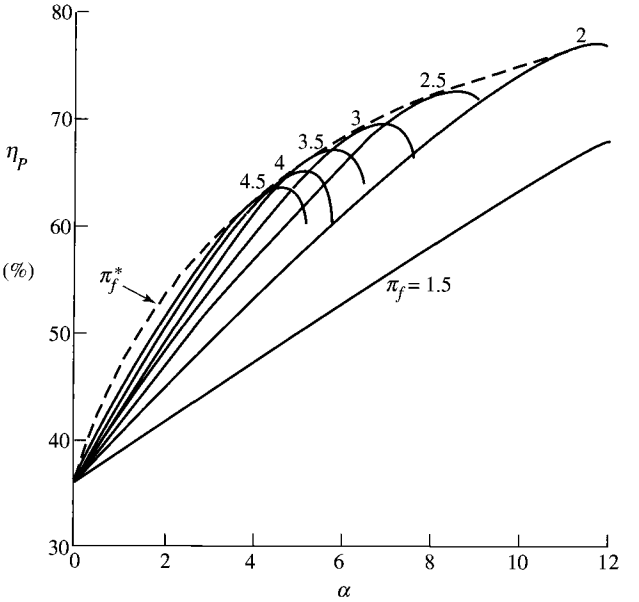

Fig. 5.26c Ideal turbofan performance vs α, for $\pi_c = 24$ and $M_0 = 0.9$: propulsive efficiency.

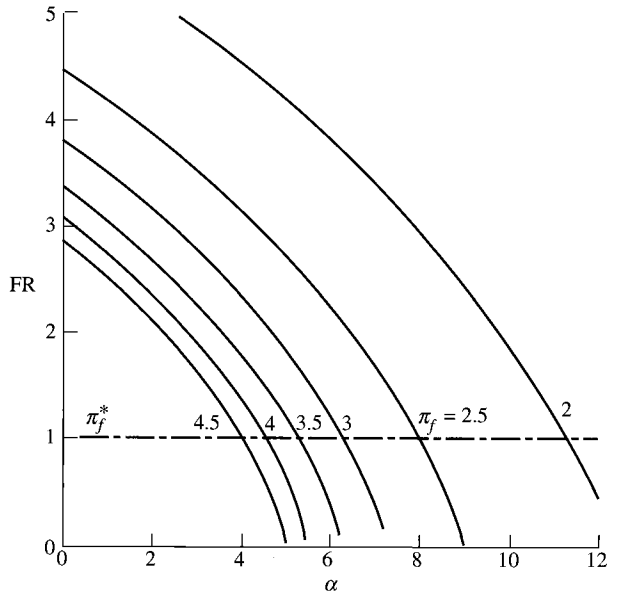

Fig. 5.26d Ideal turbofan performance vs α, for $\pi_c = 24$ and $M_0 = 0.9$: thrust ratio.

fuel consumption. We will look at this optimum bypass ratio in greater detail in another section of this chapter.

Propulsive efficiency and thrust ratio are plotted vs the bypass ratio in Figs. 5.26c and 5.26d, respectively. Figure 5.26c shows there is an optimum bypass ratio for each fan pressure ratio that will maximize propulsive efficiency. Figure 5.26d shows that thrust ratio decreases with both increasing bypass ratio and increasing fan pressure ratio.

e) Figures 5.27a–5.28e. Specific thrust and the specific fuel consumption are plotted vs the flight Mach number for different values of the bypass ratio in Figs. 5.27a, 5.27b, 5.28a, and 5.28b. The compressor pressure ratio has a value of 24 for all four plots, and the fan pressure ratio is held constant at a value of 2 for Figs. 5.27a and 5.27b and at a value of 3 for Figs. 5.28a and 5.28b. Figures 5.27a and 5.28a show that specific thrust decreases with increasing flight Mach number and with increasing bypass ratio. These four figures also show that the high-bypass-ratio engines are limited to lower flight Mach numbers and that a low-bypass-ratio engine is required for the higher flight Mach numbers.

Propulsive, thermal, and overall efficiencies are plotted vs the flight Mach number for different values of the bypass ratio in Figs. 5.27c, 5.27d, 5.28c, and 5.28d. We can see that propulsive efficiency increases with flight Mach number and that there is an optimum bypass ratio for each flight Mach number that gives maximum propulsive and overall efficiencies.

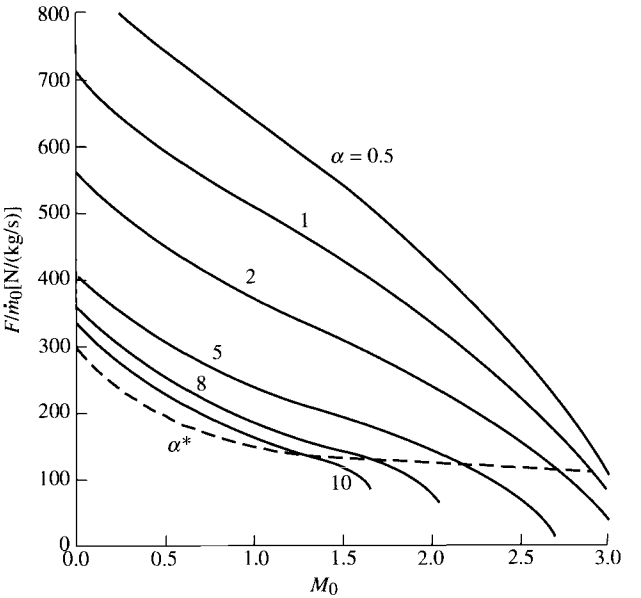

Fig. 5.27a Ideal turbofan performance vs M_0, for $\pi_c = 24$ and $\pi_f = 2$: specific thrust.

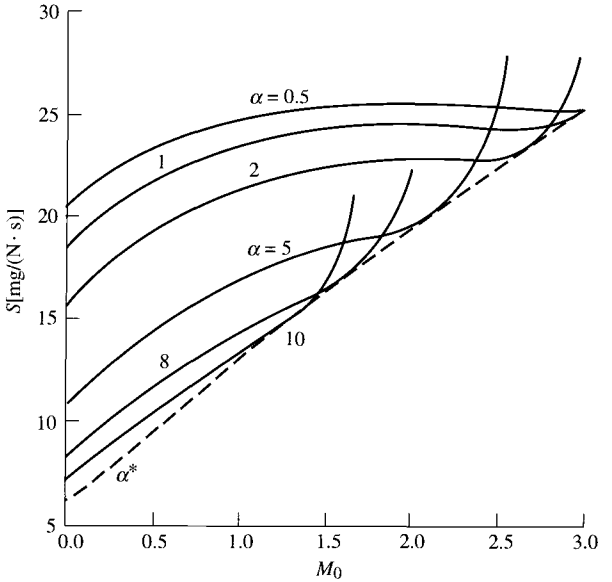

Fig. 5.27b Ideal turbofan performance vs M_0, for $\pi_c = 24$ and $\pi_f = 2$: thrust-specific fuel consumption.

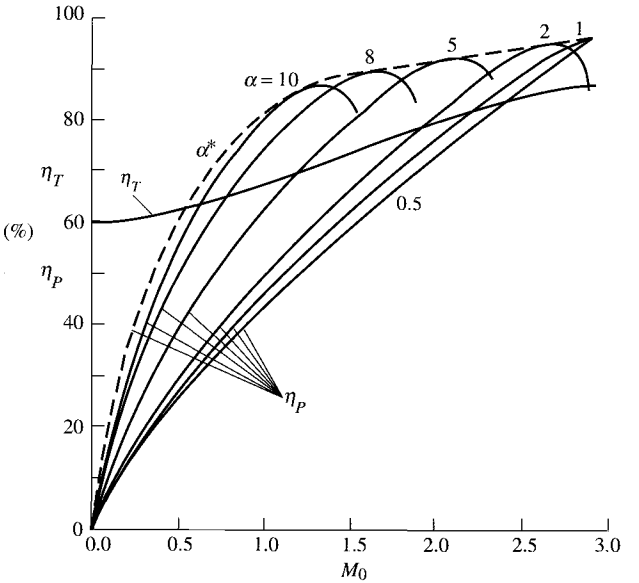

Fig. 5.27c Ideal turbofan performance vs M_0, for $\pi_c = 24$ and $\pi_f = 2$: thermal and propulsive efficiencies.

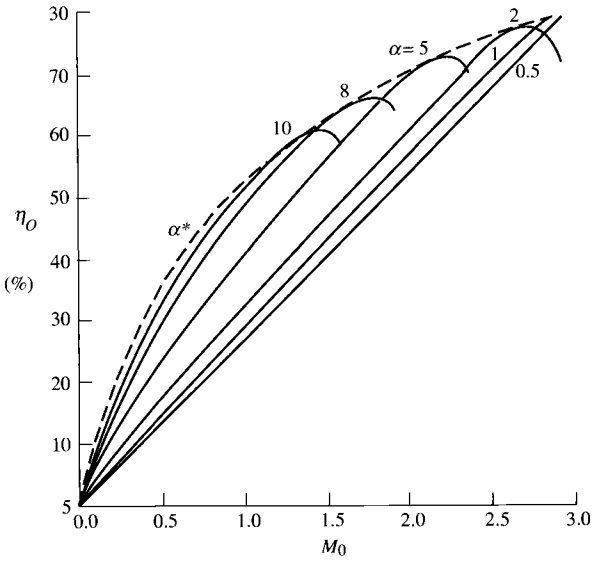

Fig. 5.27d Ideal turbofan performance vs M_0, for $\pi_c = 24$ and $\pi_f = 2$: overall efficiency.

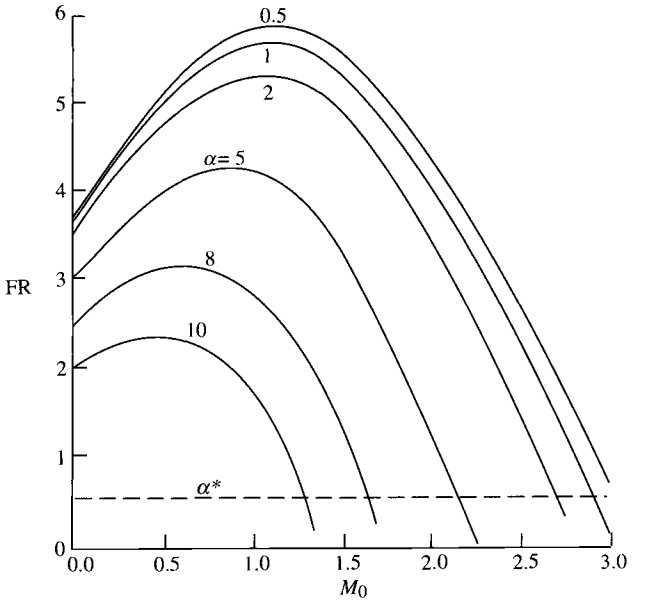

Fig. 5.27e Ideal turbofan performance vs M_0, for $\pi_c = 24$ and $\pi_f = 2$: thrust ratio.

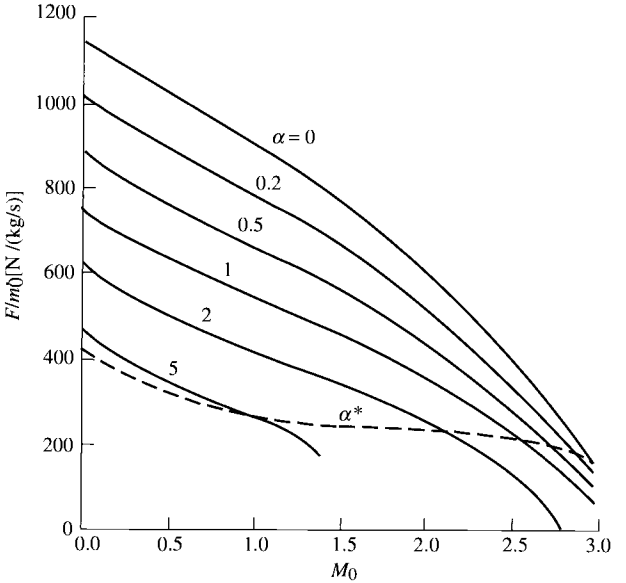

Fig. 5.28a Ideal turbofan performance vs M_0, for $\pi_c = 24$ and $\pi_f = 3$: specific thrust.

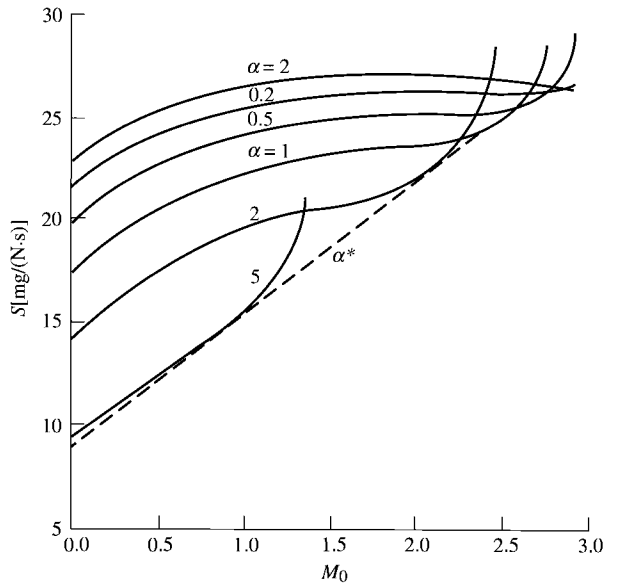

Fig. 5.28b Ideal turbofan performance vs M_0, for $\pi_c = 24$ and $\pi_f = 3$: thrust-specific fuel consumption.

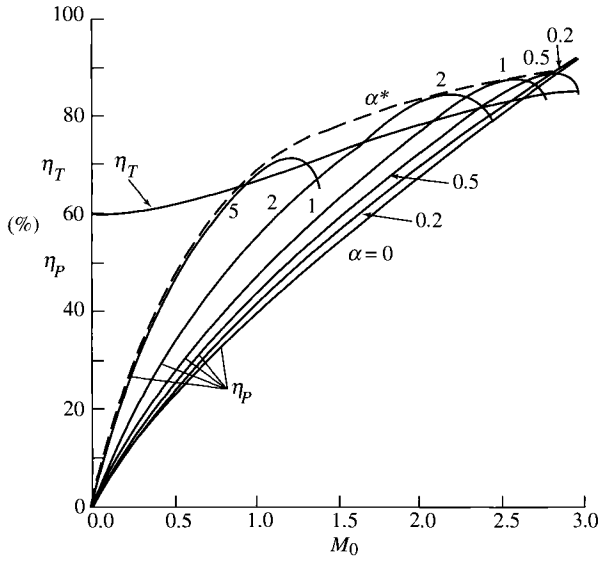

Fig. 5.28c Ideal turbofan performance vs M_0, for $\pi_c = 24$ and $\pi_f = 3$: thermal and propulsive efficiencies.

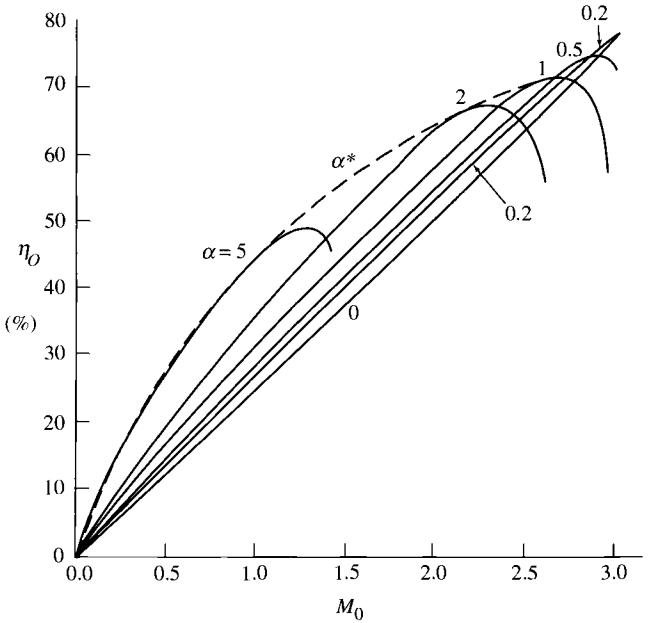

Fig. 5.28d Ideal turbofan performance vs M_0, for $\pi_c = 24$ and $\pi_f = 3$: overall efficiency.

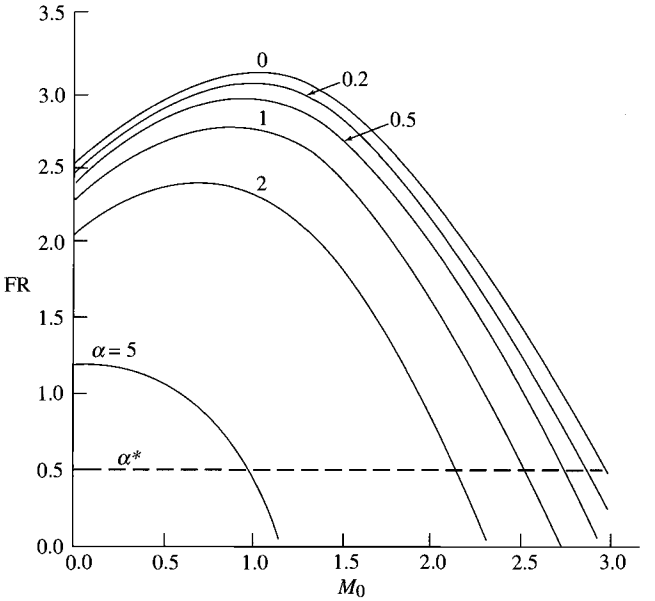

Fig. 5.28e Ideal turbofan performance vs M_0, for $\pi_c = 24$ and $\pi_f = 3$: thrust ratio.

The thrust ratio is plotted vs flight Mach number for different values of the bypass ratio in Figs. 5.27e and 5.28e. These plots show that thrust ratio decreases with increasing bypass ratio and generally decreases with increasing flight Mach number.

5.10 Ideal Turbofan with Optimum Bypass Ratio

For a given set of flight conditions T_0 and M_0 and design limit τ_λ, there are three design variables: π_c, π_f, and α. In Figs. 5.23a–5.23e and 5.24a–5.24e, we can see that by increasing the compressor ratio π_c we can increase the thrust per unit mass flow and decrease the thrust specific fuel consumption. For the data used in these figures, increases in the compressor pressure ratio above a value of 20 do not increase the thrust per unit mass flow but do decrease the thrust specific fuel consumption. In Figs. 5.25a–5.25d, we can see that an optimum fan pressure ratio exists for all other parameters fixed. This optimum fan pressure ratio gives both the maximum thrust per unit mass flow and minimum thrust specific fuel consumption. In Figs. 5.26a–5.26d, we see that an optimum bypass ratio exists for all other parameters fixed. This optimum bypass ratio gives the minimum thrust specific fuel consumption. We will look at this optimum bypass ratio first. The optimum fan pressure ratio will be analyzed in the next section of this chapter.

5.10.1 Optimum Bypass Ratio α^*

When Eq. (5.58j) for the fuel/air ratio and Eq. (5.58i) for specific thrust are inserted into the equation for specific fuel consumption [Eq. (5.58k)], an

expression in terms of the bypass ratio α and other prescribed variables results. For a given set of such prescribed variables (τ_r, π_c, π_f, τ_λ, V_0), we may locate the minimum S by taking the partial derivative of S with respect to the bypass ratio α. Because the fuel/air ratio f is not a function of the bypass ratio, we have

$$S = \frac{f}{(1+\alpha)(F/\dot{m}_0)}$$

$$\frac{\partial S}{\partial \alpha} = \frac{\partial}{\partial \alpha}\left[\frac{f}{(1+\alpha)(F/\dot{m}_0)}\right] = 0$$

$$\frac{\partial S}{\partial \alpha} = \frac{-f}{[(1+\alpha)(F/\dot{m}_0)]^2}\frac{\partial}{\partial \alpha}\left[(1+\alpha)\left(\frac{F}{\dot{m}_0}\right)\right] = 0$$

Thus $\partial S/\partial \alpha = 0$ is satisfied by

$$\frac{\partial}{\partial \alpha}\left[\frac{g_c}{V_0}(1+\alpha)\left(\frac{F}{\dot{m}_0}\right)\right] = 0$$

where, from Eq. (5.48),

$$\frac{g_c}{V_0}(1+\alpha)\left(\frac{F}{\dot{m}_0}\right) = \frac{V_9}{V_0} - 1 + \alpha\left(\frac{V_{19}}{V_0} - 1\right)$$

Then the optimum bypass ratio is given by

$$\frac{\partial}{\partial \alpha}\left[\frac{V_9}{V_0} - 1 + \alpha\left(\frac{V_{19}}{V_0} - 1\right)\right] = \frac{\partial}{\partial \alpha}\left(\frac{V_9}{V_0}\right) + \frac{V_{19}}{V_0} - 1 = 0. \tag{i}$$

However,

$$\frac{1}{2V_9/V_0}\frac{\partial}{\partial \alpha}\left[\left(\frac{V_9}{V_0}\right)^2\right] = \frac{\partial}{\partial \alpha}\left(\frac{V_9}{V_0}\right)$$

Thus Eq. (i) becomes

$$\frac{1}{2V_9/V_0}\frac{\partial}{\partial \alpha}\left[\left(\frac{V_9}{V_0}\right)^2\right] + \frac{V_{19}}{V_0} - 1 = 0 \tag{ii}$$

Since

$$\left(\frac{V_9}{V_0}\right)^2 = \frac{1}{M_0^2}\left(\frac{V_9}{a_0}\right)^2 = \frac{1}{[(\gamma-1)/2](\tau_r-1)}\left(\frac{V_9}{a_0}\right)^2$$
$$= \frac{\tau_\lambda - \tau_r[\tau_c - 1 + \alpha(\tau_f - 1)] - \tau_\lambda/(\tau_r\tau_c)}{\tau_r - 1}$$

then, using Eq. (5.53),

$$\frac{\partial}{\partial\alpha}\left[\left(\frac{V_9}{V_0}\right)^2\right] = \frac{\partial}{\partial\alpha}\left\{\frac{\tau_\lambda - \tau_r[\tau_c - 1 + \alpha(\tau_f - 1)] - \tau_\lambda/(\tau_r\tau_c)}{\tau_r - 1}\right\}$$

giving

$$\frac{\partial}{\partial\alpha}\left[\left(\frac{V_9}{V_0}\right)^2\right] = -\frac{\tau_r(\tau_f - 1)}{\tau_r - 1} \tag{iii}$$

Since, from Eq. (5.50),

$$\left(\frac{V_{19}}{V_0}\right)^2 = \frac{1}{M_0^2}\left(\frac{V_{19}}{a_0}\right)^2 = \frac{1}{[(\gamma-1)/2](\tau_r-1)}\left(\frac{V_{19}}{a_0}\right)^2 = \frac{\tau_r\tau_f - 1}{\tau_r - 1} \tag{iv}$$

then Eqs. (iii) and (iv), substituted into Eq. (ii), give

$$\frac{1}{2V_9/V_0}\left[-\frac{\tau_r(\tau_f - 1)}{\tau_r - 1}\right] + \sqrt{\frac{\tau_r\tau_f - 1}{\tau_r - 1}} - 1 = 0$$

Substitution of the preceding equation for V_9/V_0, and denoting the optimum bypass ratio as α^*, gives

$$\frac{1}{2}\frac{-\tau_r(\tau_f - 1)}{\sqrt{\{\tau_\lambda - \tau_r[\tau_c - 1 + \alpha^*(\tau_f - 1)] - \tau_\lambda/(\tau_r\tau_c)\}/(\tau_r - 1)}} + \sqrt{\frac{\tau_r\tau_f - 1}{\tau_r - 1}} - 1 = 0$$

or

$$\frac{1}{2}\frac{\tau_r(\tau_f - 1)}{\sqrt{\{\tau_\lambda - \tau_r[\tau_c - 1 + \alpha^*(\tau_f - 1)] - \tau_\lambda/(\tau_r\tau_c)\}/(\tau_r - 1)}} = \sqrt{\frac{\tau_r\tau_f - 1}{\tau_r - 1}} - 1$$

Squaring both sides, we have

$$\frac{1}{4}\frac{[\tau_r(\tau_f - 1)]^2}{\{\tau_\lambda - \tau_r[\tau_c - 1 + \alpha^*(\tau_f - 1)] - \tau_\lambda/(\tau_r\tau_c)\}/(\tau_r - 1)} = \left(\sqrt{\frac{\tau_r\tau_f - 1}{\tau_r - 1}} - 1\right)^2$$

or

$$\frac{1}{4}\frac{[\tau_r(\tau_f-1)]^2}{[\sqrt{(\tau_r\tau_f-1)/(\tau_r-1)}-1]^2}=\frac{\tau_\lambda-\tau_r[\tau_c-1+\alpha^*(\tau_f-1)]-\tau_\lambda/(\tau_r\tau_c)}{\tau_r-1} \quad \text{(v)}$$

An expression for the bypass ratio giving the minimum fuel consumption is obtained by solving Eq. (v) for α^*. Thus

$$\alpha^*=\frac{\tau_r-1}{\tau_r(\tau_f-1)}\left[\frac{\tau_\lambda-\tau_r(\tau_c-1)-\tau_\lambda/(\tau_r\tau_c)}{\tau_r-1}-\frac{1}{4}\left(\sqrt{\frac{\tau_r\tau_f-1}{\tau_r-1}}+1\right)^2\right]$$

or

$$\alpha^*=\frac{1}{\tau_r(\tau_f-1)}\left[\tau_\lambda-\tau_r(\tau_c-1)-\frac{\tau_\lambda}{\tau_r\tau_c}-\frac{1}{4}(\sqrt{\tau_r\tau_f-1}+\sqrt{\tau_r-1})^2\right] \quad (5.59)$$

Now note that we may write

$$\frac{\tau_r(\tau_f-1)}{\tau_r-1}=\frac{\tau_r\tau_f-\tau_r+1-1}{\tau_r-1}=\frac{\tau_r\tau_f-1}{\tau_r-1}-1$$

So then Eq. (v) becomes

$$\frac{1}{4}\left[\frac{\left(\sqrt{\frac{\tau_r\tau_f-1}{\tau_r-1}}\right)^2-1}{\sqrt{\frac{\tau_r\tau_f-1}{\tau_r-1}}-1}\right]^2=\frac{\tau_\lambda-\tau_r[\tau_c-1+\alpha^*(\tau_f-1]-\frac{\tau_\lambda}{\tau_r\tau_c}}{\tau_r-1}$$

Taking the square root of both sides of this equation gives

$$\frac{1}{2}\left(\sqrt{\frac{\tau_r\tau_f-1}{\tau_r-1}}+1\right)=\sqrt{\frac{\tau_\lambda-\tau_r[\tau_c-1+\alpha^*(\tau_f-1)]-\tau_\lambda/(\tau_r\tau_c)}{\tau_r-1}}$$

or

$$\frac{1}{2}\left(\sqrt{\frac{\tau_r\tau_f-1}{\tau_r-1}}-1\right)=\sqrt{\frac{\tau_\lambda-\tau_r[\tau_c-1+\alpha^*(\tau_f-1)]-\tau_\lambda/(\tau_r\tau_c)}{\tau_r-1}}-1 \quad \text{(vi)}$$

Noting from Eqs. (5.50) and (5.53) that the term within the square root on the left side of the equals sign is the velocity ratio V_{19}/V_0, and that the term within the

square root on the right side is the velocity ratio V_9/V_0, we see that Eq. (vi) becomes

$$\frac{1}{2}\left(\frac{V_{19}}{V_0} - 1\right) = \frac{V_9}{V_0} - 1 \qquad \text{or} \qquad V_9 - V_0 = \frac{1}{2}(V_{19} - V_0)$$

Thus

$$\text{FR} = \frac{V_9 - V_0}{V_{19} - V_0} = \frac{1}{2} \tag{5.60}$$

We thus note from Eq. (5.60) that when the bypass ratio is chosen to give the minimum specific fuel consumption, the thrust per unit mass flow of the engine core is one-half that of the fan. Thus the thrust ratio of an optimum-bypass-ratio ideal turbofan is 0.5. Using this fact, we may write the equation for the specific thrust simply as

$$\left(\frac{F}{\dot{m}_0}\right)_{\alpha^*} = \frac{a_0}{g_c}\frac{1 + 2\alpha^*}{2(1 + \alpha^*)}\left[\sqrt{\frac{2}{\gamma - 1}(\tau_r\tau_f - 1)} - M_0\right] \tag{5.61}$$

where α^* is obtained from Eq. (5.59).

One can easily show that the propulsive efficiency at the optimum bypass ratio is given by

$$(\eta_P)_{\min S} = \frac{4(1 + 2\alpha^*)V_0}{(3 + 4\alpha^*)V_0 + (1 + 4\alpha^*)V_{19}} \tag{5.62}$$

5.10.2 Summary of Equations—Optimum-Bypass-Ratio Ideal Turbofan

INPUTS:

$$M_0,\ T_0(\text{K, °R}),\ \gamma,\ c_p\left(\frac{\text{kJ}}{\text{kg} \cdot \text{K}}, \frac{\text{Btu}}{\text{lbm} \cdot \text{°R}}\right),\ h_{PR}\left(\frac{\text{kJ}}{\text{kg}}, \frac{\text{Btu}}{\text{lbm}}\right),$$

$$T_{t4}(\text{K, °R}),\ \pi_c,\ \pi_f$$

OUTPUTS:

$$\frac{F}{\dot{m}_0}\left(\frac{N}{\text{kg/s}}, \frac{\text{lbf}}{\text{lbm/s}}\right),\ f,\ S\left(\frac{\text{mg/s}}{\text{N}}, \frac{\text{lbm/h}}{\text{lbf}}\right),\ \eta_T,\ \eta_P,\ \eta_O,\ \alpha^*$$

EQUATIONS:

Equations (5.58a–5.58h) plus

$$\alpha^* = \frac{1}{\tau_r(\tau_f - 1)}\left[\tau_\lambda - \tau_r(\tau_c - 1) - \frac{\tau_\lambda}{\tau_r \tau_c} - \frac{1}{4}(\sqrt{\tau_r \tau_f - 1} + \sqrt{\tau_r - 1})^2\right] \tag{5.63a}$$

$$\frac{F}{\dot{m}_0} = \frac{a_0}{g_c}\frac{1 + 2\alpha^*}{2(1 + \alpha^*)}\left[\sqrt{\frac{2}{\gamma - 1}(\tau_r \tau_f - 1)} - M_0\right] \tag{5.63b}$$

$$\eta_P = \frac{4(1 + 2\alpha^*)M_0}{(3 + 4\alpha^*)M_0 + (1 + 4\alpha^*)(V_{19}/a_0)} \tag{5.63c}$$

and Eqs. (5.58j), (5.58k), (5.58l), (5.58n), and (5.60).

Example 5.5

The engine we looked at in Section 5.9 is used again in this section for an example. The following values are held constant for all plots:

$$T_0 = 216.7\,\text{K}, \qquad \gamma = 1.4, \qquad c_p = 1.004\,\text{kJ/(kg} \cdot \text{K)}$$
$$h_{PR} = 42{,}800\,\text{kJ/kg}, \qquad T_{t4} = 1670\,\text{K}$$

The optimum bypass ratio is plotted in Fig. 5.29a vs the compressor pressure ratio for a flight Mach number of 0.9 and fan pressure ratio of 2. From this plot,

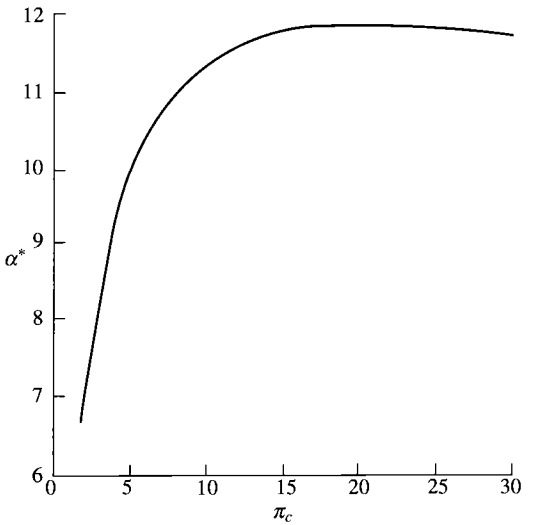

Fig. 5.29a α^* vs π_c, for $\pi_f = 2$ and $M_0 = 0.9$.

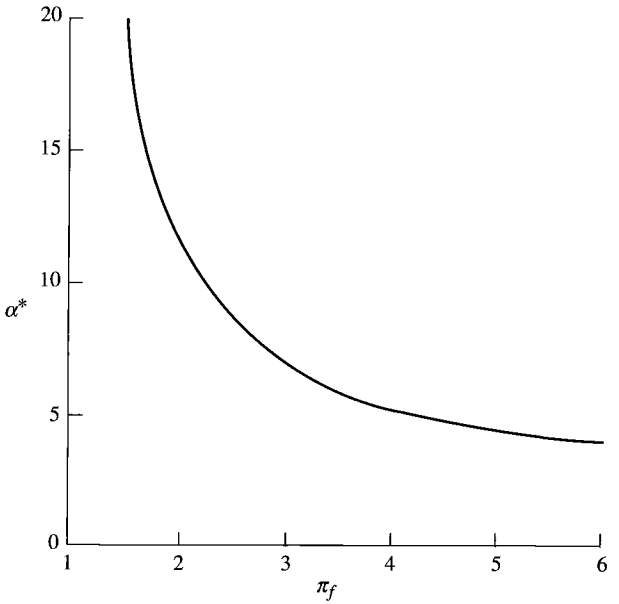

Fig. 5.29b α^* vs π_f, for $\pi_c = 24$ and $M_0 = 0.9$.

we can see that the optimum bypass ratio increases with the compressor pressure ratio. The optimum bypass ratio is plotted in Fig. 5.29b vs the fan pressure ratio, and this figure shows that optimum bypass ratio decreases with fan pressure ratio.

The optimum bypass ratio vs the flight Mach number is plotted in Fig. 5.29c for fan pressure ratios of 2 and 3. From these plots, we can see that the optimum bypass ratio decreases with the flight Mach number. Note that the optimum engine is a turbojet at a Mach number of about 3.0 for a fan pressure ratio of 3.

The plots of specific thrust and thrust specific fuel consumption for an ideal turbofan engine with optimum bypass ratio vs compressor pressure ratio are superimposed on Figs. 5.23a–5.23e by a dashed line marked α^*. The optimum-bypass-ratio ideal turbofan has the minimum thrust specific fuel consumption.

The plots of specific thrust and thrust specific fuel consumption for the optimum-bypass-ratio ideal turbofan vs fan pressure ratio are superimposed on Figs. 5.25a–5.25d by a dashed line marked α^*. As shown in these figures, the plot for α^* is the locus of the minimum value of S for each π_f.

The plots of specific thrust and thrust specific fuel consumption for the optimum-bypass-ratio ideal turbofan vs flight Mach number are superimposed on Figs. 5.27a–5.27e for a fan pressure ratio of 2 and on Figs. 5.28a–5.28e for a fan pressure ratio of 3. As shown in these figures, the plots for α^* are the locus of the minimum value of S for fixed values of π_c and π_f.

The thermal efficiency of an optimum-bypass-ratio ideal turbofan is the same as that of an ideal turbojet. The bypass ratio of an ideal turbofan affects only the

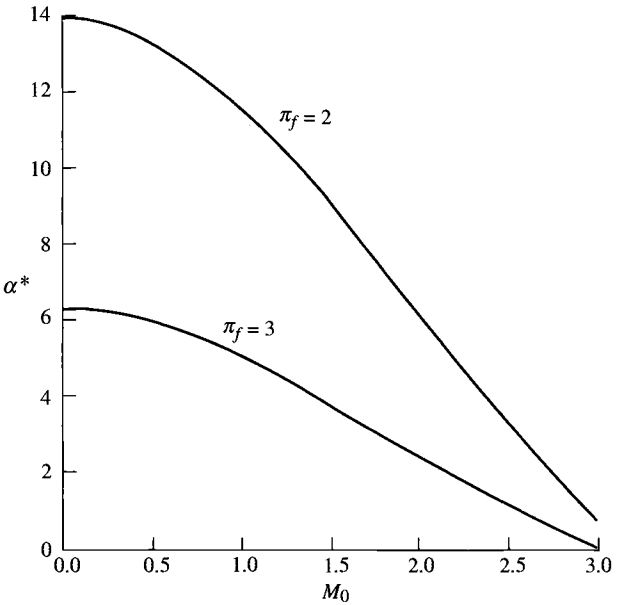

Fig. 5.29c α^* **vs** M_0**, for** $\pi_c = 24$ **and** $\pi_f = 2$ **and 3.**

propulsive efficiency. The propulsive efficiency of an optimum-bypass-ratio ideal turbofan is superimposed on those of Figs. 5.23d, 5.25c, 5.27c, and 5.28c. As can be seen, the optimum bypass ratio gives the maximum propulsive efficiency. Likewise, as shown in Figs. 5.23d, 5.25c, 5.27d, and 5.28d, the optimum bypass ratio gives the maximum overall efficiency. The thrust ratio of an optimum-bypass-ratio ideal turbofan is superimposed on those of Figs. 5.23e, 5.25d, 5.27e, and 5.28e and is equal to 0.5.

5.11 Ideal Turbofan with Optimum Fan Pressure Ratio

Figures 5.26a and 5.26b show that for given flight conditions T_0 and M_0, design limit τ_λ, compressor pressure ratio π_c, and bypass ratio α, there is an optimum fan pressure ratio π_f that gives the minimum specific fuel consumption and maximum specific thrust. As will be shown, the optimum fan pressure ratio corresponds to the exit velocity V_{19} of the fan stream, being equal to the exit velocity of the core stream V_9. It is left as a reader exercise to show that equal exit velocities ($V_9 = V_{19}$) correspond to maximum propulsive efficiency.

5.11.1 Optimum Fan Pressure Ratio π_f^*

For a given set of prescribed variables (τ_r, π_c, τ_λ, V_0, α), we may locate the optimum fan pressure ratio by taking the partial derivative of the specific

thrust with respect to the fan total temperature ratio. The derivation of an expression for the optimum fan total temperature ratio and, by Eq. (5.58f), the optimum fan pressure ratio follows. From Eq. (5.54), we have

$$\frac{\partial S}{\partial \tau_f} = \frac{-f}{[(1+\alpha)(F/\dot{m}_0)]^2} \frac{\partial}{\partial \tau_f}\left[(1+\alpha)\left(\frac{F}{\dot{m}_0}\right)\right] = 0$$

Thus

$$\frac{\partial S}{\partial \tau_f} = 0$$

is satisfied by

$$\frac{\partial}{\partial \tau_f}\left[\frac{g_c}{V_0}(1+\alpha)\left(\frac{F}{\dot{m}_0}\right)\right] = 0$$

where, from Eq. (5.48),

$$\frac{g_c}{V_0}(1+\alpha)\left(\frac{F}{\dot{m}_0}\right) = \frac{V_9}{V_0} - 1 + \alpha\left(\frac{V_{19}}{V_0} - 1\right)$$

Hence the optimum fan pressure ratio is given by solution of

$$\frac{\partial}{\partial \tau_f}\left[\frac{V_9}{V_0} - 1 + \alpha\left(\frac{V_{19}}{V_0} - 1\right)\right] = \frac{\partial}{\partial \tau_f}\left(\frac{V_9}{V_0}\right) + \alpha \frac{\partial}{\partial \tau_f}\left(\frac{V_{19}}{V_0}\right) = 0 \qquad \text{(i)}$$

Since

$$\frac{\partial}{\partial \tau_f}\left(\frac{V_9}{V_0}\right) = \frac{1}{2V_9/V_0} \frac{\partial}{\partial \tau_f}\left[\left(\frac{V_9}{V_0}\right)^2\right]$$

and

$$\frac{\partial}{\partial \tau_f}\left(\frac{V_{19}}{V_0}\right) = \frac{1}{2V_{19}/V_0} \frac{\partial}{\partial \tau_f}\left[\left(\frac{V_{19}}{V_0}\right)^2\right]$$

Eq. (i) becomes

$$\frac{1}{2V_9/V_0} \frac{\partial}{\partial \tau_f}\left[\left(\frac{V_9}{V_0}\right)^2\right] + \alpha \frac{1}{2V_{19}/V_0} \frac{\partial}{\partial \tau_f}\left[\left(\frac{V_{19}}{V_0}\right)^2\right] = 0 \qquad \text{(ii)}$$

To determine the first term of Eq. (ii), we start with

$$\left(\frac{V_9}{V_0}\right)^2 = \frac{1}{M_0^2}\left(\frac{V_9}{a_0}\right)^2 = \frac{1}{[(\gamma-1)/2](\tau_r-1)}\left(\frac{V_9}{a_0}\right)^2$$
$$= \frac{\tau_\lambda - \tau_r[\tau_c - 1 + \alpha(\tau_f - 1)] - \tau_\lambda/(\tau_r\tau_c)}{\tau_r - 1} \qquad \text{(iii)}$$

Thus

$$\frac{\partial}{\partial\tau_f}\left[\left(\frac{V_9}{V_0}\right)^2\right] = \frac{-\alpha\tau_r}{\tau_r - 1} \qquad \text{(iv)}$$

To determine the second term of Eq. (ii), we start with

$$\left(\frac{V_{19}}{V_0}\right)^2 = \frac{1}{M_0^2}\left(\frac{V_{19}}{a_0}\right)^2 = \frac{1}{[(\gamma-1)/2](\tau_r-1)}\left(\frac{V_{19}}{a_0}\right)^2 = \frac{\tau_r\tau_f - 1}{\tau_r - 1} \qquad \text{(v)}$$

Thus

$$\frac{\partial}{\partial\tau_f}\left[\left(\frac{V_{19}}{V_0}\right)^2\right] = \frac{\tau_r}{\tau_r - 1} \qquad \text{(vi)}$$

Substitution of Eqs. (iv) and (vi) into Eq. (ii) gives

$$\frac{1}{2V_9/V_0}\left(\frac{-\alpha\tau_r}{\tau_r - 1}\right) + \alpha\frac{1}{2V_{19}/V_0}\frac{\tau_r}{\tau_r - 1} = 0 \qquad \text{(vii)}$$

Thus we can conclude from Eq. (vii) that the optimum fan pressure ratio corresponds to that value of τ_f yielding

$$V_9 = V_{19} \qquad (5.64)$$

Also

$$\text{FR} = 1 \qquad (5.65)$$

To solve for the optimum fan temperature ratio, we equate Eqs. (iii) and (v):

$$\left(\frac{V_9}{V_0}\right)^2 = \frac{\tau_\lambda - \tau_r[\tau_c - 1 + \alpha(\tau_f - 1)] - \tau_\lambda/(\tau_r\tau_c)}{\tau_r - 1}$$
$$= \left(\frac{V_{19}}{V_0}\right)^2 = \frac{\tau_r\tau_f - 1}{\tau_r - 1}$$

giving

$$\tau_f^* = \frac{\tau_\lambda - \tau_r(\tau_c - 1) - \tau_\lambda/(\tau_r\tau_c) + \alpha\tau_r + 1}{\tau_r(1+\alpha)} \tag{5.66}$$

An equation for the specific thrust of an optimum-fan-pressure-ratio turbofan can be obtained by starting with the simplified expression

$$\left(\frac{F}{\dot{m}_0}\right)_{\tau_f^*} = \frac{a_0}{g_c}\left(\frac{V_{19}}{a_0} - M_0\right)$$

which becomes

$$\left(\frac{F}{\dot{m}_0}\right)_{\tau_f^*} = \frac{a_0}{g_c}\left[\sqrt{\frac{2}{\gamma-1}(\tau_r\tau_f^* - 1)} - M_0\right] \tag{5.67}$$

The propulsive efficiency for the optimum-fan-pressure-ratio turbofan engine is simply

$$(\eta_P)_{\tau_f^*} = \frac{2}{V_{19}/V_0 + 1} \tag{5.68}$$

5.11.2 Summary of Equations—Optimum-Fan-Pressure-Ratio Ideal Turbofan

INPUTS:

$$M_0,\ T_0(\mathrm{K},\ ^\circ\mathrm{R}),\ \gamma,\ c_p\left(\frac{\mathrm{kJ}}{\mathrm{kg}\cdot\mathrm{K}},\ \frac{\mathrm{Btu}}{\mathrm{lbm}\cdot{}^\circ\mathrm{R}}\right),\ hr_{PR}\left(\frac{\mathrm{kJ}}{\mathrm{kg}},\ \frac{\mathrm{Btu}}{\mathrm{lbm}}\right),\ T_{t4}(\mathrm{K},\ ^\circ\mathrm{R}),\ \pi_c,\ \alpha$$

OUTPUTS:

$$\frac{F}{\dot{m}_0}\left(\frac{\mathrm{N}}{\mathrm{kg/s}},\ \frac{\mathrm{lbf}}{\mathrm{lbm/s}}\right), f,\ S\left(\frac{\mathrm{mg/s}}{\mathrm{N}},\ \frac{\mathrm{lbm/h}}{\mathrm{lbf}}\right),\ \eta_T,\ \eta_P,\ \eta_O,\ \pi_f^*$$

EQUATIONS:

Equations (5.58a–5.58e), (5.58j), (5.58l), plus

$$\tau_f^* = \frac{\tau_\lambda - \tau_r(\tau_c - 1) - \tau_\lambda/(\tau_r\tau_c) + \alpha\tau_r + 1}{\tau_r(1+\alpha)} \tag{5.69a}$$

$$\pi_f^* = (\tau_f^*)^{\gamma/(\gamma-1)} \tag{5.69b}$$

$$\frac{V_{19}}{a_0} = \sqrt{\frac{2}{\gamma - 1}(\tau_r \tau_f^* - 1)} \tag{5.69c}$$

$$\frac{F}{\dot{m}_0} = \frac{a_0}{g_c}\left(\frac{V_{19}}{a_0} - M_0\right) \tag{5.69d}$$

$$\eta_P = \frac{2M_0}{V_{19}/a_0 + M_0} \tag{5.69e}$$

and Eqs. (5.58k), (5.58n), and (5.60).

5.11.3 Effect of Bypass Ratio on Specific Thrust and Fuel Consumption

Data for several turbofan engines are listed in Table 5.2. The bypass ratio ranges from 0.76 for the engine in the smaller A-7D fighter attack airplane to 5 for engines in the commercial transports, to 8 for the C-5A/B heavy logistics military transport engine. The specific thrust and specific fuel consumption for the fighter are about twice their values for the three transport-type airplanes. Let us look at the interrelationship between the bypass ratio, specific thrust, and specific fuel consumption to help explain the trends in the values of these quantities, as exhibited by the table.

We can examine how these quantities interact for the ideal turbofan with optimum fan pressure ratio by plotting specific thrust and thrust specific fuel consumption vs bypass ratio. Such plots are given in Fig. 5.30 for

$$M_0 = 0.8, \quad T_0 = 216.7 \text{ K}, \quad \tau_\lambda = 6.5, \quad \pi_c = 24, \quad h_{PR} = 42{,}800 \text{ kJ/kg}$$
$$\gamma = 1.4, \qquad c_p = 1.004 \text{ kJ/(kg} \cdot \text{K)}$$

Table 5.2 Data for several turbofan engines

Engine	Bypass ratio α	$F/\dot{m}_0$, [N/(kg/s)] [lbf/(lbm/s)]	S, [(mg/s)/N] [(lbm/h)/lbf]	π_f	π_c	Aircraft
TF-39	8.0	251.8 (25.68)	8.87 (0.313)	1.45	22.0	C5A/B
JT9D	5.1	253.4 (25.84)	9.80 (0.346)	1.54	22.3	Boeing 747
CF6	4.32	255.6 (26.06)	9.86 (0.348)	1.71	30.2	DC-10
TF-41	0.76	498.0 (50.78)	17.8 (0.629)	2.45	21.0	A-7D

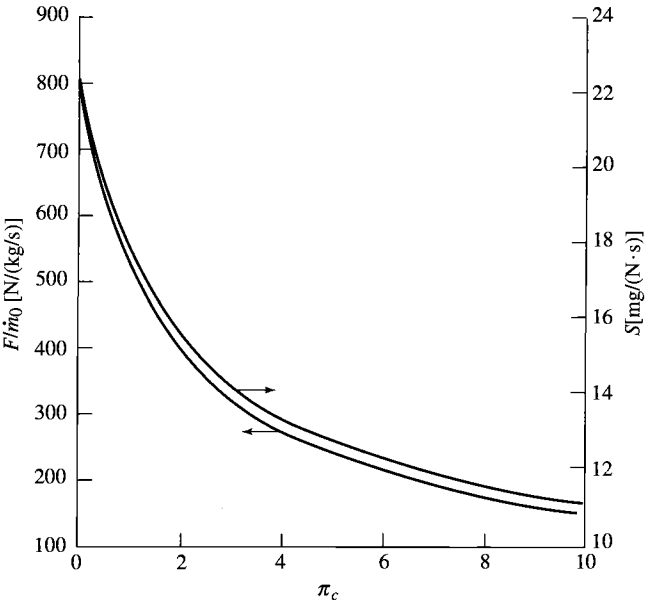

Fig. 5.30 Peformance at π_f^* vs α, for $\pi_c = 24$ and $M_0 = 0.8$.

The optimum fan pressure ratio that gives $V_9 = V_{19}$ is plotted vs the bypass ratio α in Fig. 5.31.

We can see, in Fig. 5.30, a sharp reduction in specific fuel consumption as α increases from zero. An equally marked, but unfavorable, decrease in thrust per unit mass flow occurs. A large fraction of the beneficial decrease in S is obtained by selecting an α of about 5, as was done for the engines in the DC-10 and 747 transports. At a bypass ratio of 8, corresponding to the C-5A engines, a further decrease in specific fuel consumption is realized. Because engine weight is a small fraction of the takeoff gross weight for these airplanes, it is of secondary importance compared to fuel weight and hence specific fuel consumption. Thus we find a relatively large bypass ratio for the engines in the transporters tabulated compared to the 0.76 value of the A-7D engine.

Example 5.6

The engine that we looked at in Section 5.9 is used again in this section for an example. The following values are held constant for all plots:

$$T_0 = 216.7\,\text{K}, \quad \gamma = 1.4, \quad c_p = 1.004\,\text{kJ/(kg K)}$$
$$h_{PR} = 42{,}800\,\text{kJ/kg}, \qquad T_{t4} = 1670\,\text{K}$$

The optimum fan pressure ratio is plotted vs the compressor pressure ratio in Fig. 5.32 and vs the bypass ratio in Fig. 5.33. From Fig. 5.32, we can see that the

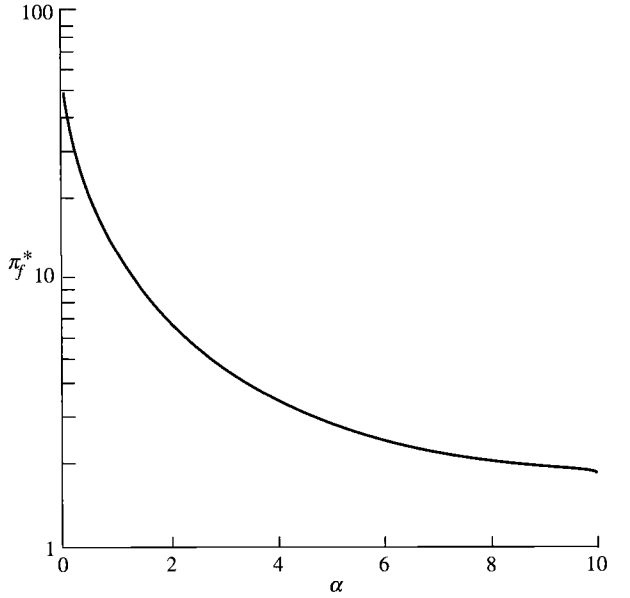

Fig. 5.31 π_f^* vs α, for $\pi_c = 24$ and $M_0 = 0.8$.

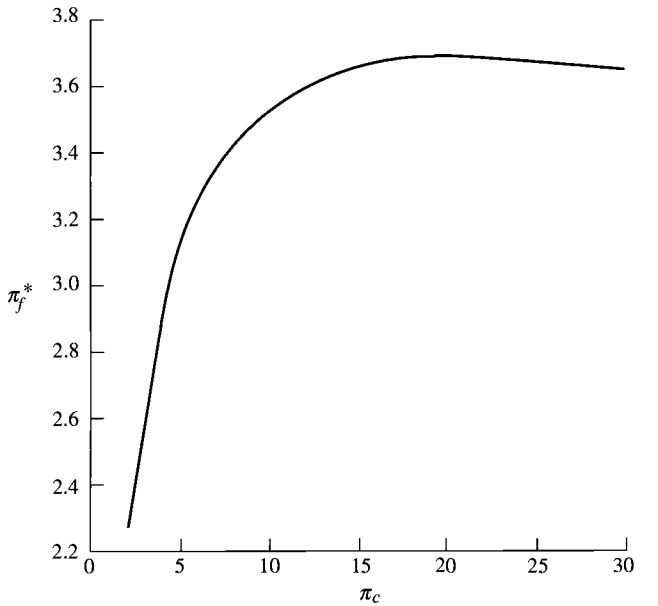

Fig. 5.32 π_f^* vs π_c, for $M_0 = 0.9$ and $\alpha = 5$.

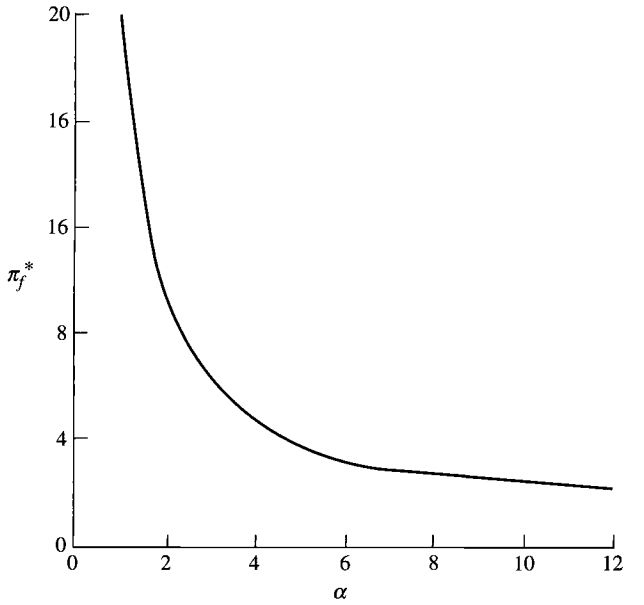

Fig. 5.33 π_f^* **vs** α, **for** $M_0 = 0.9$ **and** $\pi_c = 24$.

optimum fan pressure ratio increases with the compressor pressure ratio. Figure 5.33 shows that the optimum fan pressure ratio decreases with the bypass ratio.

Plots of specific thrust, thrust specific fuel consumption, propulsive efficiency, overall efficiency, and thrust ratio for the optimum-fan-pressure-ratio ideal turbofan engines are superimposed on Figs. 5.24 and 5.26 as dashed lines marked π_f^*. The plots for optimum fan pressure ratio are the loci of the optimums for specific thrust, thrust specific fuel consumption, propulsive efficiency, and overall efficiency. The thrust ratio of the optimum-fan-pressure-ratio ideal turbofan engines is equal to 1.

5.11.4 Comparison of Optimum Ideal Turbofans

A comparison of the two optimum ideal turbofan engines can be made by looking at contour plots of specific thrust $F/\dot{m}_0$ and thrust specific fuel consumption S vs fan pressure ratio π_f and bypass ratio α. For our example problem (Examples 5.4, 5.5, and 5.6), contours of constant specific thrust values and contours of constant thrust specific fuel consumption are plotted in Figs. 5.34a and 5.34b, respectively. Also plotted are the curves for π_f^* and α^* for each optimum engine. Figures 5.34a and 5.34b show that π_f^* is the fan pressure ratio giving maximum specific thrust and minimum thrust specific fuel consumption for a given bypass ratio. Figure 5.34b shows that α^* is the bypass ratio giving

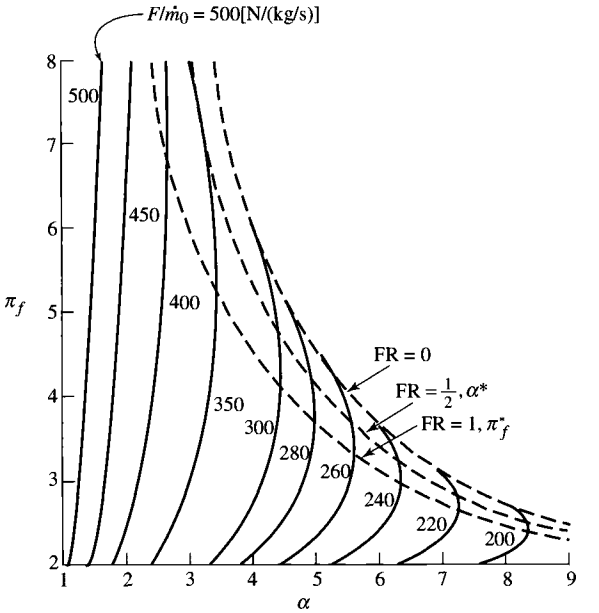

Fig. 5.34a Contours of constant specific thrust and curves for π_f^* and α^*.

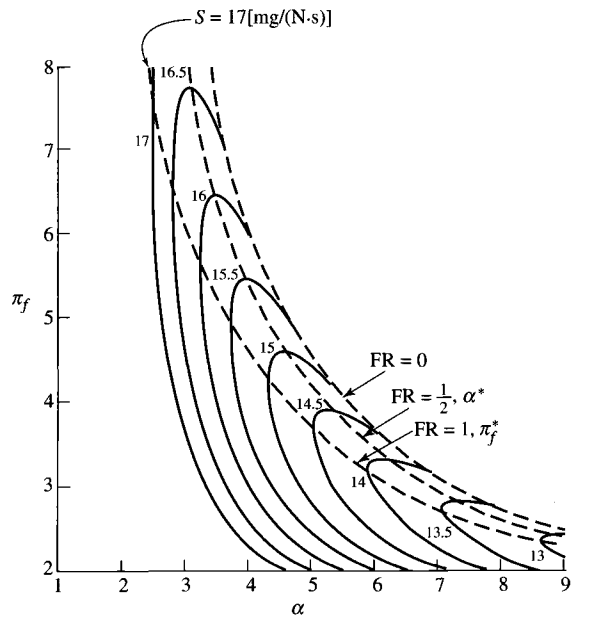

Fig. 5.34b Contours of constant fuel consumption and curves for π_f^* and α^*.

minimum thrust specific fuel consumption for a given fan pressure ratio. Also shown in Fig. 5.34b are that the α^* curve is the locus of horizontal tangents to contours of constant S and the π_f^* curve is the locus of vertical tangents to contours of constant S.

5.12 Ideal Pulse Detonation Engine

The classical, calorically perfect gas, closed thermodynamic cycle analysis should always be considered for the initial evaluation of ideal propulsion devices because it often provides transparent algebraic results that reveal fundamental behavior almost effortlessly. This is particularly true because the T-s diagram is not anchored in space or time, but represents the succession of states experienced by every element of the working fluid, and can therefore be applied equally well to steady (e.g., Brayton and Carnot) and unsteady (e.g., Diesel and Otto) cycles.

The pulse detonation engine (PDE) is a contemporary example of a novel propulsion cycle. Because of its inherently unsteady behavior, it has been difficult to conveniently classify and evaluate it relative to its steady-state counterparts by means of unsteady gas dynamic calculations alone. The classical, closed thermodynamic cycle analysis of the ideal PDE is identical to that of the ideal turbojet (see Section 5.7), except that the heat is released by a detonation wave that passes through the working fluid containing fuel that has been brought essentially to rest in the combustor. Please note that the compression process may include both ram compression due to forward flight and mechanical compression driven by the fluid leaving the combustor. The T-s diagram for an example PDE is shown in Fig. 5.35, where $\psi = T_3/T_0$ is the cycle thermal compression ratio, $\tilde{q}$ is the dimensionless heat release, and $\gamma = 1.36$. This approach takes advantage of the fact that entropy is a thermodynamic state property, independent of velocity reference frame, as opposed to, for example, the total pressure and total temperature. The complete version of this analysis can be found in Ref. 31.

We therefore direct our attention to the pulse detonation wave process. The reader is advised that the ensuing mathematical analyses will be straightforward, and is therefore encouraged to focus on the physical phenomena involved.

The generally accepted model of a normal detonation wave in PDP devices is that of a Zeldovich/von Neumann/Doering or ZND wave (see Refs. 32 and 33), a compound wave consisting of a normal shock wave progressing into the undisturbed fuel-air mixture, which is nearly at rest at the combustor entry condition (*point 3*), followed by release of sensible heat in a constant-area region (Rayleigh flow) terminating at *point 4*. The strength (Mach number, pressure ratio, or temperature ratio) of the leading shock wave, from point 3 to point 3a, is uniquely determined by the initial conditions and the amount of heat added. The entire process is constrained by the Chapman-Jouguet condition, which requires that the local Mach number at the termination of the heat addition region (point 4) be one (sonic or choked flow). The heat addition region is followed by a very complex constant-area region of nonsteady expansion waves, the most important

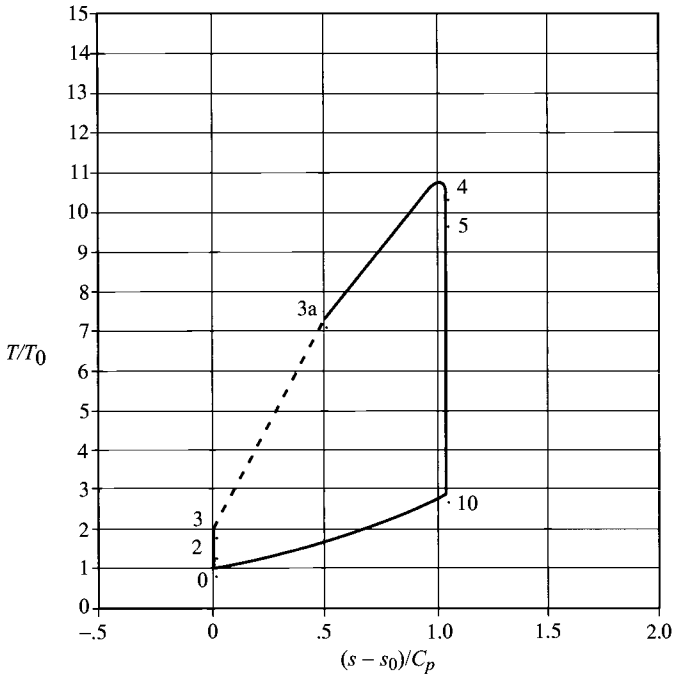

Fig. 5.35 Temperature-entropy diagram for the ideal PDE cycle, for $\psi = 2$, $\tilde{q} = 5$, and $\gamma = 1.36$.

property of which is that they are assumed to be isentropic. This ZND wave structure is stationary in detonation wave coordinates from the undisturbed flow to the end of the heat addition process. To ensure the greatest cycle performance, it is further assumed that 1) the nonsteady expansion (point 4 to point 10) of the detonated mixture is isentropic, 2) every fluid particle experiences the same normal detonation process, and 3) there is no energy penalty to the cycle for whatever spark or ignition torch may be required to initiate the detonation process.

Closed-form, algebraic solutions for the leading normal shock wave (Chapman-Jouguet) Mach number M_{CJ} and the entropy rise in the detonation wave have been derived by Shapiro[34] and others[33,35] for calorically perfect gases, and are given, respectively, by

$$M_{CJ}^2 = (\gamma+1)\frac{\tilde{q}}{\psi} + 1 + \sqrt{\left[(\gamma+1)\frac{\tilde{q}}{\psi} + 1\right]^2 - 1}$$

where

$$\tilde{q} \equiv \frac{q_{\text{supp}}}{c_p T_0} = \frac{f h_{PR}}{c_p T_0} \tag{5.70}$$

and

$$\frac{s_4 - s_3}{c_p} = -\ell n\left[M_{CJ}^2\left(\frac{\gamma+1}{1+\gamma M_{CJ}^2}\right)^{\frac{\gamma+1}{\gamma}}\right] \tag{5.71}$$

Consequently, the constant-pressure heat rejected and the cycle thermal efficiency become

$$\begin{aligned} q_{\text{rej}} &= h_{10} - h_0 = c_p(T_{10} - T_0) = c_p T_0\left(e^{\frac{s_{10}-s_0}{c_p}} - 1\right) \\ &= c_p T_0\left(e^{\frac{s_4-s_3}{c_p}} - 1\right) = c_p T_0\left[\frac{1}{M_{CJ}^2}\left(\frac{1+\gamma M_{CJ}^2}{\gamma+1}\right)^{\frac{\gamma+1}{\gamma}} - 1\right] \end{aligned} \tag{5.72}$$

and

$$\eta_{\text{th}} = 1 - \frac{\frac{1}{M_{CJ}^2}\left(\frac{1+\gamma M_{CJ}^2}{\gamma+1}\right)^{\frac{\gamma+1}{\gamma}} - 1}{\bar{q}} \tag{5.73}$$

Since

$$\frac{F}{\dot{m}_0} \equiv \frac{1}{g_c}\left[\sqrt{V_0^2 + 2\eta_{\text{th}} q_{\text{supp}}} - V_0\right] \tag{5.74}$$

and

$$S \equiv \frac{\dot{m}_f}{F} = \frac{f\dot{m}_0}{F} = \frac{f}{F/\dot{m}_0} \tag{5.75}$$

then generalized ideal PDE performance information, such as that shown in Figs. 5.36 and 5.37, are easily calculated. The ideal Brayton (ramjet/turbojet) is included for reference.

In summary, Figs. 5.36 and 5.37 clearly show that the thermal compression inherent in the PDE normal shock wave, albeit irreversible (see Fig. 5.35), leads to superior propulsion performance for the ideal PDE cycle vs the ideal Brayton cycle when $\psi = T_3/T_0$ is small. However, when $\psi \geq$ about 3 (due to combined ram and mechanical compression), the difference between PDE and Brayton performance is significantly reduced. Readers are now empowered to freely investigate comparisons of their own choice.

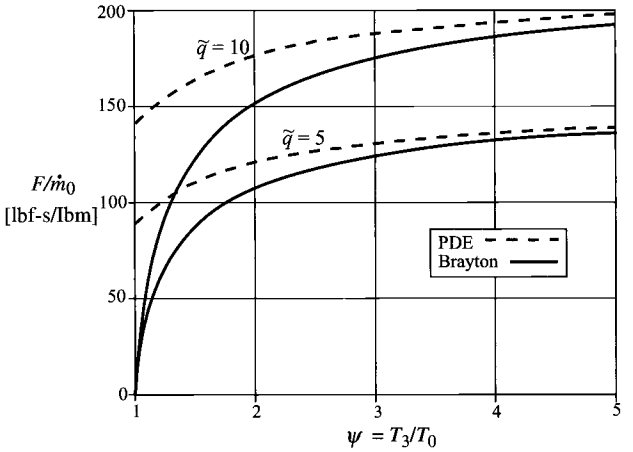

Fig. 5.36 Specific thrust $F/\dot{m}_0$ of ideal PDE and Brayton cycles as functions of ψ, for $\tilde{q} = 5$ and 10, $\gamma = 1.36$, and vehicle speed $V_0 = 0$.

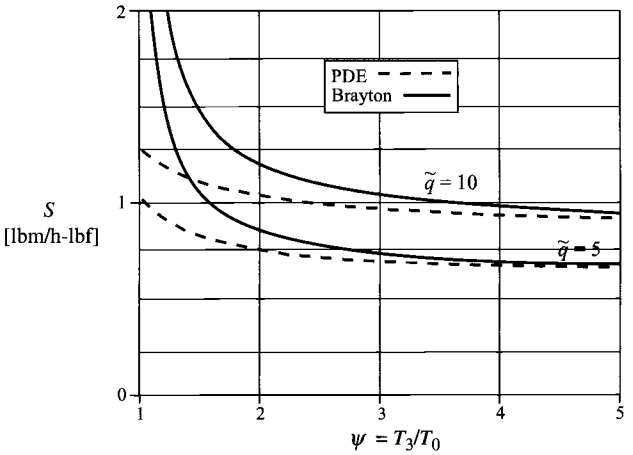

Fig. 5.37 Specific fuel consumption S of ideal PDE and Brayton cycles as functions of ψ, for $\tilde{q} = 5$ and 10, $\gamma = 1.36$, $h_{PR} = 19{,}000$ Btu/lbm, and $V_0 = 0$.

Problems

5.1 Show that the thermal and propulsive efficiencies for an ideal ramjet engine are given by Eqs. (5.17a) and (5.17b), respectively.

5.2 Calculate the variation with T_{t4} of exit Mach number, exit velocity, specific thrust, fuel/air ratio, and thrust specific fuel consumption of an ideal

turbojet engine for compressor pressure ratios of 10 and 20 at a flight Mach number of 2 and $T_0 = 390°R$. Perform calculations at T_{t4} values of 4400, 4000, 3500, and 3000°R. Use $h_{PR} = 18{,}400$ Btu/lbm, $c_p = 0.24$ Btu/(lbm · °R), and $\gamma = 1.4$. Compare your results with the output of the PARA computer program.

5.3 Calculate the variation with T_{t4} of exit Mach number, exit velocity, specific thrust, fuel/air ratio, and thrust specific fuel consumption of an ideal turbojet engine for compressor pressure ratios of 10 and 20 at a flight Mach number of 2 and $T_0 = 217$ K. Perform calculations at T_{t4} values of 2400, 2200, 2000, and 1800 K. Use $h_{PR} = 42{,}800$ kJ/kg, $c_P = 1.004$ kJ/(kg · K), and $\gamma = 1.4$. Compare your results with the output of the PARA computer program.

5.4 Show that the thermal efficiency for an ideal turbojet engine is given by Eq. (5.22).

5.5 Show that the thermal efficiency for an ideal afterburning turbojet is given by Eq. (5.42).

5.6 A major shortcoming of the ramjet engine is the lack of static thrust. To overcome this, it is proposed to add a compressor driven by an electric motor, as shown in the model engine in Fig. P5.1. For this new ideal engine configuration, show the following:

(a) The specific thrust is given by

$$\frac{F}{\dot{m}_0} = \frac{a_0}{g_c}\left[\sqrt{\frac{2}{\gamma - 1}\frac{\tau_\lambda}{\tau_r \tau_c}(\tau_r \tau_c - 1)} - M_0\right]$$

(b) The compressor power requirement is given by

$$\dot{W}_c = \dot{m}_0 c_p T_0 \tau_r (\tau_c - 1)$$

(c) Determine the static thrust of this engine at the following conditions:

$$T_0 = 518.7°R, \qquad T_{t4} = 3200°R, \qquad \pi_c = 4$$

$$c_P = 0.24\,\text{Btu/(lbm} \cdot °R), \qquad \gamma = 1.4$$

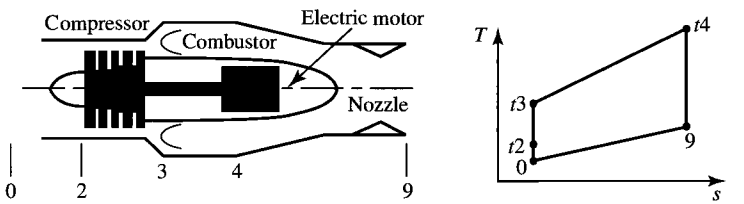

Fig. P5.1 Model engine.

5.7 Determine the optimum compressor pressure ratio, specific thrust, and thrust specific fuel consumption for an ideal turbojet engine giving the maximum specific thrust at the following conditions:

$$M_0 = 2.1,\ T_0 = 220\ \text{K}, \qquad T_{t4} = 1700\ \text{K}, \qquad h_{PR} = 42{,}800\ \text{kJ/kg}$$
$$c_p = 1.004\ \text{kJ/(kg} \cdot \text{K)}, \qquad \gamma = 1.4$$

5.8 Show that the thermal efficiency for an ideal turbojet engine with optimum compressor pressure ratio is given by $\eta_\tau = 1 - 1/\sqrt{\tau_\lambda}$.

5.9 Show that the thermal efficiency for an ideal turbofan engine is given by Eq. (5.22).

5.10 Compare the performance of three ideal turbofan engines with an ideal turbojet engine at two flight conditions by completing Table P5.1. The first flight condition (case 1) is at a flight Mach number of 0.9 at an altitude of 40,000 ft, and the second flight condition (case 2) is at a flight Mach number of 2.6 and an altitude of 60,000 ft. Note that the fuel/air ratio need be calculated only once for each case since it is not a function of α or π_f. The following design information is given:

$$\pi_c = 20, \qquad T_{t4} = 3000^\circ\text{R}, \qquad c_p = 0.24\ \text{Btu/(lbm} \cdot {}^\circ\text{R)}$$
$$\gamma = 1.4, \qquad h_{PR} = 18{,}400\ \text{Btu/lbm}$$

5.11 Repeat Problem 5.10 with the first flight condition (case 1) at a flight Mach number of 0.9 and altitude of 12 km and the second flight condition (case 2) at a flight Mach number of 2.6 and an altitude of 18 km. Use the following design information:

$$\pi_c = 20, \qquad T_{t4} = 1670\ \text{K}, \qquad c_p = 1.004\ \text{kJ/(kg} \cdot \text{K)}$$
$$\gamma = 1.4, \qquad h_{PR} = 42{,}800\ \text{kJ/kg}$$

Table P5.1

Engine	α	π_f	V_9/a_0	V_{19}/a_0	F/m_0	f	S
Turbofan							
(a) Case 1	1	4					
Case 2	1	4					
(b) Case 1, α^*		4					
Case 2, α^*		4					
(c) Case 1, π_f^*	1						
Case 2, π_f^*	1						
Turbojet							
(a) Case 1	0	n/a		n/a			
Case 2	0	n/a		n/a			

5.12 Show that the propulsive efficiency for an ideal turbofan engine with optimum bypass ratio is given by Eq. (5.62).

5.13 Show that the propulsive efficiency for an ideal turbofan engine with optimum fan pressure ratio is given by Eq. (5.68).

5.14 For an ideal turbofan engine, the maximum value of the bypass ratio corresponds to $V_9 = V_0$.

(a) Starting with Eq. (5.53), show that this maximum bypass ratio is given by

$$\alpha_{\max} = \frac{\tau_\lambda + 1 - \tau_r\tau_c - \tau_\lambda/(\tau_r\tau_c)}{\tau_r(\tau_f - 1)}$$

(b) Show that the propulsive efficiency for this maximum bypass ratio is given by

$$\eta_P = \frac{2}{\sqrt{(\tau_r\tau_f - 1)/(\tau_r - 1) + 1}}$$

5.15 Under certain conditions, it is desirable to obtain power from the freestream. Consider the ideal air-powered turbine shown in Fig. P5.2. This cycle extracts power from the incoming airstream. The incoming air is slowed down in the inlet and then heated in the combustor before going through the turbine. The cycle is designed to produce no thrust ($F = 0$), so that $V_9 = V_0$ and $P_9 = P_0$.

(a) Starting with Eq. (5.29), show that

$$\tau_t = \frac{1}{\tau_r} + \frac{1}{\tau_\lambda}\frac{\gamma - 1}{2}M_0^2$$

(b) Then show that the turbine output power is given by

$$\dot{W}_i = \dot{m}c_pT_0\left(\frac{\tau_\lambda}{\tau_r} - 1\right)\frac{\gamma - 1}{2}M_0^2$$

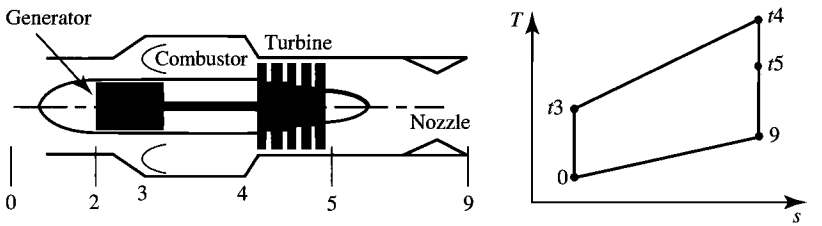

Fig. P5.2 Ideal air-powered turbine.

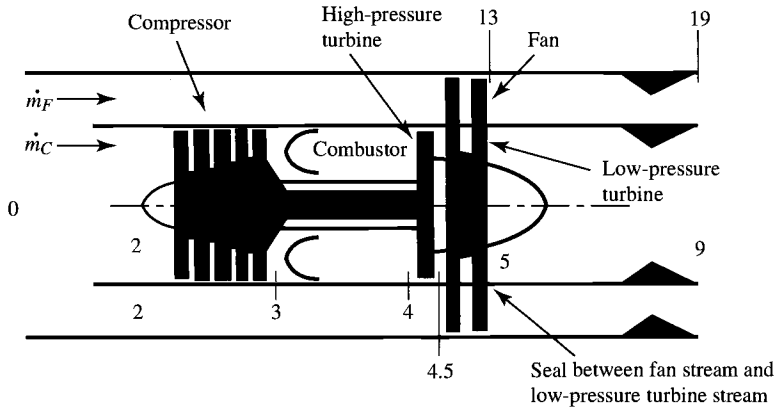

Fig. P5.3 Turbofan engine with aft fan.

5.16 In the early development of the turbofan engine, General Electric developed a turbofan engine with an aft fan, as shown in Fig. P5.3. The compressor is driven by the high-pressure turbine, and the aft fan is directly connected to the low-pressure turbine. Consider an ideal turbofan engine with an aft fan.

(a) Show that the high-pressure turbine temperature ratio is given by

$$\tau_{tH} = \frac{T_{t4.5}}{T_{t4}} = 1 - \frac{\tau_r}{\tau_\lambda}(\tau_c - 1)$$

(b) Show that the low-pressure-turbine temperature ratio is given by

$$\tau_{tL} = \frac{T_{t5}}{T_{t4.5}} = 1 - \frac{\alpha\tau_r}{\tau_\lambda \tau_{tH}}(\tau_f - 1)$$

5.17 Starting with Eq. (5.48), show that for known values of M_0, T_0, T_{t4}, π_c, and πf, the bypass ratio α giving a specified value of specific thrust $F/\dot{m}_0$ is given by the solution to the quadratic equation

$$A\alpha^2 + B\alpha + C = 0$$

where

$$A = \frac{\gamma - 1}{2} D^2$$

$$B = (\gamma - 1)\left(D^2 + D\frac{V_{19}}{a_0}\right) + \tau_r(\tau_f - 1)$$

$$C = \frac{\gamma - 1}{2}\left(D^2 + 2D\frac{V_{19}}{a_0}\right) - E$$

$$D = \frac{F}{\dot{m}_0}\frac{g_c}{a_0} - \left(\frac{V_{19}}{a_0} - M_0\right)$$

$$E = \tau_\lambda - \tau_r(\tau_c - 1) - \frac{\tau_\lambda}{\tau_r \tau_c} - (\tau_r \tau_f - 1)$$

$$\frac{V_{19}}{a_0} = \sqrt{\frac{2}{\gamma - 1}(\tau_r \tau_f - 1)}$$

5.18 Using the system of equations listed in Problem 5.17, determine the bypass ratio that gives a specific thrust of 400 N/(kg/s) for the following data:

$$T_0 = 216.7 \text{ K}, \quad T_{t4} = 1670 \text{ K}, \quad M_0 = 0.8, \quad \pi_c = 24, \quad \pi_f = 4$$
$$\text{with } \gamma = 1.4, \; c_p = 1.004 \text{ kJ/(kg} \cdot \text{K)}, \; h_{PR} = 42{,}800 \text{ kJ/kg}$$

5.19 Using the system of equations listed in Problem 5.17, determine the bypass ratio that gives a specific thrust of 40.0 lbf/(lbm/s) for the following data:

$$T_0 = 390°\text{R}, \quad T_{t4} = 3000°\text{R}, \quad M_0 = 2, \quad \pi_c = 16, \quad \pi_f = 5$$
$$\text{with } \gamma = 1.4, \quad c_p = 0.24 \text{ Btu/(lbm} \cdot °\text{R)}, \quad h_{PR} = 18{,}400 \text{ Btu/lbm}$$

Problems for Supporting Material

SM5.1 Considerable research and development effort is going into increasing the maximum T_{t4} in gas turbine engines for fighter aircraft. For a mixed-flow turbofan engine with $\pi_c = 16$ at a flight condition of $M_0 = 2.5$ and $T_0 = 216.7$ K, use the PARA computer program to determine and plot the required engine fan pressure, specific thrust, and specific fuel consumption vs T_{t4} over a range of 1600 to 2200 K for bypass ratios of 0.5 and 1. Use $h_{PR} = 42{,}800$ kJ/kg, $c_p = 1.004$ kJ/(kg · K), and $\gamma = 1.4$. Comment on your results in general. Why do the plots of specific fuel consumption vs specific thrust for these engines all fall on one line?

SM5.2 Considerable research and development effort is going into increasing the maximum T_{t4} in gas turbine engines for fighter aircraft. For a mixed-flow turbofan engine with $\pi_c = 20$ at a flight condition of $M_0 = 2$ and $T_0 = 390°$R, use the PARA computer program to determine and plot the required engine bypass ratio α, specific thrust, and specific fuel consumption vs T_{t4} over a range of 3000 to 4000°R for fan pressure ratios of 2 and 5. Use $h_{PR} = 18{,}400$ Btu/lbm, $c_p = 0.24$ Btu/(lbm · °R), and $\gamma = 1.4$. Comment on your results.

SM5.3 Show that the thermal efficiency of the afterburning mixed-flow turbofan engine given by Eq. (SM5.16) can be rewritten as

$$\eta_T = \frac{c_p T_0}{f_0 h_{PR}} \left[\tau_\lambda \text{AB} \left(1 - \frac{1}{\tau_r \tau_f} \right) - (\tau_r - 1) \right]$$

SM5.4 For an afterburning mixed-flow turbofan engine with $\pi_c = 16$ and $T_{t7} = 2200$ K at a flight condition of $M_0 = 2.5$ and $T_0 = 216.7$ K, use the PARA computer program to determine and plot the required engine fan pressure, specific thrust, and specific fuel consumption vs T_{t4} over a range of 1600 to 2200 K for bypass ratios of 0.5 and 1. Use $h_{PR} = 42{,}800$ kJ/kg, $c_p = 1.004$ kJ/(kg · K), and $\gamma = 1.4$. Comment on your results in general. Why do the plots of specific fuel consumption vs specific thrust for these engines all fall on one line? Compare these results to those for Problem SM5.1, and comment on the differences.

SM5.5 For an afterburning mixed-flow turbofan engine with $\pi_c = 20$ and $T_{t7} = 4000°$R at a flight condition of $M_0 = 2$ and $T_0 = 390°$R, use the PARA computer program to determine and plot the required engine bypass ratio α, specific thrust, and specific fuel consumption vs T_{t4} over a range of 3000 to 4000°R for fan pressure ratios of 2 and 5. Use $h_{PR} = 18{,}400$ Btu/lbm, $c_p = 0.24$ Btu/(lbm · °R), and $\gamma = 1.4$. Comment on your results. Compare these results to those for Problem SM5.2, and comment on the changes.

SM5.6 Use the PARA computer program to determine and plot the thrust specific fuel consumption vs specific thrust for the turboprop engine of Example SM5.2 over the same range of compressor pressure ratios for turbine temperature ratios of 0.8, 0.7, 0.6, 0.5, 0.4, and optimum.

SM5.7 Use the PARA computer program to determine and plot the thrust specific fuel consumption vs specific thrust for the turboprop engine over the range of compressor pressure ratios from 2 to 40 at $T_0 = 425°$R, $M_0 = 0.65$, $\gamma = 1.4$, $c_p = 0.24$ Btu/(lbm · °R), $h_{PR} = 18{,}400$ Btu/lbm, $T_{t4} = 2460°$R, and $\eta_{\text{prop}} = 0.8$ for turbine temperature ratios of 0.8, 0.7, 0.6, 0.5, 0.4, and optimum.

SM5.8 Use the PARA computer program to determine and plot the power specific fuel consumption vs specific power for the turboshaft engine with regeneration over compressor pressure ratios of 4 to 18 at $T_0 = 290$ K, $M_0 = 0$, $\gamma = 1.4$, $c_p = 1.004$ kJ/(kg · K), $h_{PR} = 42{,}800$ kJ/kg, and $x = 1.02$ for combustor exit temperatures T_{t4} of 1300, 1400, 1500, and 1600 K.

SM5.9 Use the PARA computer program to determine and plot the power specific fuel consumption vs specific power for the turboshaft engine with regeneration of Example SM5.3 at $x = 1.02$ over the same range of compressor ratios for combustor exit temperatures T_{t4} of 2400, 2600, 2800, and 3000°R.

Gas Turbine Design Problems

5.D1 You are to determine the range of compressor pressure ratios and bypass ratios for ideal turbofan engines that best meet the design requirements for the hypothetical passenger aircraft, the HP-1.

Hand-Calculate Ideal Performance (HP-1 Aircraft). Using the parametric cycle analysis equations for an ideal turbofan engine with $T_{t4} = 1560$ K, hand-calculate the specific thrust and thrust specific fuel consumption for an ideal turbofan engine with a compressor pressure ratio of 36, fan pressure ratio of 1.8, and bypass ratio of 10 at the 0.83 Mach, 11-km-altitude cruise condition. Assume $\gamma = 1.4$, $c_p = 1.004$ kJ/(kg · K), and $h_{PR} = 42{,}800$ kJ/kg. Compare your answers to results from the parametric cycle analysis program PARA.

Computer-Calculated Ideal Performance (HP-1 Aircraft). For the 0.83 Mach, 11-km-altitude cruise condition, determine the performance available from turbofan engines. This part of the analysis is accomplished by using the PARA computer program with $T_{t4} = 1560$ K. Specifically, you are to vary the compressor pressure ratio from 20 to 40 in increments of 2. Fix the fan pressure ratio at your assigned value of ___. Evaluate bypass ratios of 4, 6, 8, 10, 12, and the optimum value. Assume $\gamma = 1.4$, $c_p = 1.004$ kJ/(kg · K), and $h_{PR} = 42{,}800$ kJ/kg.

Calculate Minimum Specific Thrust at Cruise (HP-1 Aircraft). You can calculate the minimum uninstalled specific thrust at cruise based on the following information:

1) The thrust of the two engines must be able to offset drag at 0.83 Mach and 11-km altitude and have enough excess thrust for P_s of 1.5 m/s. Determine the required installed thrust to attain the cruise condition using Eq. (1.28). Assuming $\phi_{\text{inlet}} + \phi_{\text{noz}} = 0.02$, determine the required uninstalled thrust.

2) Determine the maximum mass flow into the 2.2-m-diam inlet for the 0.83 Mach, 11-km-altitude flight condition, using the equation given in the background section for this design problem in Chapter 1.

3) Using the results of steps 1 and 2, calculate the minimum uninstalled specific thrust at cruise.

4) Perform steps 2 and 3 for inlet diameters of 2.5, 2.75, 3.0, 3.25, and 3.5 m.

Select Promising Engine Cycles (HP-1 Aircraft). Plot thrust specific fuel consumption vs specific thrust (thrust per unit mass flow) for the engines analyzed in the preceding. Plot a curve for each bypass ratio, and cross-plot the values of the compressor pressure ratio (see Fig. P5.D1). The result is a *carpet plot* (a multivariable plot) for the cruise condition. Now draw a dashed horizontal line on the carpet plot corresponding to the maximum allowable uninstalled thrust specific fuel consumption $S_{\max}$ for the cruise condition (determined in the Chapter 1 portion of this design problem). Draw a dashed vertical line for each minimum uninstalled specific thrust

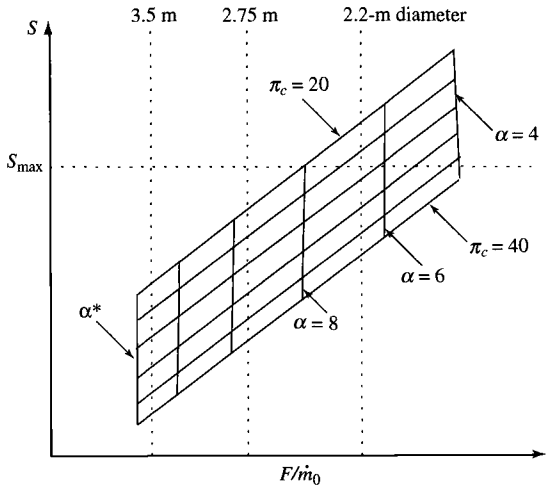

Fig. P5.D1 Example carpet plot for HP-1 aircraft engine.

determined in the preceding. Your carpet plots will look similar to the example shown in Fig. P5.D1. What ranges of bypass ratio and compressor pressure ratio look most promising?

5.D2 You are to determine the ranges of compressor pressure ratio and bypass ratio for ideal mixed-flow turbofan engines that best meet the design requirements for the hypothetical fighter aircraft, the HF-1.

Hand-Calculate Ideal Performance (HF-1 Aircraft). Using the parametric cycle analysis equations for an ideal mixed-flow turbofan engine with $T_{t4} = 3250°R$, hand-calculate the specific thrust and thrust-specific fuel consumption for an ideal turbofan engine with a compressor pressure ratio of 25 and bypass ratio of 0.5 at the 1.6 Mach, 40-kft-altitude supercruise condition. Assume $\gamma = 1.4$, $c_p = 0.24$ Btu/(lbm · °R), and $h_{PR} = 18{,}400$ Btu/lbm. Compare your answers to the results from the parametric cycle analysis program PARA.

Computer-Calculated Ideal Performance (HF-1 Aircraft). For the 1.6 Mach, 40-kft-altitude supercruise condition, determine the performance available from turbofan engines. This part of the analysis is accomplished by using the PARA computer program with $T_{t4} = 3250°R$. Specifically, you are to vary the bypass ratio from 0.1 to 1.0 in increments of 0.05. Evaluate compressor pressure ratios of 16, 18, 20, 22, 24, and 28. Assume $\gamma = 1.4$, $c_p = 0.24$ Btu/(lbm · °R), and $h_{PR} = 18{,}400$ Btu/lbm.

Calculate Minimum Specific Thrust at Cruise (HF-1 Aircraft). You can calculate the minimum uninstalled specific thrust at supercruise based on the following information:

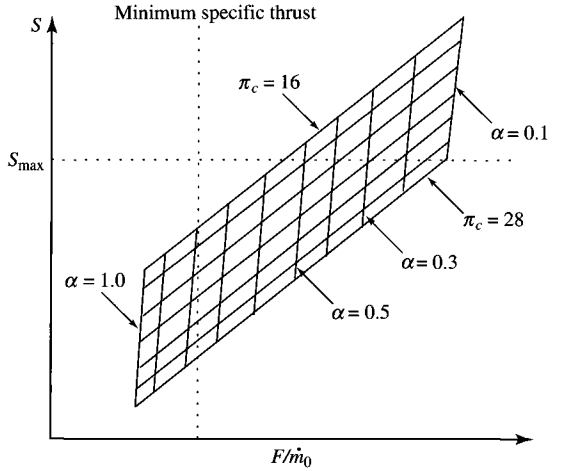

Fig. P5.D2 Example carpet plot for HF-1 aircraft engine.

1) The thrust of the two engines must be able to offset drag at 1.6 Mach, 40-kft altitude, and 92% of takeoff weight. Assuming $\phi_{inlet} + \phi_{noz} = 0.05$, determine the required uninstalled thrust for each engine.

2) The maximum mass flow into a 5-ft^2 inlet for the 1.6 Mach, 40-kft-altitude flight condition is $\dot{m} = \rho AV = \sigma\rho_{ref}AMa = (0.2471 - 0.07647)(5)\ (1.6 \times 0.8671 \times 1116) = 146.3$ lbm/s.

3) Using the results of steps 1 and 2, calculate the minimum uninstalled specific thrust at supercruise.

Select Promising Engine Cycles (HF-1 Aircraft). Plot the thrust specific fuel consumption vs specific thrust (thrust per unit mass flow) for the engines analyzed in the preceding. Plot a curve for each bypass ratio, and cross-plot the values of compressor pressure ratio (see Fig. P5.D2). The result is a carpet plot (a multivariable plot) for the supercruise condition. Now draw a dashed horizontal line on the carpet plot corresponding to the maximum allowable uninstalled thrust specific fuel consumption S_{max} for the cruise condition (determined in the Chapter 1 portion of this design problem). Draw a dashed vertical line for the minimum uninstalled specific thrust determined in the preceding section. Your carpet plots will look similar to the example shown in Fig. P5.D2. What ranges of bypass ratio and compressor pressure ratio look most promising?